3151

SAND78-1015
Unlimited Release

Limitations and Corrections in Measuring Dynamic Characteristics of Structural Systems

Patrick L. Walter

Sandia Laboratories

SF 2900 Q(7-73)

SAND78-1015
Unlimited Release
Printed October 1978

LIMITATIONS AND CORRECTIONS IN MEASURING DYNAMIC CHARACTERISTICS OF STRUCTURAL SYSTEMS

Patrick L. Walter
Telemetry Components and Transducers Division 1585
Sandia Laboratories, Albuquerque, NM 87185

ABSTRACT

This work deals with limitations encountered in measuring the dynamic characteristics of structural systems. Structural loading and response are measured by transducers possessing multiple resonant frequencies in their transfer function. In transient environments, the resultant signals from these transducers are shown to be analytically unpredictable in amplitude level and frequency content. Data recorded during nuclear effects simulation testing on structures are analyzed. Results of analysis can be generalized to any structure which encounters dynamic loading. Methods to improve the recorded data are described which can be implemented on a frequency selective basis during the measurement process. These improvements minimize data distortion attributable to the transfer characteristics of the measuring transducers.

ACKNOWLEDGMENT

This report resulted from work sponsored at Arizona State University under Sandia Laboratories Doctoral Studies Program.

CONTENTS

CONTENTS (cont)

TABLES

FIGURES

FIGURES (cont)

FIGURES (cont)

FIGURES (cont)

FIGURES (cont)

CHAPTER I

INTRODUCTION

This work describes limitations encountered when recording signals intended to measure the dynamic characteristics of structural systems. These limitations are demonstrated by analyzing structural test data, and corrective methods are developed so that meaningful data can be initially recorded. These recorded data enhance the analytical modeling of the structural dynamicist, resulting in more valid test specifications and greater structural system reliability.

A sequence of events which might be followed to assure an engineering system's structural reliability under dynamic loading is listed below.

1. A mathematical model is created to represent the physical system.
2. An instrumented test is performed on either a mechanical model of the system or, preferably, on a full scale system, and data regarding loads applied to, and the resulting response of, the structure are transmitted and recorded.
3. The mathematical model is adjusted or redefined to provide correlation between the results it predicts and the recorded test data.
4. The redefined model is used to synthesize those dynamic environments where testing cannot be performed readily.
5. Based on the preceding results, test specifications are originated for various critical system components. Shock

spectra techniques are one method used to establish these specifications.

6. System reliability is assured through an extensive component test program during manufacture and assembly.

Measurement transducers used to acquire the structural dynamics test data of step 2 can be described as resonant devices. Resonant devices are dynamic systems possessing multiple peaks in the magnification factor associated with their transfer function. The transfer function of a transducer is the ratio of its Fourier transformed output to the transformed input causing that output. The magnification factor of a transducer's transfer function is the factor by which its zero frequency response must be multiplied to determine the magnitude of its steady state response at any given frequency.

The presence of multiple peaks in the transfer function of a transducer indicate a potential for problems when the transducer responds to a transient stimulus. The problem is more severe if the stimulus contains significant amplitude at frequencies near these peaks. Distortion of the recorded signal will occur.

While inverse problem treatment can often correct for signal distortion, limitations in experimentally characterizing the measuring transducer's transfer function prohibit its application in this work. The inverse problem consists of determining the corresponding excitation associated with a particular system model and a given response.

In some situations, the resultant signal may be conditioned by multiplexed data channels which do not possess adequate frequency response to reveal the presence of the distortion. As a result,

erroneous experimental data are frequently recorded and accepted for analysis.

The fact that erroneous data are accepted for analysis is generally because the data user does not know enough about the limitations of the measurement system. Similarly, the measurement engineer often does not know enough about the test requirements and the use and analysis of the data.

Figure I.1 is an acceleration record from an actual test on a structure. The amplitude range of the recording system was ±10,000 g (1 g = 9.8 m/s^2). The specified test accelerometer linear range was ±5000 g, with some over-range capability. Transfer characteristics of the recording channel were analogous to those of a low-pass RC filter with a -3dB frequency at 10,000 Hz. The response of the accelerometer was verified as flat over this 0 to 10,000 Hz frequency range. Initially, these data appear valid for mathematical model comparison and the generation of test specifications. In subsequent chapters, the data's validity will be investigated further. For future reference, this data channel will be identified as A5.

Development of this topic requires eight additional chapters. Chapter II introduces the subject of transient response and analysis of structures. Chapter III introduces measurement systems, with emphasis on special requirements for dynamic measurements. In Chapter IV the particular problem of interest is synthesized, and the work performed by previous researchers is reviewed. Chapter V illustrates this problem with "real world" data. Chapter VI describes limitations which prevent inverse problem treatment, and Chapter VII characterizes the resonant transducer model. Finally, in Chapter VIII techniques for optimizing the

instrumentation channel are investigated leading towards problem solution. Chapter IX summarizes the contributions of this work and indicates additional areas for productive research.

Two points should be emphasized. First, the experimental data for this topic are associated with ballistic armospheric reentry vehicles experiencing nuclear weapon effects testing. However, this should not overshadow the general applicability of the results to all structures which experience dynamic loading. Second, these experimental data contain only pressure and acceleration records; force data are excluded. This last point is not a limitation if the topic is understood. The common factor is that the measuring transducers are "resonant devices." This topic is developed around actual test data rather than contrived experiments. Reference 1 provides adequate examples of the applicability of this study to force measurements in such diverse environments as material test machines, mechanical die and drop forging equipment, and rocket thrust measurements.

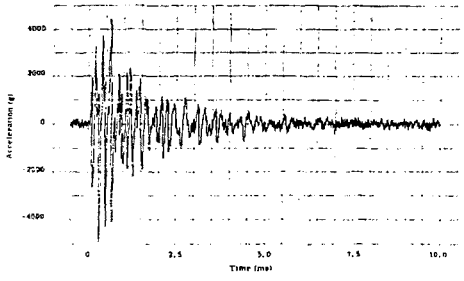

Figure I.1. Acceleration versus time from channel A5

CHAPTER II

INTRODUCTION TO TRANSIENT RESPONSE AND ANALYSIS OF STRUCTURES

Mechanical structural elements of interest to engineers for analysis include plates, beams, and shells. These structural elements are generally individual contributors to a more complex engineering system. In addition to these elements, the system typically contains a combination of joints, welds, bonds, fasteners, and coatings. Such a system can also be characterized by an assemblage of various materials such as metals, foams, rubbers, plastics, etc. These systems can be as diverse as aircraft, automobiles, reentry vehicles, or any of hundreds of other structurally complex items. A prime responsibility of the design engineer is to ensure that these systems maintain their structural integrity and perform reliably under the conditions of dynamic load which they will experience in service.

Some of the more severe examples of these dynamic loads are transient in nature and can be found in crash, impact, and blast environments. These environments may be characterized in one of two manners. Crash and impact environments are typified by a rapid change in momentum of the test system. Total linear impulse (LI) applied in time T over an area A^* of the system is:

$$LI = \int_0^T \int_0^{A^*} p(t,A)\,dA\,dt \qquad (II.1)$$

where $p(t,A)$ represents either pressure or stress as a function of both time and area. This linear impulse is usually delivered in a time which is short relative to the system structural response, enabling the system

forcing function to be represented as:

$$(L1)\,\delta(t) \qquad \text{(II.2)}$$

where $\delta(t)$ is the Dirac delta function. Blast environments are characterized not so much by their short durations as by the instantaneous loading produced by a compressional wave traveling through space. The common characteristics of all these environments are both the discontinuities and the high frequencies in the dynamic loading they impose upon the system.

Examples of this loading are numerous. Explosive devices are used in missiles and space vehicles to perform a variety of functions, including stage separation, jettisoning, launch separation, circuit switching, actuation, and propulsion ignition. When one of these devices is exploded, it induces loads and motions which propagate through the entire vehicle structure, including secondary structure and equipment. These loads and motions may result in mechanical failure or performance degradation of sensitive electronics and guidance equipment. Experiments and analysis on 1/4 inch and 3/8 inch diameter explosive bolts have documented that their associated force-time outputs are less than 12 microseconds in duration. The predicted pressure impulse on nose tips of a specific geometry at an impact velocity of 1000 feet/second is 35,000 taps (1 tap = 1 dyne-second/cm^2) for approximately 30 microseconds. The increasing government requirements for automobiles to withstand frontal crashes into stationary objects has led to crash barrier testing, with a typical approach generating a high frequency impact into a concrete wall. Blast waves propagated from gun muzzles impart severe transient loads to structures or personnel in the vicinity. Cold gas shock tubes,

used for aerodynamic as well as other experimental studies, are capable of producing shock waves with rise times of less than one microsecond. When a gas-tight diaphragm is burst in the shock tube, the high pressure gas released creates a shock wave which travels from the compression chamber into the expansion chamber. Reflections from the closed end of the compression chamber introduce additional compressional shocks.

Subsequent chapters analyze structural data acquired during nuclear effects simulation testing. This testing will provide a final example of blast and impulsive loading of engineering systems. Testing techniques have evolved in which mechanical effects simulation of these loadings is attempted by means of pulsed electron beams, magnetically or explosively driven flyer plates, and explosively driven shock tubes. Testing is performed to reduce weapons vulnerability and allow hardening against countermeasure effects.

To understand these mechanical effects, it is necessary to consider the categories of energy in a nuclear detonation. They consist of:

1. the kinetic energy of electrons, atoms, and molecules;
2. the internal energy of these same particles; and
3. the thermal radiation energy (this energy category is not significant in conventional chemical explosions because the temperatures involved are lower by four orders of magnitude).

The fraction of the nuclear explosion yield received as thermal energy at some distance from the burst point depends to some extent on the nature of the weapon, but primarily it depends on the environment of the

explosion. A typical energy distribution for an airburst of a fission weapon at an altitude below 100,000 feet is:[2*]

Blast and shock	50%
Thermal radiation	35%
Residual nuclear radiation from fission products which emit gamma and beta particles	10%
Initial nuclear radiation consisting primarily of gamma rays	5%

At higher altitudes, a greater percentage of the energy appears as thermal radiation and a lesser percentage as blast and shock due to the less dense atmosphere. Because of the high temperatures associated with nuclear explosions, 60 to 70 percent of this total radiation energy may be in the form of X-rays. In a lower altitude detonation, the low energy portion of these X-rays is absorbed by the atmosphere by conversion into kinetic and internal energy of the oxygen and nitrogen molecules.

During exoatmospheric flight of a reentry vehicle near a nuclear detonation, impulsive loadings are experienced by the reentry vehicle due to the lower energy X-rays being absorbed by the heat shield. This X-ray energy causes instantaneous heating of the surface material, resulting in very rapid spallation and vaporization of an outside layer. The rapid material "blow-off" results in an impulsive force being imparted to the vehicle structure. Flyer plates are typically employed to simulate this circumstance in experiments.

Vulnerability testing of the reentry vehicle through simulation attempts to answer the question of how much load a vehicle can take and still remain functional. Generally, impulses supplied to the vehicle are less than a few thousands taps. Transient loads imparted to the vehicle may be in the tens of kilobars region. After vulnerability

*Superscripts refer to numbers in bibliography.

testing is complete, static load deflection tests, vibration resonance surveys, or an actual vehicle flight may be performed to verify that functional integrity and reliability have been maintained.

Lethality testing is an attempt to simulate reentry vehicle failure criteria. The test objective is to determine how much load a vehicle can withstand before it is no longer functional. Impulse levels imposed may be tens of thousands of taps.

Within the atmosphere, the mechanical effects of a nuclear detonation consist primarily of blast waves transmitted through the air. Explosively driven shock tubes simulate this air blast event. In the shock tubes, not only is the total impulse in the air blast environment simulated but an attempt is made to duplicate the actual pressure-time profile. Since the energy deposited by the air blast is not instantaneous, reproducing the actual pressure-time profile also simulates the frequency content of the transient loads a vehicle may encounter in service. Figure II.1 illustrates the air blast front from a nuclear explosion traveling through space with time. At initial time, the blast front is still connected to the fireball. Figure II.2 illustrates a more complex airblast experienced at a point above ground level and attributable to a reflection from the earth's surface.

In any of the previously described loading situations where forces are applied for very short time periods or are rapidly changing, it is convenient to consider two different types of system response and analysis. The initial response of a structurally complex system to this loading will be defined as its material response. This is the response which lasts until waves propagating in the structure have essentially dissipated. Dependent upon the magnitude and rate of dynamic loading, as

well as the types of materials which comprise the structure, these waves may be elastic, viscoelastic, plastic, or shock.[54] The system response which occurs once wave propagation is no longer a consideration will be defined as structural response. Depending on the structure, this response may persist for one, tens, or hundreds of milliseconds. Dynamic analysis of a complex system to predict structural response treats it as an assemblage of a finite number of elements connected at a discrete number of nodes. The complete dynamics problem is defined only when both responses are considered.

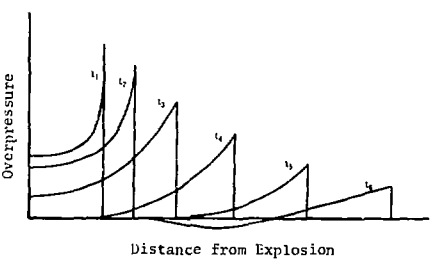

Figure II.1. Peak overpressure from nuclear blast showing breakaway from fireball

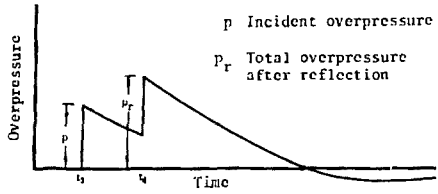

Figure II.2. Variation of overpressure at a point above earth's surface with reflection

Some care must be taken in applying the preceding distinctions. Geometrically simple continuous structures, such as long slender rods, could in theory have their wave propagation problem studied by adequate refinement of a finite-element approach. The distinction between structural and material response in this case would become meaningless. For the more complex structural systems of concern in this study, these special cases are of minor interest.

An initial discussion of material response will consider engineering materials as hydrodynamic solids. This assumption implies that strength effects, i.e., resistance to shear, are small enough to be ignored. Also implied is that the materials are of a single homogeneous phase. A further restriction will be to permit only plane waves in the material. This implies a condition of uniaxial strain with particle motion only in the direction of wave propagation. Uniaxial strain can be achieved in the central region of large flat plates for times shorter

than the time required for an elastic relief wave to propagate from the edge of the plate into this central region. Figure II.3 illustrates this occurrence. These restrictions focus interest on strong shock waves.

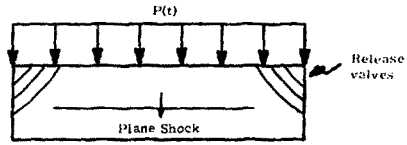

Figure II.3. Plane wave propagating through material

Shock waves result from the fact that most materials transmit sound at a speed which increases with increasing pressure. A compressional wave traveling in such a material will gradually steepen until it propagates as a jump or discontinuous disturbance called a shock. The speed with which a disturbance moves is denoted by:

$$c + u \qquad \text{(II.3)}$$

where c is the sound speed and u is the particle velocity or the velocity at which the material at the point of interest is moving. The speed with which the shock wave moves after formation is U. Once formed, the shock produces discontinuous jumps in density, pressure, particle velocity, energy, temperature, and entropy. Figure II-4 illustrates this process. Shock wave formation is evidence of nonlinear wave propagation. Since shock impedance is a function of pressure, superposition of solutions is not valid.

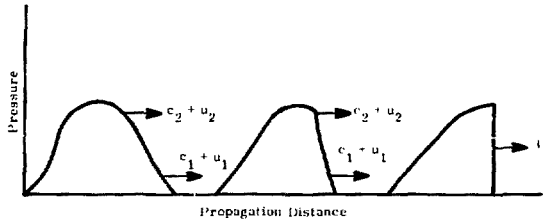

Figure II.4. Shock formation

In any shock front, there are two competing effects. A compressional wave is attempting to steepen into a discontinuity while viscosity and heat flow try to smooth it out. Once these effects cancel each other, the shock wave becomes steady. A stable shock propagates with velocity $U < c + u$. This prevents small perturbations at the shock front from being swept away by the flow.

In most materials, the same property of materials which causes compression waves to steepen causes release waves to spread; that is, increasing sound speed with pressure causes release waves to "fan." They must then be treated differently from shocks. The Rankine-Hugoniot[55] jump conditions relate the pressure, energy, and density of a material behind a shock traveling with velocity U to those same properties in the unshocked material across the shock front. These conditions are derivable from considerations regarding the conservation of mass, momentum, and energy. The state o refers to the unshocked material:

$$\frac{\rho_o}{\rho} = 1 - \frac{u - u_o}{U - u_o} \qquad \text{(II.4)}$$

$$P - P_o = \rho_o (U - u_o)(u - u_o) \qquad \text{(II.5)}$$

$$E - E_o = (1/2)(P + P_o)(v_o - v) \qquad \text{(II.6)}$$

where ρ is the density, u is the particle velocity, U is the shock velocity, P is the pressure, E is the energy, and v is the specific volume. If an equation of state is available for the material, $E = E(P,v)$, energy can be eliminated from Eq. (II.6), thus providing a locus of P,v states attainable behind a shock front. This locus of P,v states is the Hugoniot. The Hugoniot is derived experimentally by measuring any two of the four quantities (P,u,U,v). The jump conditions permit calculation of the other two quantities. This experimental work has established that almost all metals exhibit a linear relationship between shock velocity and particle velocity:

$$U = c_o + su \quad (s \approx 1.5) \qquad \text{(II.7)}$$

where c_o is the adiabatic sound speed for very weak shocks in a material. The Hugoniot then defines the locus of end states obtainable behind a shock front but also remains a good approximation to a relief isentrope along which unloading occurs.

A graphical analysis of a transient loading situation is presented to assist in problem development. The analysis involves blast loading of an "infinite" aluminum flyer plate one centimeter thick. The "infinite" assumption is made in order to satisfy the initial restriction of plane strain.

Detonating high explosives in contact with an inert material can produce shocks in the material. The use of flyer plates is a technique which achieves much higher pressures than are achievable by direct methods.

High explosives liberate energy in the form of heat when they detonate. When this happens, the gaseous products are raised to very high temperatures and, as long as they remain confined, very high pressures. A detonation wave passing through the high explosive initiates the chemical reaction, and the pressure produced continues to feed the shock so that it does not attenuate as it passes through the high explosive. At the instant a detonation wave has completely burned all the explosive, the explosive products are at the Chapman-Jouget (C-J) point;[56] that is, after detonation the products of the burned explosive are at a known pressure, density, and particle velocity.

Figure II.5 illustrates the left going curve for the explosion products of TNT. Note that the explosive products are at the C-J point. The intersection of the Hugoniot for aluminum, starting at zero pressure and particle velocity, with that for the detonation products occurs at state (2), which is the initial pressure and particle velocity imparted to the loaded surface of the flyer plate. At state (3), the shock wave in the aluminum has traversed the plate thickness and arrived at its front surface. At state (4), a rarefaction wave has traversed back to the loaded surface and again interacted with the detonation products. These reflections continue until the plate is traveling at zero pressure and uniform particle velocity; this occurs at approximately state (9).

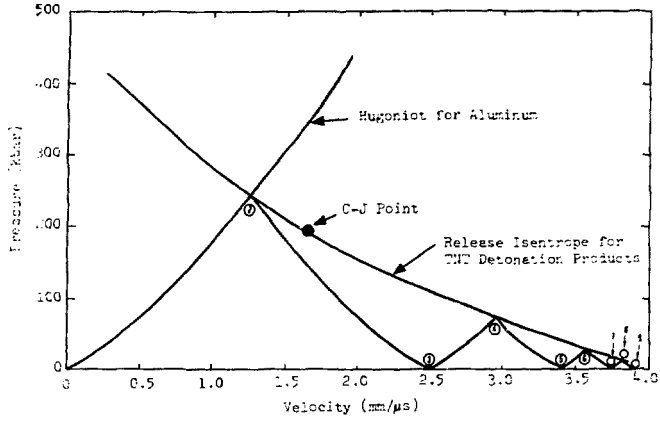

Figure II.5. Pressure versus particle velocity for aluminum plate explosively loaded by TNT

Figure II.6 illustrates the same process on a position-time plot. The assumption of an "infinite" amount of explosive allows the possibility of relief waves mitigating the blast front to be ignored over the time scale of the analysis. Figures II.7 and II.8 illustrate the velocity time and acceleration time history of the blast loaded surface of the aluminum flyer plate. Over the time interval that the velocity of the flyer plate is stepwise increasing, the rear surface pressure loading of the flyer is stepwise decreasing.

In the preceding example, the material response is of interest until the shock waves are attenuated. In more complicated situations, the shock waves may be attenuated by release waves and reflections in various materials, dissipated by viscous effects, and mitigated by lost

energy associated with the irreversible process of shocking a material. The time duration of response depends on material types and geometries but is on the order of microseconds, or at most tens of microseconds.

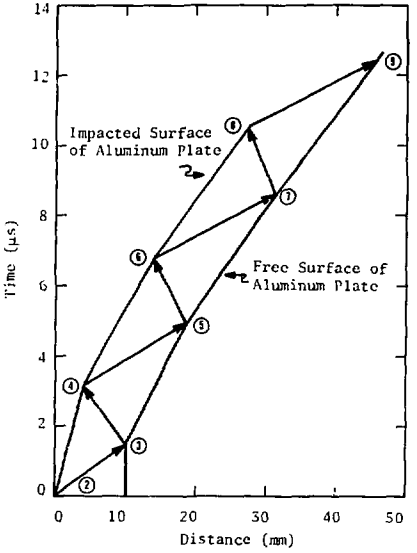

Figure II.6. Time versus position for aluminum plate explosively loaded by TNT

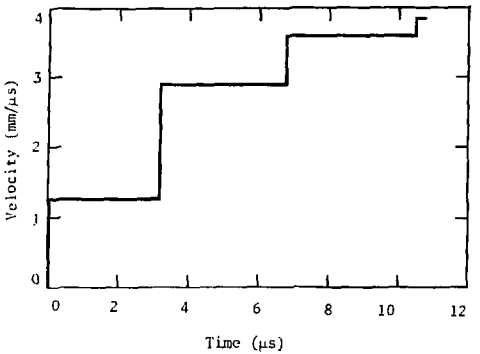

Figure II.7. Velocity versus time of loaded surface of aluminum plate interfacing TNT

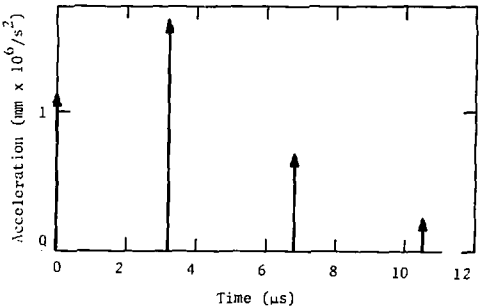

Figure II.8. Acceleration versus time of loaded surface of aluminum plate interfacing TNT

Material failure during this response mode occurs by spall. A spall occurs when a pair of free surfaces is created internally in a solid. Spall can be achieved if tension of sufficient magnitude is

produced when two rarefactions interact. Ultrasonic inspection after testing can check for the presence of spall if its effects are not externally evident.

The preceding example, as well as Figure II.2, illustrates several important points. In blast, crash, and impact environments, the loading process possesses step discontinuities, is impulsive in nature, and is complicated by reflected shocks. Material response of free surfaces to these environments can be typified by step discontinuities in material particle velocities with corresponding sudden acceleration impulses.

While illustrative, the preceding simple example of hydrodynamic shock does not indicate the complexity of the material loading and response of structurally more complicated systems in the type of environments being considered in this study:

1. Impact velocities may be lower, so that material strength cannot be ignored. This results in elastic precursor waves traveling in front of the plastic shock.
2. The loading does not produce a simple state of plane strain.
3. Complex geometries and various materials, as well as joints and welds in engineering systems, initiate multiple reflections of the waves.
4. Material properties may be rate sensitive.

The experimental determination of either wave propagation during system material response or pressure fronts associated with blast waves in gases requires measuring instruments or transducers which are characterized in terms of their own wave propagation properties. The experimental determination of system structural response, which is the ultimate concern of this work, requires measuring transducers which are

characterized in terms of their own structural response. This distinction is discussed in Appendix A.

It was previously indicated that structural analysis of mechanically complex engineering systems can be performed by treating the structure as an assemblage of a finite number of elements connected at a discrete number of nodes. The linear response of the structure at the element locations can be determined by the solution of the equations of motion of the system of finite-elements if the system of elements indeed represents the structure correctly.

For any system with generalized displacements q_i, generalized forces Q_i, and potential and kinetic energy functions of the respective forms:

$$V = \frac{1}{2}\bar{q}^T \underline{K}\bar{q} \tag{II.8}$$

$$T = \frac{1}{2}\dot{\bar{q}}^T \underline{M}\dot{\bar{q}} \ , \tag{II.9}$$

Lagrange's equations can be applied to derive the equations of motion. In some systems, T must be modified to include the effects of rotational kinetic energy expressed in Eulerian coordinates. Separating the nonconservative viscous forces from the generalized nonconservative forces allows these equations to be written

$$\underline{M}\ddot{\bar{q}} + \underline{C}\dot{\bar{q}} + \underline{K}\bar{q} = \bar{Q} \tag{II.10}$$

where:

$\underline{M}$ is the square inertia matrix whose elements M_{ij} represent the negative inertia force at point i in the system attributable

to a unit acceleration at point j with all other accelerations set equal to zero;

$\underline{C}$ is the square damping matrix whose elements C_{ij} represent the negative viscous force at point i in the system attributable to a unit velocity change at point j with all other velocities set equal to zero;

$\underline{K}$ is the square stiffness matrix whose elements K_{ij} represent the negative spring force at point i in the system attributable to a unit displacement at point j with all other displacements set equal to zero;

$\overline{Q}$ is a column matrix of nonconservative external forces acting on various elements of the system and ignoring viscous forces accounted for in the damping matrix; and

$\overline{q}$, $\dot{\overline{q}}$, and $\ddot{\overline{q}}$ are column matrices representing generalized system displacement, velocity, and acceleration.

Before Eq. (II.10) can be formulated, equations of motion for each individual element must be derived. The element equations of motion have the form:

$$\underline{m}\ddot{\overline{x}} + \underline{c}\dot{\overline{x}} + \underline{k}\overline{x} = \overline{f}\ (\text{internal}) + \overline{f}\ (\text{external}) \qquad (II.11)$$

where the coordinates $\overline{x}$ define each element's motion, $\overline{f}$ represents the force state on the element, and $\underline{m}$, $\underline{c}$, and $\underline{k}$ have the same significance to the element as their counterparts in Eq. (II.10) have to the system. The coefficients of the inertia and stiffness matrices are acquired by various techniques. One technique is to estimate these coefficients based on judgment and experimental data. The applied load is also discretized. The coefficients of the damping matrix are typically

ignored in the element equations and subsequently inserted as a linear combination of the system's mass and stiffness matrices in the system equations in order to provide modal damping.

More sophisticated techniques for determining the inertia and stiffness matrices and discretizing the applied load can be based on an integral energy formulation. This latter technique requires the assumption of some shape function for an element. The shape function is a polynomial of some assumed displacement field in terms of the nodal degrees of freedom. This shape function can be directly calculated or devised by intuition, trial, or familiarity with similar but simpler elements. As long as the assumed shape function is continuous, compatibility is satisfied within an element.

The coordinates for each individual element of Eq. (II.11) are then aligned for assembly in system space through some linear transformation:

$$\bar{x} = \underline{R}\bar{y}. \tag{II.12}$$

This substitution is made in Eq. (II.11), and a premultiplication is performed by $\underline{R}^T$; this results in a transformed element equation of motion. These elements are then reassembled based on geometric compatibility. A final linear transformation, reflecting this reassembly procedure, forms the system equations of motion given as Eq. (II.10). If some of the physical coordinates in Eq. (II.10) have specified displacements, the generalized displacement and force vectors can be partitioned into specified and unspecified segments. Specified forces correspond to unspecified displacements and vice versa. The static homogeneous equations may be used to relate the specified and unspecified coordinates. A matrix of static constraint modes can be

formulated to transform Eq. (II.10) so that the left hand side of the equality is always expressed in terms of only unspecified coordinates. The forcing function impressed on the model to simulate the earlier discussed transient environments may be based on the Dirac delta function or, where longer time durations are encountered, may require pressure or force-time data.

It should be noted that since this analysis is formulated for an engineering system containing continuously distributed mass and elasticity, the description of system motion requires an infinite number of independent coordinates. An infinite number of degrees of freedom, as implied by the number of independent coordinates, implies an infinite number of characteristic frequencies of vibration for the system. The effect of an analysis based on Eq. (II.10), where a continuous system is approximated by an n degree of freedom system, is to identify a maximum frequency above which experimental data do not support the mathematical model.

The fact that structural analysis should extend to some maximum upper frequency of interest agrees with insight into the physical problem. Since materials typically have loss factors[4] of 10^{-4} to 10^{-3}, damping of mechanically complex structures is dominated by joints. Damping resulting from the slippage of parts in a fabricated structure is denoted as slip damping. These frictional effects are not suited to analysis except under ideal conditions. As guidance to a designer, it may be convenient to define the damping in terms of equivalent viscous damping to allow estimation of the severity of a resonance. Some values are:[5]

Assembly Type	Equivalent Viscous Damping
Welded	0.02
Riveted	0.03
Bolted	0.04

The conclusion to be drawn is that damping exists in all physical systems. The value of this damping typically increases with frequency. For this reason, in any system there will exist some maximum upper frequency limit above which amplitude of structural response will become insignificant enough to be ignored.

If the matrix size in Eq. (II.10) is not excessive, the problem may be solved by direct integration. However, information is not acquired regarding system mode shapes or resonant frequencies. Usually, solution of Eq. (II.10) first involves solution of the free undamped vibration problem:

$$\underline{M}\ddot{\bar{q}} + \underline{K}\bar{q} = \bar{0} \ . \tag{II.13}$$

A solution form $\bar{q} = \bar{u}f(t)$ physically implies that coordinates perform synchronous motions and that the system configuration does not change its shape but only its amplitude during motion. The resultant eigenvalue problem has the form:

$$(\underline{M}\omega^2 - \underline{K})\bar{u} = \bar{0} \ . \tag{II.14}$$

Solution of the eigenvalue problem provides the n eigenvalues (ω^2), or characteristic frequencies of interest, along with the associated eigenvectors. The eigenvectors can be combined as $\bar{u}^1\bar{u}^2\ldots\bar{u}^n$ to form a modal matrix $\underline{B}$ so that when the linear transformation:

$$\bar{q} = \underline{B}\bar{z} \tag{II.15}$$

is performed in Eq. (II.10) and the equation is premultiplied by $\underline{B}^T$, the inertia matrix and stiffness matrix diagonalize through the property of orthogonality. It is at this point that a diagonalized modal damping matrix is typically inserted. The uncoupled equations, along with their transformed initial conditions, can be solved through numerical integration. The solution in physical coordinates then can be obtained through the transformation just presented by relating the physical or system coordinates $\overline{q}$ to the uncoupled coordinates $\overline{z}$ through the modal matrix $\underline{B}$. Acceleration, $\ddot{\overline{q}}$, is typically the response variable measured on the structural system to support analysis.

Slight variations in the analysis approach may occur. For example, a different form of the eigenvalue problem of Eq. (II.14) arises if the damping matrix is not proportional, implying that it is not a linear combination of the system mass and stiffness matrix. Similarly, gyroscopic moments introduce skew-symmetry into the damping matrix, requiring biorthogonal relations as opposed to orthogonal relations to uncouple the equations. The overall concept remains the same. Results of analysis include predictions for system frequency response, mode shapes, and time history of structural response.

Structural failure in this type of analysis is motion related. Excessive motion can produce failure which is predictable from the theory of elasticity. Motion can damage valving, sever tubing or electrical connections, and change thermal insulating properties. Motion of certain critical amplitudes or frequencies can cause premature electrical switching in circuits or otherwise reduce the performance reliability of control components within a system.

Summary and Conclusions

1. Numerous examples of transient loading associated with blast, crash, and impact environments have been identified in the transportation, aerospace, and ordnance industries. Additional examples also exist in other industries such as metal forming and construction.
2. The loading process in the referenced environments is impulsive in nature, is characterized by discontinuities in the forcing function, and is complicated by reflections.
3. The mechanical response of engineering systems in the referenced environments can be divided into two time regimes. The early time regime is characterized by the material response of the system. Structural response characterizes the system response in the later time regime.
4. Material response in the referenced environments is characterized by discontinuities in particle velocities with corresponding sudden acceleration impulses.
5. The structural response measurement parameters of interest are displacement, velocity, or acceleration. Acceleration is the response typically measured, while the loading function is determined by measuring applied force or pressure. If the transient load is applied in a time duration which is short relative to the period of the highest structural natural frequency, it may be approximated by the Dirac delta function.
6. Measurements conducted for comparison with structural analysis extend to some maximum upper frequency limit whose value is

limited by the discrete representation of the continuous system. In early testing, additional frequency bandwidth is allotted the data channel to allow for frequencies not predicted in the analysis process. The majority of data requirements are in the range of 10 to 2000 Hz. Only a few percent of requirements may be for frequencies as high as 10,000 Hz.[6] This frequency limit is considerably lower than the frequency content of the physical transient loading being considered.

CHAPTER III

INTRODUCTION TO MEASUREMENTS

Chapter II provided an introduction to the response and analysis of structures to transient loads. Those measurands which have to be determined to permit comparison between experimental data and the results of analysis were identified. The present chapter provides an introduction to the type of design considerations which must be made to acquire the needed measurements.

A measurand is the object of a measurement. It is the physical or chemical process to be measured. In structural response studies, typical measurands are force, pressure, and acceleration. The values of these measurands are usually acquired by transducers which transform them into electrical quantities.

A basic component of any instrumentation or measurement system is the transducer. The measurement transducer both transfers information about the process being measured and transfers energy from the process. A measurement system is a chain of transducers which links the measurand to the recorded data. Cables, attenuators, filters, amplifiers, digitizers, multiplexers, plotters, and other system components are transducers which can distort the signal intended to define the measurand.

In this work, two types of noise are distinguished. One type of noise is the ever present "spontaneous fluctuations" of voltage and current in the physical world. This type of noise represents a basic limitation in the transmission of information and is the subject of statistical treatment in communication theory. Any remaining distortion

of the signal which prevents it from defining the measurand is classified as measurement noise.

Every component within a measuring system will respond in every way it can to all variables in its environment. The total environment for a transducer contains both desired and undesired stimuli. The following paragraph elaborates on this distinction.

Various technical organizations, such as the Instrument Society of America, have sponsored committees that have written specifications and test guides[60] for different types of transducers. One such publication is ISA-RP37.2 1964, "Guide for Specifications and Tests for Piezoelectric Acceleration Transducers for Aero-Space Testing." Included within this document are specifications to minimize the response of accelerometers to such undesired stimuli as steady state and transient temperature, base strain, acoustic pressure, magnetic fields, humidity, radio interference, and nuclear radiation. Another Instrument Society of America publication is ISA-S37.10 1969, "Specifications and Tests for Piezoelectric Pressure and Sound-Pressure Transducers." It is interesting to note that while ISA-RP37.2 contains specifications to minimize the response of piezoelectric accelerometers to acoustic pressure, ISA-S37.10 contains specifications to minimize the response of piezoelectric acoustic pressure transducers to acceleration. One transducer's desired environmental stimulus then becomes another transducer's undesired environmental stimulus.

An undesired response from a transducer can even originate from its desired stimulus. For example, instruments such as accelerometers and force transducers are intended to be directionally selective in their response. Any signal generated by a transverse component of the desired

stimulus must then be considered to be noise. ISA-RP37.2 provides specifications against accelerometer response to transverse accelerations, while ISA-S37.8 1975, "Specifications and Tests for Strain Gage Force Transducers," provides specifications against force transducer transverse response to angular loads. A second example can be provided by the spurious electrical signal generated by strain gages encountering impact loading while without electrical power.

The objective of any measurement discussed in this study is to define either the loading to or the response of a structure as if the transducer were not there to disturb the process being investigated. Among other information, Chapter VI contains detailed descriptions of how the measurand can be modified by the presence of the transducer.

A generalized transducer has been modeled as a three-port, six terminal device.[7,8] Figure III.1 illustrates such a model. Real transducers can be synthesized from one or more of these devices. This basic model is adequate both for the following discussion and to develop techniques for noise documentation and suppression within the instrumentation system.

Physically, the ports in Figure III.1 represent boundary surfaces on the transducer across which information and energy are transferred. The terminals are a mathematical necessity to acknowledge the existence of two energy-related components at each port.

Inputs to transducers are measurands which are directly available. They require no activation. They are temporal or spatial functions of energy components or are energy components themselves. Two are required at each port of a transducer. Their product possesses dimensions of energy, energy rate, energy flux, etc.

One of the directly available measurands at each transducer port carries the information to be processed. The second measurand coexists because of physical necessity, and its effects are usually undesired. It is desired to measure the pressure loading of a structure without an accompaning volume change of the pressure transducer. Similarly, it is desired to measure mechanical force at impact with a transducer possessing infinite mechanical impedance. Any accompaning deflection of the force transducer is undesired. The impedance considerations of Chapter VI illustrate how the presence of the coexisting measurand *modifies the information carrying measurand.*

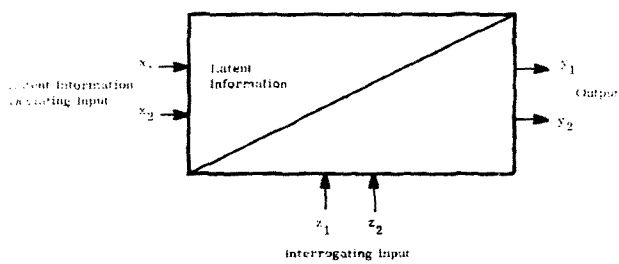

Figure III.1. Three-port, six-terminal transducer model

Contained within the transducer are indirectly available measurands (latent information) which must be activated or interrogated by some energy source. In Figure III.1, z_1 and z_2 represent inputs from an interrogating energy source. Similarly, x_1 and x_2 represent inputs at a port where the latent information is modified about some initial condition or operating point. At the remaining port, y_1 and y_2 are

outputs which transmit information and energy for processing elsewhere in the instrumentation system.

From this simple transducer model, two types of response can be produced. They include a self-generating and a nonself-generating response. Since piezoelectric and piezoresistive transducers are commonly used in structural dynamics measurements, they will be discussed in terms of the two response types. This discussion will also illustrate utilization of the transducer model.

In piezoresistive transducers, it is the nonself-generating response which is desired to be used. In this instance, the interrogating inputs z_1 and z_2 are voltage and current, both of which are controlled by design. For the specific example of a piezoresistive force transducer, the environmentally controlled inputs x_1 and x_2 are force and displacement which modify the resistance (latent information) about its initial condition and produce output voltage and current, which are represented by y_1 and y_2.

For piezoelectric transducers, it is the self-generating response which is desired to be used. The latent information takes the form of the piezoelectric coefficients of the particular material. Since x_1 and x_2 deviate the latent information, they must be controlled by design to maintain invariant piezoelectric coefficients during the test. Again using the specific example of a piezoelectric force transducer, the interrogating inputs z_1 and z_2 are force and displacement. The energy related components y_1 and y_2 at the output port represent charge and voltage.

Both of the latent information parameters (resistance = volts/amps $= \partial V/\partial I$, and piezoelectric coefficient = coulombs/newton $= \partial Q/\partial F$) are

expressed as partial derivatives since they are a function of more than one variable. In addition, they may also be nonlinear. These parameters therefore have specified values only at specified operating points. This explains why the performance of instruments in an actual environment may be considerably different from that which occurred in a calibration laboratory. The calibration laboratory often does not accurately duplicate the environment that the transducer encounters in application. An exact calibration would have to simultaneously expose the transducer to both the same level of desired environmental stimulus and the same level and combination of undesired environmental stimuli it will experience in service at the same boundary conditions of application. Reference 9 elaborates on this point in greater detail.

In any real transducer, both self-generating and nonself-generating responses are simultaneously present. For example, transducers using semiconductor strain gages typically have these gages interconnected by various materials into a spatially distributed electrical bridge network. Even with the bridge power removed, self-generating electrical output signals are still possible. These signals are attributable to different material properties and interfaces as well as the spatial distribution of the materials. Thermoelectric, electromagnetic, pyroelectric, piezoelectric, triboelectric, and photovoltaic effects are just a few of the possible signal sources still available even though the electrical power supplied to a transducer is removed.

Previously, it has been noted that a transducer can respond to desired and undesired stimuli in its environment. It was also noted

that its response type can be classified as either self-generating or nonself-generating. Its response evidence can be classified as either temporary or permanent.

An example of a temporary response is that exhibited by a piezoelectric transducer measuring the transient propellant chamber pressure in artillery motars and ammunition. For over 100 years, this same measurement has also been acquired by a different type of transducer using a spherical copper crusher deformed by an anvil face while in the chamber. The deformation of the copper crusher represents a permanent self-generating response whose magnitude is proportional to peak dynamic pressure.[10]

A second example which illustrates the permanent nonself-generating response of a transducer is the depolarization of certain piezoelectric materials by the passage of shock waves. Numerous other examples can also be provided.

In any measurements application, it must be documented that the desired environmental response combination (signal) has been recorded. It is not possible to have prior knowledge of every hostile environment the measuring system will encounter nor every manner in which it can respond to these environments. Signal validation then involves either the concept of redundant or check channels or sequential switching circuits to determine the presence or absence of noise. References 11 and 12 identify documentation techniques for noise levels and also describe techniques for implementing these check channels.

An obvious problem is encountered when noise is present to the extent that it significantly degrades signal quality within the instrumentation system. Methods for suppressing this noise must then be

considered in order to improve the system's dynamic range. The dynamic range is the ratio of the linear channel range to the channel noise level.

Figure III.2 schematically represents a constant current model for a transducer having both self-generating and nonself-generating responses. In this figure, v represents the transducer's self-generating response to the environmental stimuli and R represents its nonself-generating response to these stimuli when interrogated by (I - i). D symbolizes a desired environmental stimulus, and U symbolizes all undesired environmental stimuli. The differential transducer output voltage can be expressed in a Taylor series as:

$$dv = (I - i)\, R\left[\frac{1}{R}\frac{\partial R}{\partial D}\,dD + \frac{1}{R}\frac{\partial R}{\partial U}\,dU + \frac{1}{2R}\frac{\partial^2 R}{\partial U^2}\overline{dU}^2 + \frac{1}{2R}\frac{\partial^2 R}{\partial D^2}\overline{dD}^2 - \frac{1}{2R}\frac{\partial^2 R}{\partial U \partial D}\,dD\,dU + \frac{1}{2R}\frac{\partial^2 R}{\partial D \partial U}\,dU\,dD + \ldots\right] + \left[\frac{\partial v}{\partial D}\,dD + \frac{\partial v}{\partial U}\,dU + \frac{1}{2}\frac{\partial^2 v}{\partial U^2}\overline{dU}^2 + \frac{1}{2}\frac{\partial^2 v}{\partial D^2}\overline{dD}^2 + \frac{1}{2}\frac{\partial^2 v}{\partial U \partial D}\,dD\,dU - \frac{1}{2}\frac{\partial^2 v}{\partial D \partial U}\,dU\,dD + \ldots\right]. \qquad \text{(III.1)}$$

This output voltage is seen to be attributable to both response types. The signal, depending on whether the desired response is self-generating or nonself-generating, is either the $(I - i)\,(\partial R/\partial D)dD$ term or the $(\partial v/\partial D)dD$ term. All other terms are measurement noise.

The final response classification categorizes a transducer's response effects as being either additive or multiplicative. A force

transducer using semiconductor strain gages and operating in a nuclear radiation environment produces an additive output that it is hoped is attributable to force. The undesired environment (nuclear radiation), however, may change the basic sensitivity of the force transducer by disturbing the atomic lattice of the semiconductor material. This sensitivity change represents a multiplicative effect.

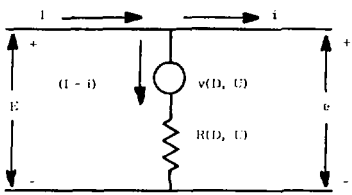

Figure III.2. Model of transducer possessing both a self-generating and a nonself-generating response

It is now convenient to summarize the preceding environment/-response combinations systematically. Every transducer has its response characterized according to the following four classifications.

1. Environmental stimuli (desired or undesired)
2. Response type (self-generating or nonself-generating)
3. Response evidence (temporary or permanent)
4. Response effect (additive or multiplicative)

Based on these classifications, there are 16 environmental response combinations. Only one of the 16 combinations uniquely represents the measurand. The other 15 combinations undesirably influence the signal producing measurement noise. In the situation previously described for a

piezoelectric pressure transducer measuring propellant chamber pressure, signal is defined as the additive, temporary, self-generating response to the pressure environment.

The methods available for measurement noise suppression are those which minimize or eliminate the undesired terms from the Taylor series. For example, the self-generating response can be separated from the nonself-generating response in the frequency or time domain by information conversion. This conversion requires application of a sine wave or pulse power supply to an impedance based transducer (such as a piezorestive type) and results in an amplitude modulated signal. For transducers measuring transient pressures, undesired heating from a hot gas environment can be eliminated by a thermal shield on the transducer diaphragm ($dU \cong 0$). Some piezoelectric materials used in force, pressure, and acceleration transducers can be formulated to permit operation over a wide range of temperature ($\partial^2 v/\partial U \partial D \cong 0$). In blast environments, the amplifier input can remain shorted until the noise pulse resulting from the electrical firing set which ignites the explosive has ended. This prevents any interrogating input to the amplifier ($(I - i) = 0$). Since all terms in the Taylor series are frequency dependent, either electrical or mechanical filtering may be able to separate them. A systematic approach to noise suppression based on this Taylor series is documented in References 8 and 11.

Additional requirements are placed on measurement systems intended to record dynamic data without distortion. One such requirement is for a linear channel input versus output relationship. For data whose time

history is important, a requirement also exists for a channel transfer function with a flat amplitude-frequency and a linear phase-frequency response.

If a system is linear, it can be characterized by a linear differential equation. Linear systems satisfy the principle of superposition. For instance, in a linear system if $o_1(t)$ results from the application of $i_1(t)$ and $o_2(t)$ results from the application of $i_2(t)$, then $ao_1(t) + bo_2(t)$ results from the application of $ai_1(t) + bi_2(t)$. One simple check for linearity in measuring systems is to change the system's balance or operating point. A change in output waveform of an initially applied signal indicates a nonlinear system.

The requirement for a linear channel input versus output relationship to preclude distortion of dynamic data is verified by the following argument. The symbol i represents system input, and o represents system output. It is arbitrarily assumed that a third order polynomial relationship exists between input and output. This may be expressed as:

$$o = ai + bi^2 + ci^3 \quad . \tag{III.2}$$

The input i can be of a single frequency so that:

$$i = \sin\omega t \quad . \tag{III.3}$$

The output o is then:

$$o = a \sin \omega t + b \sin^2 \omega t + c \sin^3 \omega t \quad . \tag{III.4}$$

Applying a power relation to the higher order sine functions results in:

$$o = a \sin \omega t + b/2\,(1 - \cos 2\omega t) + c/4\,(3 \sin \omega t - \sin 3\omega t) \quad . \qquad \text{(III.5)}$$

The nonlinearity has resulted in second and third harmonics of the input as well as a dc component. The cubic term has even resulted in a contribution at the system input frequency. The fact that nonlinear systems distort dynamic data through a frequency creative process will be referred to numerous times in subsequent chapters of this work.

It last remains to justify why both a flat amplitude and a linear phase versus frequency response are necessary to preclude distortion of data whose time history is of interest. System input will be represented by $i(t)$ with its corresponding Fourier transform $I(j\omega)$. System output will be represented by $o(t)$ with its corresponding Fourier transform $O(j\omega)$. A transfer function with flat amplitude response and linear phase characteristics can be represented as:

$$H(j\omega) = A\, e^{-j\omega T} \quad , \qquad \text{(III.6)}$$

where A and T are constants. For a linear system, the relationship between input and output can be expressed as:

$$O(j\omega) = AI(j\omega)\, e^{-j\omega T} \quad . \qquad \text{(III.7)}$$

System output $o(t)$ is then:

$$o(t) = \frac{A}{2\pi} \int_{-\infty}^{\infty} I(j\omega)\, e^{j\omega(t-T)}\, d\omega \qquad \text{(III.8)}$$

or

$$o(t) = Ai(t - T) \quad . \qquad \text{(III.9)}$$

For this situation, the output is a scaled time delay replica of the input.

When any signal becomes distorted due to measurement noise, this distortion can, in theory, be corrected if the response of the measuring system to the noise source is time invariant. Time invariance in this connotation implies that once characterized the system response to a given measurement noise source remains fixed over its time interval of application. For example, assume a given measurement system responds to temperature in addition to its desired measurand. If the measurement system is time invariant, if its thermal response can be characterized, and if temperature is recorded as a separate measurement during the experiment, the distorted signal can be corrected.

In general, even if a measurement system is time invariant, any of four factors can prevent correction of a recorded signal to account for distortion. They are:

1. Inability to identify the cause of the distortion,
2. Inability to properly quantify the cause of the distortion,
3. Inability to characterize the relationship between the measurement system and the cause of the distortion, and
4. The presence of "spontaneous fluctuation" noise.

The combined tolerances of these four factors must also be considered.

Summary and Conclusions

1. The design of measuring systems can be conducted in a methodical and analytical manner to acquire meaningful data the first time. Noise documentation and suppression is required to assure that

the recorded signal represents the desired environmental response combination.

2. Measurement system requirements to prevent distortion of data whose time history is of interest include:
   a. a linear input versus output relationship,
   b. flat amplitude-frequency response, and
   c. linear phase-frequency response.
3. Signals are undesirably influenced by either or both measurement noise and "spontaneous fluctuation" noise. In theory, distortion attributable to measurement noise can be corrected if the measuring system is time invariant. In practice, these corrections can not always be applied.

CHAPTER IV

PROBLEM DEVELOPMENT

All transducers containing mechanical flexures can be described as resonant devices. Resonant devices are dynamic systems possessing multiple peaks in the magnification factor associated with their transfer function. The transfer function of a transducer is the ratio of its Fourier transformed output to the transformed input causing that output. The magnification factor of a transducer's transfer function is the factor by which its zero frequency response must be multiplied to determine the magnitude of its steady state response at any frequency. Transducers used to measure structural dynamics are resonant devices.

The presence of multiple peaks in the transfer function of a transducer indicates a potential for problems when the transducer responds to a transient stimulus. The problem is more severe if the stimulus contains significant amplitude at frequencies near these peaks. Distortion of the recorded signal will occur.

The preceding chapter stated that if a transducer's response was time invariant, distortion attributable to measurement noise could in theory be corrected. If the transducer's transfer function was completely characterized, the data distortion could be treated as an inverse problem. The inverse problem consists of determining the corresponding excitation associated with a particular system model and a given response.

The present chapter begins specific problem development. It will subsequently be demonstrated that the measurement of structural dynamics cannot be treated as an inverse problem. Regardless of this limitation, problem solution will ultimately be achieved.

The dynamic model most frequently presented in literature for force, pressure, and acceleration transducers is that of a single degree of freedom system which is characterized by a linear second order differential equation with constant mass (m), damping (c), and stiffness (k) coefficients. Figure IV.1 illustrates such a model subjected to harmonic excitation. For a force or pressure transducer, x represents the absolute motion of the mass. For an accelerometer, x represents the relative motion between mass and base. The governing equation for either situation has the form:

$$m\ddot{x} + c\dot{x} + kx = Ke^{j\omega t} \quad . \tag{IV.1}$$

In this equation, energy dissipation is assumed to occur by viscous damping. Mass motion is resisted by a force that has a magnitude proportional to the magnitude of the velocity and is in a direction which opposes motion.

Another technique to account for internal damping in linear structures involves treating the elastic constants governing vibration as complex quantities. For a one-dimensional stress distribution, the relationship between stress (σ) and strain (ϵ) can be expressed as:

$$\sigma/\epsilon = E(\omega,\theta)[1 + j\delta(\omega,\theta)] \quad , \tag{IV.2}$$

where ω represents frequency and θ represents temperature. $E(\omega,\theta)$ represents the real part of the complex Young's modulus, and $\delta(\omega,\theta)$ is the loss factor or ratio of the imaginary to the real part of the complex modulus.

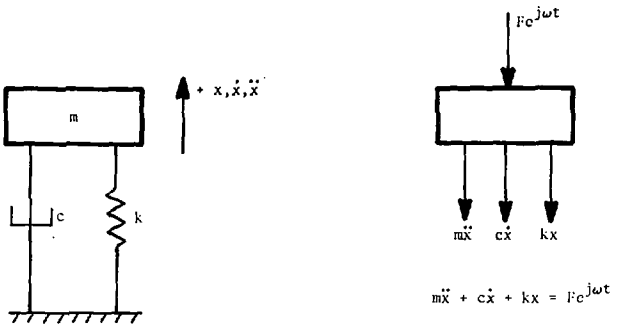

Force or pressure transducer

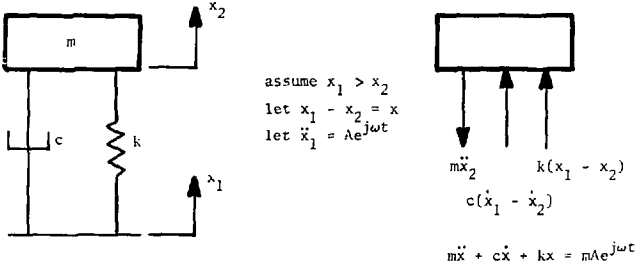

Accelerometer

Figure IV.1. Elementary dynamic model for force transducer, pressure transducer, and accelerometer

Hysteretic damping is one method which can be used to describe the internal damping of metals. The modulus is assumed to be independent of

both frequency and temperature over the range of interest so that:

$$\sigma/\epsilon = E(1 + j\delta) \quad . \tag{IV.3}$$

For all transducers which have metal sensing mechanisms, hysteretic damping can be incorporated into the governing differential equation for the transducer's dynamic response. The resultant equation has the form:

$$m\ddot{x} + k(1 + j\delta)x = Ke^{j\omega t} \quad . \tag{IV.4}$$

A typical value for the maximum magnification factor of the transfer function of a pressure, force, or acceleration transducer is 50. Figure IV.2 plots the magnitude of the transfer function as determined from each of the two preceding differential equations which incorporate viscous and hysteretic damping. Parameters within each equation are adjusted to achieve this maximum magnification factor of 50. The abscissa is normalized to the undamped natural frequency, defined as $(k/m)^{1/2}$, while the ordinate is normalized to the value the transfer function possesses at zero frequency. The two transfer functions superimpose on one another so that it is not readily apparent that Figure IV.2 actually contains two plots.

Figure IV.3 plots the phase angle associated with each transfer function. The phase angle identifies the number of degrees by which the transducer output lags its input. The abscissa is normalized to the undamped natural frequency as in Figure IV.2. The phase plots for the two transfer functions also superimpose on one another. In Figures IV.2 and IV.3, the transfer functions are computed for a viscous damping factor $c/(2(km)^{1/2})$ equal to 0.01 and a loss factor equal to 0.02. These transfer functions are applicable to any linear second order system where m, c, and k represent equivalent coefficients of the time derivatives of the secondary or dependent quantities.

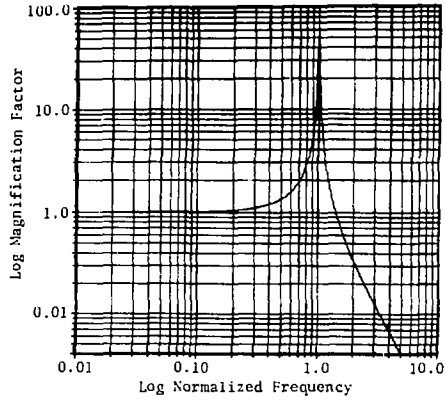

Figure IV.2. Linear second order system amplitude-frequency response for either 0.01 viscous damping factor or 0.02 loss factor

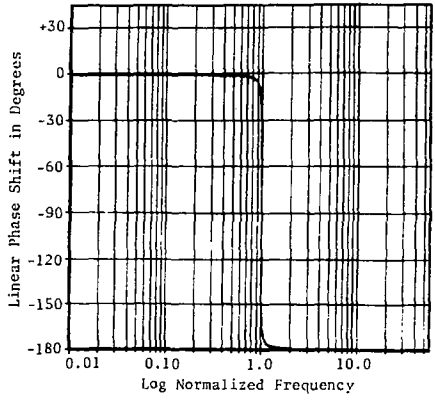

Figure IV.3. Linear second order system phase-frequency response for either 0.01 viscous damping factor or 0.02 loss factor

The preceding discussion has demonstrated that as long as its magnitude remains small, the type of damping placed in the transducer model is of little consequence. In discussions involving this simple dynamic model, viscous damping will arbitrarily be assumed.

An inconsistency exists in the literature between the simple single degree of freedom dynamic model described by the preceding equations and the physical models of the sensing mechanisms of various transducers illustrated in Figure IV.4. The top portion of Figure IV.4 illustrates six types of diaphragm designs found in pressure transducers. A flat diaphragm is the simplest form of pressure receiver and deflects in accordance with theories applicable to circular plates. Annular diaphragms include the addition of a central circular reinforcement to facilitate the transition of diaphragm deflection into a subsequent mechanical displacement. The central portion of Figure IV.4 illustrates both rod or column and beam type sensing elements found in accelerometers. Four resistance strain gages are mounted on each element so that at any time two are operating in tension and two in compression. The beam is notched to provide strain amplification to gages mounted on its surfaces. The lower portion of Figure IV.4 provides cross-sectional views of piezoelectric accelerometers with piezoelectric elements operating in a bending and a shear mode. Also illustrated in these lower views are the accelerometer housing, connector, and mounting base.

When discussing systems comprised of the beams, plates, and columns of Figure IV.4 assembled within some housing, the continuous nature of the system response must be emphasized. The validity of the commonly used single degree of freedom dynamic model for the transducers of interest must be questioned.

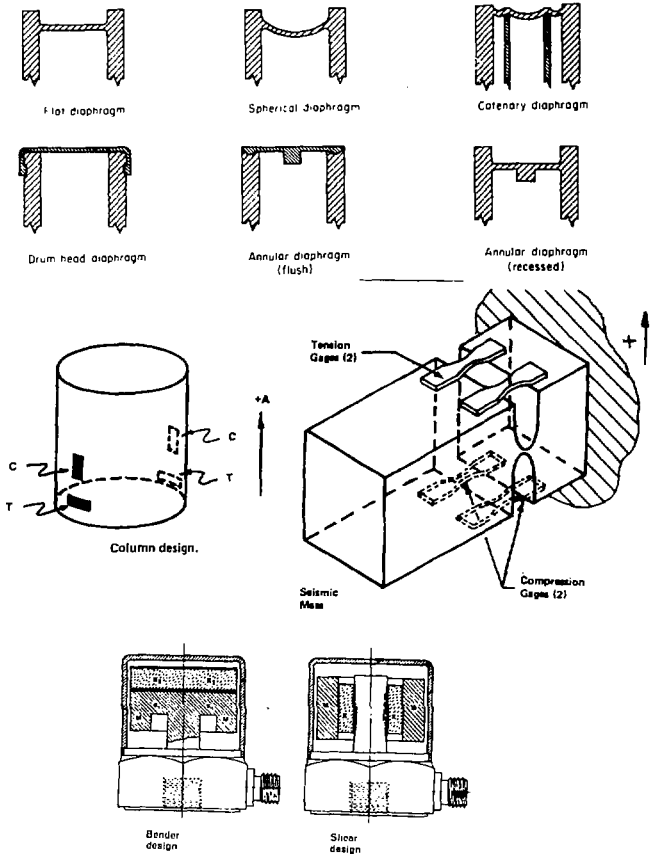

Figure IV.4. Sensing mechanisms of various transducer types

A transfer function will be computed for the circular rod or column in Figure IV.4 by analyzing it as a continuous element. The rod will be assumed to have a large length-to-diameter ratio. Its cross sectional area will be denoted as A and its length as l. An analysis will be performed for the rod in tension with one end fixed and the other end driven by a harmonic force $P\cos\omega t$.

The partial differential equation governing the rod's free vibration is:

$$\frac{\partial^2 u}{\partial x^2} = \frac{1}{c^2}\frac{\partial^2 u}{\partial t^2} \quad . \tag{IV.5}$$

In this equation, u is rod particle motion, x is the longitudinal rod coordinate, t is time, and c^2 is the ratio of Young's modulus to the mass density of the rod material or E/ρ. Boundary conditions for the particular problem are:

$$u(o,t) = 0 \tag{IV.6}$$

and

$$EA\frac{\partial u(l,t)}{\partial x} = P\cos\omega t \quad . \tag{IV.7}$$

The transfer function of the rod is the ratio of the displacement of its harmonically excited end to the displacement of this same end under an applied static load P. The magnitude of this computed transfer function is:

$$\frac{c}{l\omega}\left|\frac{\sin\omega l/c}{\cos\omega l/c}\right| \quad . \tag{IV.8}$$

Figure IV.5 plots the magnitude of the transfer function with the abscissa normalized to the rod's fundamental resonant frequency and the

ordinate normalized to the static deflection. For more complex transducer sensing elements, these resonant frequencies are not harmonically related.

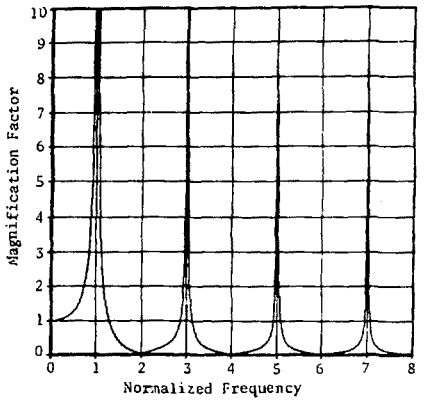

Figure IV.5. Amplitude-frequency response of a thin rod fixed at one end and harmonically excited at the other

Of significance in Figure IV.5 is the fact that the continuous model of a transducer sensing element indicates the presence of multiple resonant frequencies or eigenvalues. The simple dynamic model discussed earlier allows just one. It is then desired to determine if this continuous model represents any improvement over the simple model.

One method of evaluating the validity of this continuous model is to determine if the response it predicts to a given initial condition is consistent with intuition. With one end of the rod still fixed, the free end can be stretched from its undeformed length l to some new length l' and then released. Boundary conditions for the rod are:

$$u(o,t) = 0 \tag{IV.9}$$

and

$$\frac{\partial u(l, t)}{\partial x} = 0 \ . \tag{IV.10}$$

Initial conditions for the rod are:

$$u(x, o) = \frac{(l' - l)x}{l} \tag{IV.11}$$

and

$$\frac{\partial u(x, o)}{\partial t} = 0 \ . \tag{IV.12}$$

The solution for the displacement response at the rod's free end is:

$$u(l, t) = \frac{8(l' - l)}{\pi^2} \sum_{n=1, 3, 5, \ldots}^{\infty} \frac{(-1)^{[(n-1)/2]}}{n^2} \sin \frac{n\pi}{2} \cos \frac{cn\pi t}{2l} \ . \tag{IV.13}$$

This displacement response is plotted in Figure IV.6. The particular plot is for a one-inch long steel rod which could represent a size consistent with a transducer's sensing element. The ordinate of the plot is normalized to $8(l' - l)/\pi^2$. The abscissa extends over a period of 200 microseconds. Only the first eight modes of response are summed in Figure IV.6. Response modes above the eighth contribute less than 0.5 percent of that of the first mode.

Results of Figure IV.6 are not consistent with the manner in which physical systems respond. The amplitude of the rod's response does not decay with time. Neither do the high frequency modes damp out, as indicated by the sharp peaks on each half-cycle of response. The undamped continuous model of the transducer also appears invalid, as did the simple dynamic model described earlier.

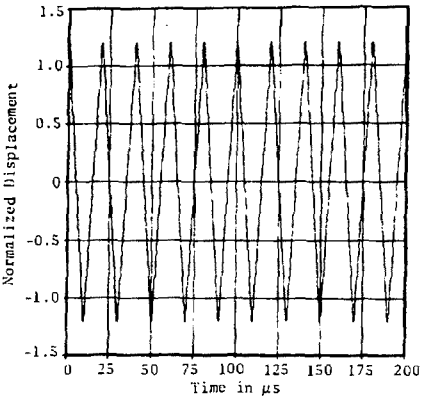

Figure IV.6. Vibration response of free end of one-inch long undamped thin steel rod fixed at one end and initially displaced at the free end

A final attempt to improve this continuous model will include within it the addition of some damping mechanism. One way of including this damping is to express the stress-strain relationship for a material as:

$$\sigma = E\epsilon + \eta\dot{\epsilon} \quad . \tag{IV.14}$$

The parameter η is a constant to be defined. Materials defined by this form of stress-strain relationship are denoted as Kelvin solids.

Finally, a rod treated as a Kelvin solid will be evaluated for its initial condition response when its free end is displaced and then released. Boundary and initial conditions remain unchanged. The partial differential equation, by virtue of the new stress-strain relationship, becomes:

$$E\frac{\partial^2 u}{\partial x^2} + \eta\frac{\partial^3 u}{\partial x^2 \partial t} = \rho\frac{\partial^2 u}{\partial t^2} \quad . \tag{IV.15}$$

The displacement response for this free end can again be solved. Rather than writing out the equation for this response, since results become more tedious, the response is plotted as Figure IV.7. The plot is again for a one-inch steel rod, and the parameter η has been adjusted to correspond to a 0.01 viscous damping factor in the first mode. The plot is scaled the same as is Figure IV.6.

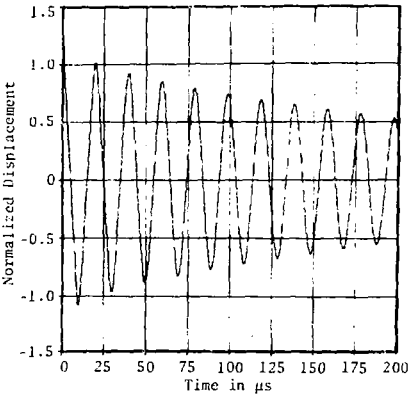

Figure IV.7. Vibration response of free end of one-inch long damped thin steel rod fixed at one end and initially displaced at the free end

Figure IV.7 is consistent with the manner in which physical systems respond. The sharp peaks on the first one or two cycles of response indicate that high frequency modes are initially present. These higher modes soon damp out, and with increasing time the motion of the rod end

appears more nearly sinusoidal. In addition, the response decays with increasing time, as is characteristic of real physical systems. This shows that transducers do not possess a transfer function as elementary as the one presented for them in literature. Instead, the transfer function may well contain multiple resonant peaks and damping.

The preceding conclusion can also be arrived at by considering other types of transducer sensing elements. Beam elements are characterized by a higher order partial differential equation which governs their dynamic response. The equation for free beam vibration, to include a Kelvin solid stress-strain relationship, becomes:

$$EI\frac{\partial^4 y}{\partial x^4} + \eta I\frac{\partial^5 y}{\partial x^4 \partial t} + \rho A\frac{\partial^2 y}{\partial t^2} = 0 \ , \qquad \text{(IV.16)}$$

Additional parameters to be defined in this equation include the beam cross-sectional area moment of inertia I, its transverse motion y, and its mass per unit length, ρ.

The beam's vibration equation can be solved for the response of the free end of a cantilevered beam which is initially deflected and then released. The parameter η can again be adjusted to provide a 0.01 viscous damping factor to the first vibrational mode. Because the solution becomes lengthy and provides little additional information, it is not stated here. Although the beam resonant frequencies are not harmonically related, the response predicted and the conclusions which result from it are consistent with those based on the rod response of Figure IV.7.

With the preceding discussion as background, it is desired to investigate the transfer function of some actual transducers. Figure IV.8 illustrates the instrumentation setup used to determine the

transfer function of a group of accelerometers. Test results are presented in Figure IV.9 through IV.12. Both the sweep rate and the amplitude of vibratory input were limited during testing to assure the validity of these transfer functions. For reasons which will be detailed in following chapters, Figures IV.9 through IV.12 are quantitative in amplitude to 10,000 Hz but only qualitative at higher frequencies.

Figures IV.9 and IV.10 present experimentally determined transfer functions for two typical piezoelectric accelerometers. Each figure contains a single major resonant frequency. Both also contain minor disturbances in the transfer function before this major resonance. These minor disturbances are not valid data, as evidenced by the fact that they are harmonically related to the major resonance. They are attributable to some small amount of harmonic distortion in the input sinusoidal forcing function.

The elementary, single degree of freedom dynamic model for a transducer would appear adequate if an opinion were based only on Figures IV.9 and IV.10. However, Figure IV.11 illustrates the transfer function for an accelerometer that possesses minor resonances that occur before its major resonant frequency. Since these minor resonances are not harmonically related to the major resonance, it is highly unlikely that they are attributable to test technique but should be valid data. Figure IV.12 illustrates the transfer function for another accelerometer for which a major resonance occurs low enough in frequency that the test setup is capable of demonstrating the presence of two additional resonances at higher frequencies. Both Figures IV.11 and IV.12 demonstrate the concept that transducers possess a dynamic response which is characterized by a continuous system model.

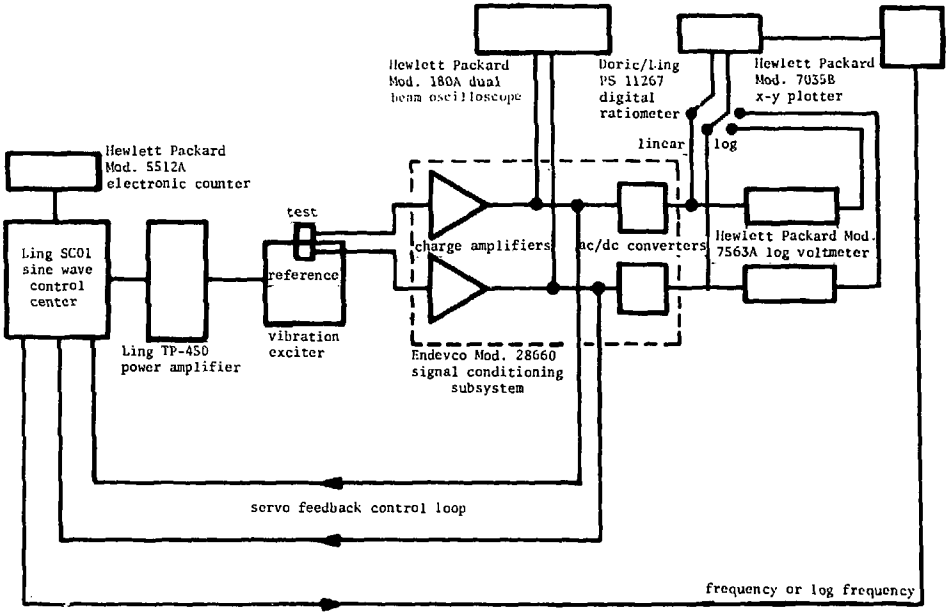

Figure IV.8. Ling-Endevco System 50 instrumentation schematic

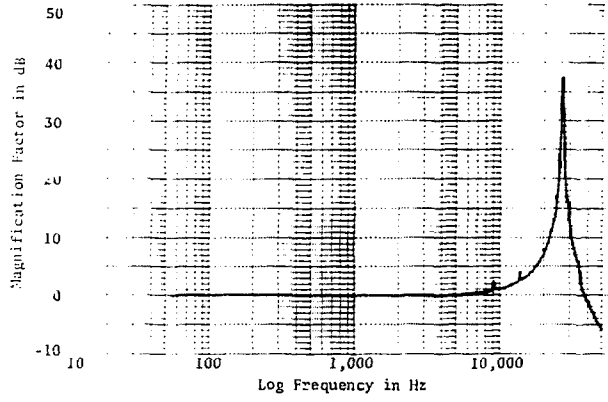

Figure IV.9. Magnitude of transfer function of piezoelectric accelerometer containing single piezoelectric element

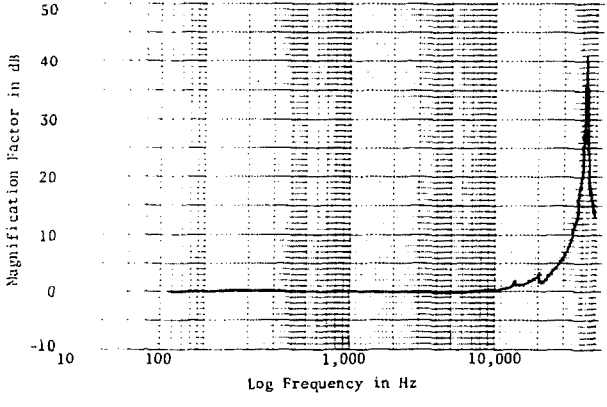

Figure IV.10. Magnitude of transfer function of piezoelectric accelerometer containing quartz crystal stack

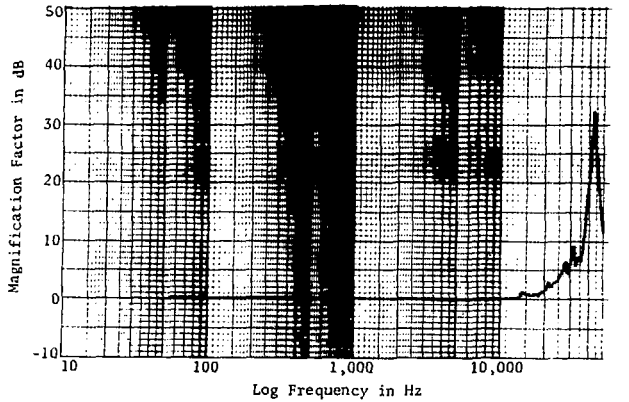

Figure IV.11. Magnitude of transfer function of piezoresistive accelerometer containing beam type sensing element

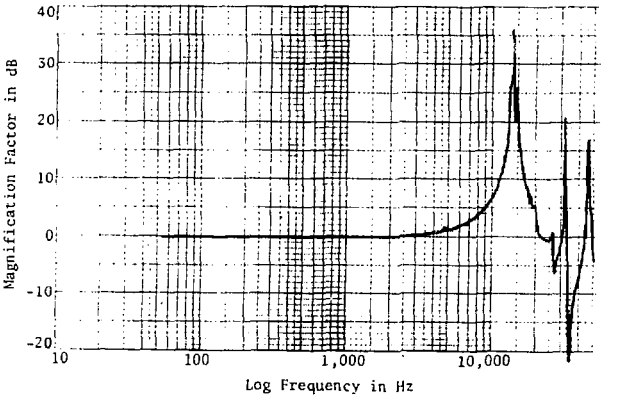

Figure IV.12. Magnitude of transfer function of piezoresistive accelerometer illustrating resonant frequencies above its major resonant frequency

Figures IV.13 and IV.14 illustrate the time response of two pressure transducers. These transducers were monitoring the step pressure achieved in a closed end helium to air shock tube. The instrumentation system used to record and digitize these responses is similar to that shown in Figure V.5 in the following section. An approximate transfer function can be derived from each of these time responses and is presented as Figures IV.15, IV.16, IV.17, and IV.18. The computer program TRANFUNC, which was used to approximate these transfer functions, as well as shock tube theory, are discussed in Chapter VI.

The data in both Figure IV.13 and Figure IV.14 were acquired by sampling 1024 points over a 0.002-second time interval. Figures IV.15 and IV.17 reveal major resonant frequencies at approximately 21,000 Hz and 45,000 Hz, respectively. The presence of minor resonances in addition to these major resonances again confirms that a transducer's dynamic response is characterized by a continuous system model.

Subsequently, it will be necessary to discuss limitations which occur when dynamically characterizing the type of transducers of interest. The present discussion has emphasized only that the transfer function of these devices contains multiple resonances, with one resonance typically dominant.

It is next desired to illustrate the potential for error when measuring transient phenomena with such resonant devices. Initially, the elementary dynamic transducer model of Figure IV.1 will be used. The preceding experimental data indicated that 0.01 was a reasonable viscous damping factor to insert into this model to allow problem development.

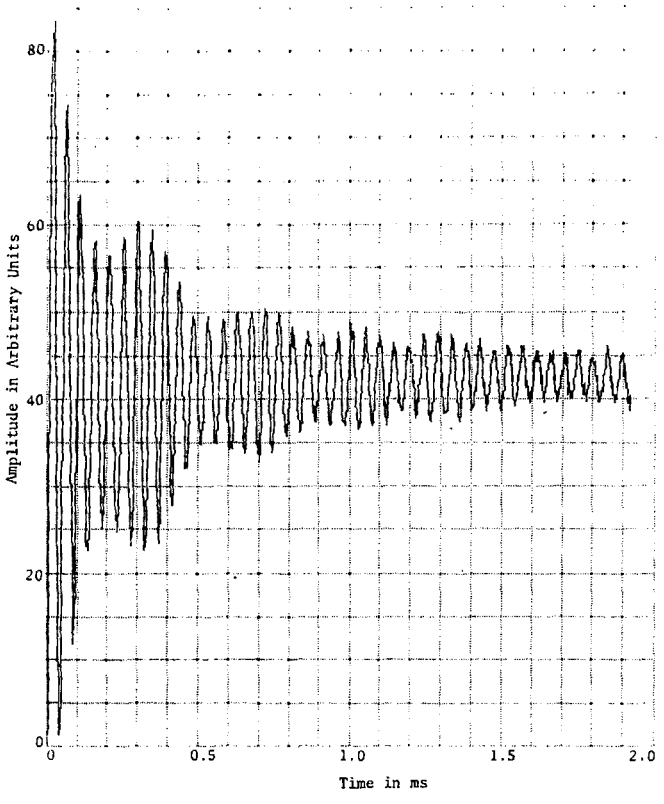

Figure IV.13. Shock tube step response of flush diaphragm metallic strain gage type pressure transducer

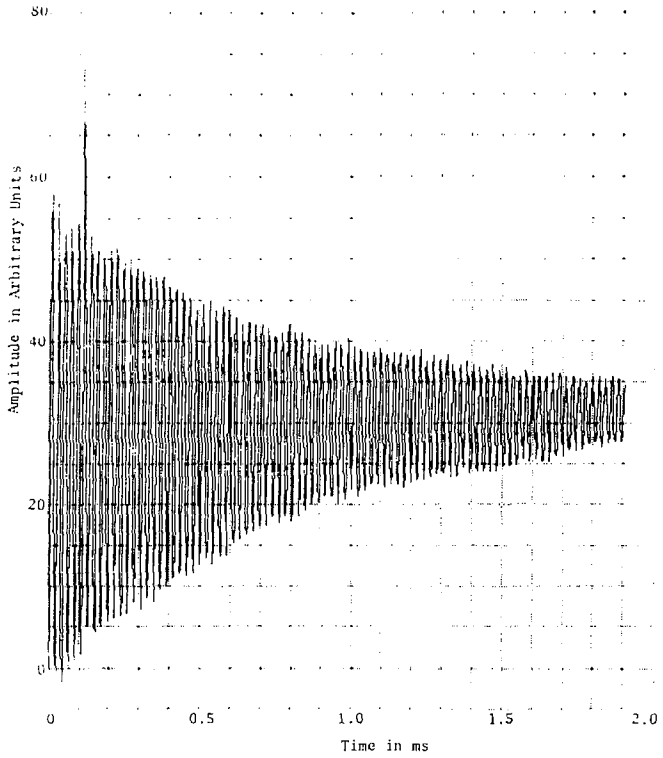

Figure IV.14. Shock tube step response of flush diaphragm semiconductor strain gage type pressure transducer

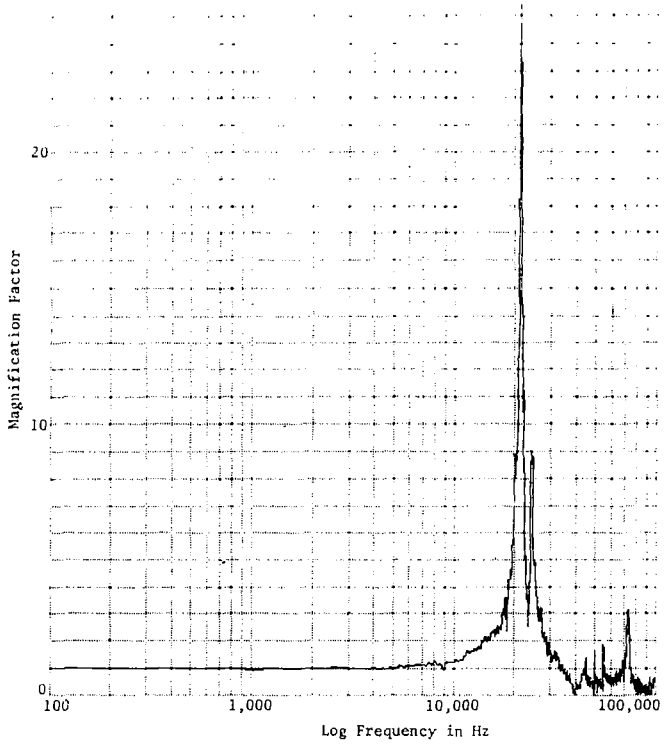

Figure IV.15. Approximate amplitude-frequency response computed for metallic strain gage type pressure transducer

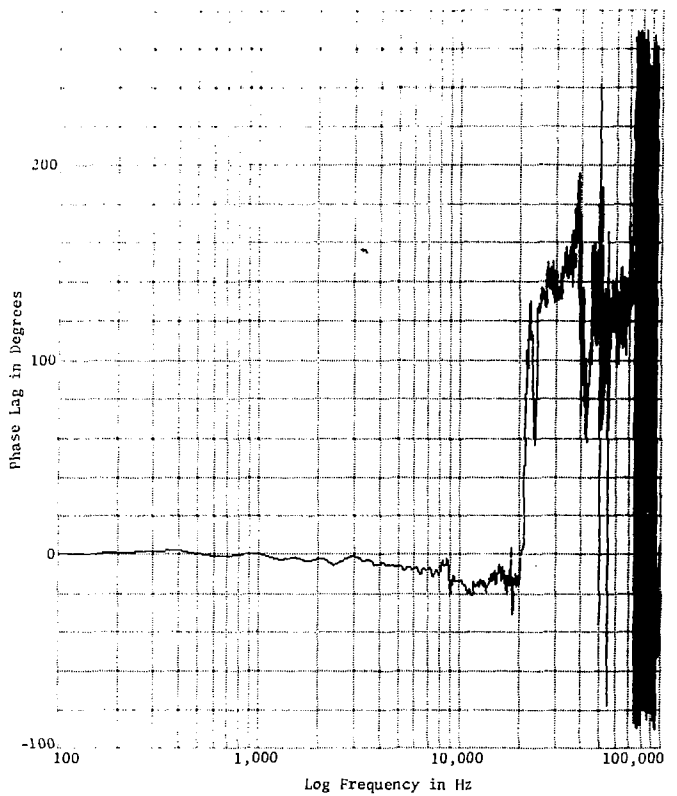

Figure IV.16. Approximate phase-frequency response computed for metallic strain gage type pressure transducer

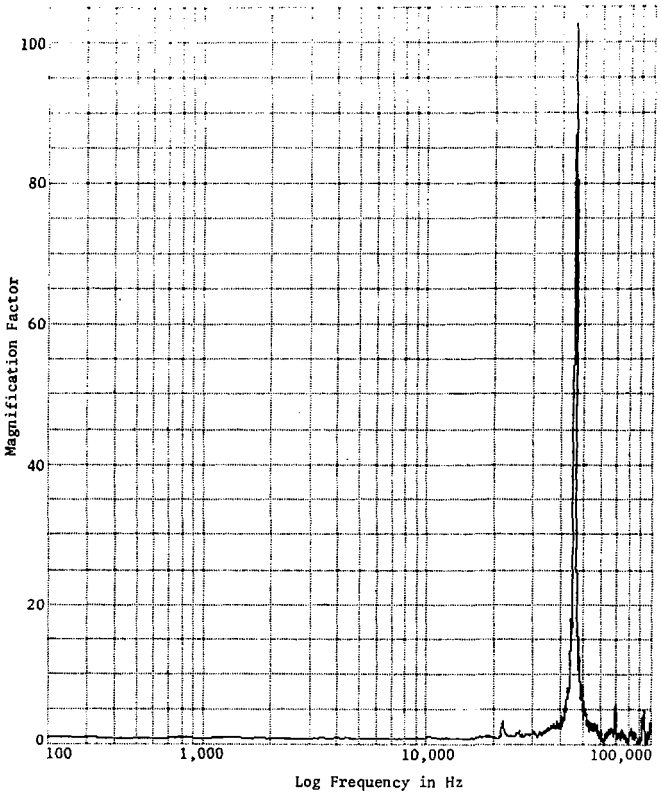

Figure IV.17. Approximate amplitude-frequency response computed for semiconductor strain gage type pressure transducer

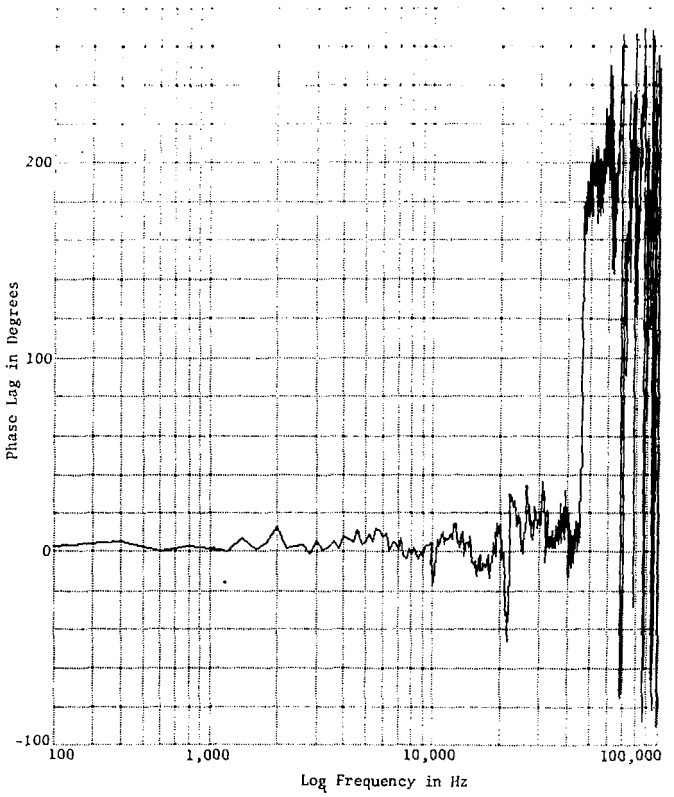

Figure IV.18. Approximate phase-frequency response computed for semiconductor strain gage type pressure transducer

When considering errors in measuring transient phenomena, it will be assumed that adequate low frequency response exists in the measuring system to assure accurate reproduction of the phenomena. Simple ac circuit theory permits verification of this assumption and suggests a solution, if a problem exists.

The transducer model schematically depicted in Figure IV.1 can be discussed in terms of its undamped natural frequency, its damped natural frequency, and its resonant frequency. These are respectively $(k/m)^{1/2}$, the frequency at which an underdamped system responds to any transient, and the frequency of maximum response to a sinusoidal forcing function. For the small value of viscous damping being included in the model, these frequencies are essentially identical.

The response of this elementary dynamic model to various transient phenomena will now be investigated. Its unit impulse response can be analytically computed to be:

$$h(t) = \frac{e^{-\zeta\omega_n t}}{\omega_n\sqrt{1-\zeta^2}} \sin\left(\omega_n\sqrt{1-\zeta^2}t\right), \qquad \text{(IV.17)}$$

where ζ is the viscous damping factor (0.01 assumed) and ω_n is the undamped natural frequency. The transducer's natural period is the reciprocal of the circular undamped natural frequency. Its response $o(t)$ to any transient forcing function $f(t)$ for zero initial conditions can be computed by the convolution integral as:

$$o(t) = \int_0^t f(\tau)h(t-\tau)\,d\tau \ . \qquad \text{(IV.18)}$$

This convolution integral has been numerically integrated to achieve the results shown in Figures IV.19 through IV.34.

A perfectly elastic impact of a lumped mass onto a linear spring would generate an ideal half-sine deceleration pulse. However, because of nonlinearities and losses, deceleration pulses associated with phenomena such as dirt impact typically take on the characteristics of a versed sine.

Figure IV.19 illustrates a unit versed sine forcing function input to this transducer model. The transducer has a natural period equal to the base duration of the versed sine. Also illustrated is the transducer response which possesses a peak error of 68 percent.

The fact that the transducer response does not reproduce the unit versed sine forcing function is not surprising. The transfer function of the transducer does not possess the flat frequency response established in Chapter III as a desirable characteristic of measuring systems.

Figure IV.20 illustrates this same forcing function input to a transducer with a natural period of 0.2, which corresponds to an undamped natural frequency five times higher than that of Figure IV.19. This effectively places a larger portion of the frequency spectrum of the versed sine in the flat region of Figure IV.2. For this situation, the transducer response more closely reproduces the input.

Once a blast wave breaks away from its source, its waveshape can be approximated by a decaying exponential function. Figure IV.21 illustrates such an exponential function and the accompanying transducer response. The natural period of the transducer is equal to the duration of the exponential function at its ten percent amplitude point.

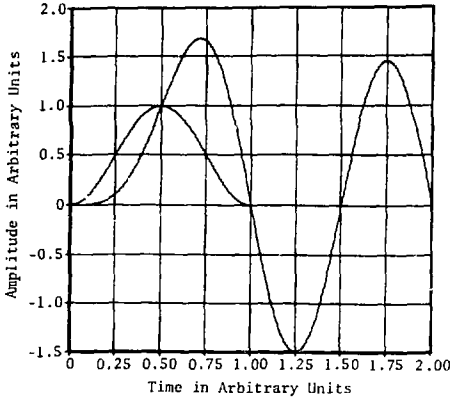

Figure IV.19. Elementary dynamic transducer model response to unit versed sine input (natural period = 1.00)

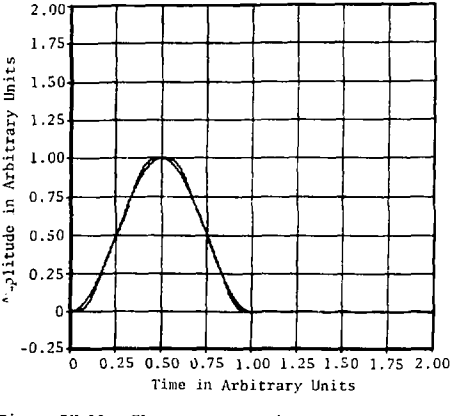

Figure IV.20. Elementary dynamic transducer model response to unit versed sine input (natural period = 0.20)

In an attempt to improve upon the response shown in Figure IV.21, the undamped natural frequency of the measuring instrument is increased by a factor of ten. Figure IV.22 illustrates that even with this increased undamped natural frequency, the transducer response does not represent its input. It is then desired to determine if the undamped natural frequency of the transducer can ever be made high enough so that the exponential function can be defined as successfully as was the versed sine function previously.

The amplitude-frequency and phase-frequency spectrum associated with the exponential function can be computed by first evaluating its Fourier integral as:

$$F(j\omega) = \int_0^{\infty} e^{-(2.8956-j\omega)t} dt \quad . \tag{IV.19}$$

The magnitude of the spectrum is plotted in Figure IV.23 for a one-second duration pulse. Significant high frequency content is contained within this spectrum. The phase angle associated with each frequency can be normalized by the frequency so that time delay can be plotted versus frequency in Figure IV.24. This last figure illustrates that the high frequencies in the exponential forcing function are encountered at initial time by the transducer. The transducer will respond with significant output at its damped natural frequency. The blast front associated with the exponential function can never be defined perfectly by a resonant transducer.

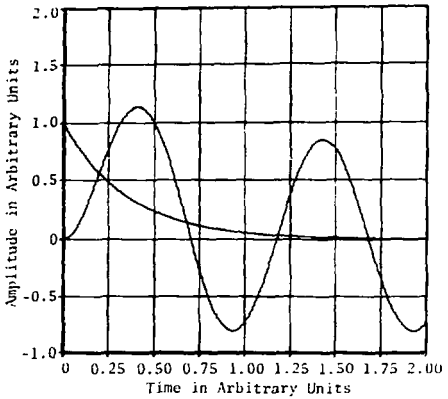

Figure IV.21. Elementary dynamic transducer model response to decaying exponential input (natural period = 1.00)

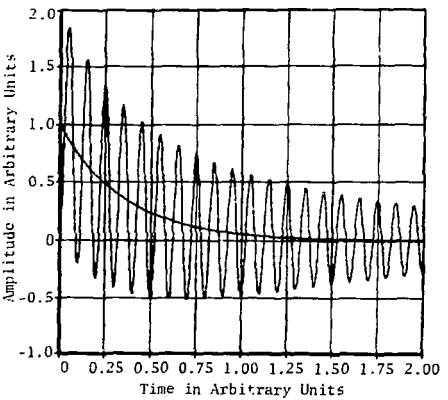

Figure IV.22. Elementary dynamic transducer model response to decaying exponential input (natural period = 0.10)

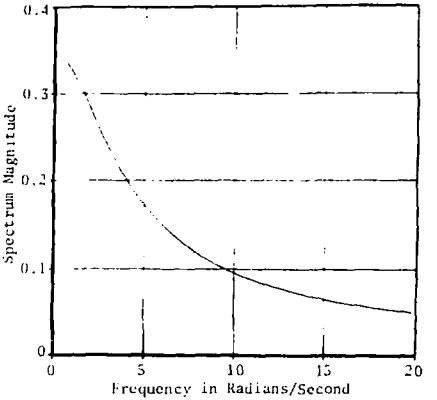

Figure IV.23. Magnitude of Fourier integral of exponential function

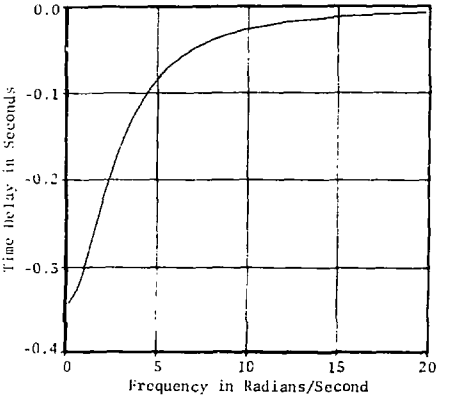

Figure IV.24. Time delay of Fourier integral of exponential function

The previous discussion has considered only two forcing functions and a small number of ratios of pulse durations to transducer natural periods. Figures IV.25 to IV.29 provide a better estimate of the magnitude of error which can occur for various transient forcing functions and various ratios of pulse durations to natural periods.

Each plot of Figures IV.25 to IV.29 is comprised of 40 data points representing 40 different ratios of pulse duration to transducer natural period. The convolution integral is evaluated for each of the 40 values. Maximum transducer response over the time the pulse occurs is ratioed to the maximum pulse amplitude. For example, a versed sine pulse recorded by a transducer with a natural period of one-half the pulse duration (T/TN = 2) can be determined from Figure IV.25 to result in a 32-percent error in recorded pulse peak.

While informative, the preceding examples do not begin to illustrate the potential for error which exists when using resonant devices to define structural dynamics under transient loading. Resonant transducers are used because they are available with flat frequency response and zero phase distortion over the range of frequencies to which structures can significantly respond. It is the idiosyncrasy in their transfer function at high frequencies which makes the transducers' response analytically unpredictable.

In Chapter II it was shown that the loading process to structures in the more severe transient environments was characterized by step discontinuities and complicated by reflections. Early-time material response was characterized by a string of sudden acceleration impulses or Dirac delta acceleration functions.

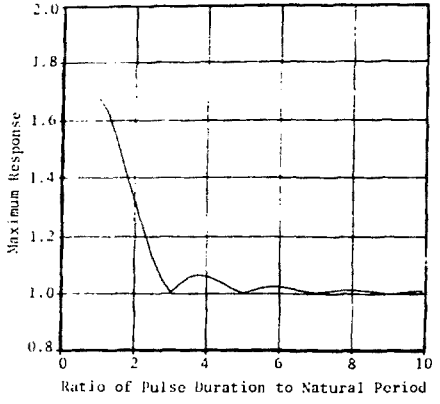

Figure IV.25. Elementary dynamic transducer model maximum response to a unit versed sine pulse

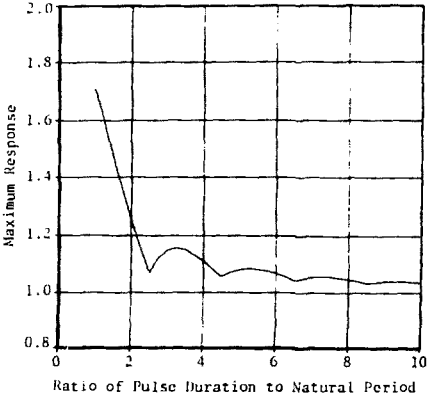

Figure IV.26. Elementary dynamic transducer model maximum response to a unit half sine pulse

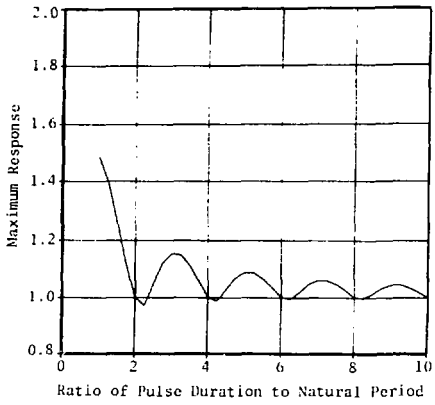

Figure IV.27. Elementary dynamic transducer model maximum response to a unit symmetric triangular pulse

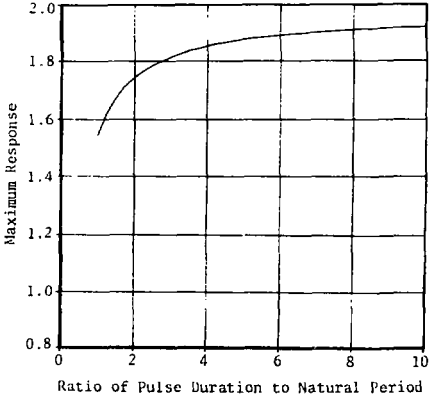

Figure IV.28. Elementary dynamic transducer model maximum response to a unit initial peak sawtooth pulse

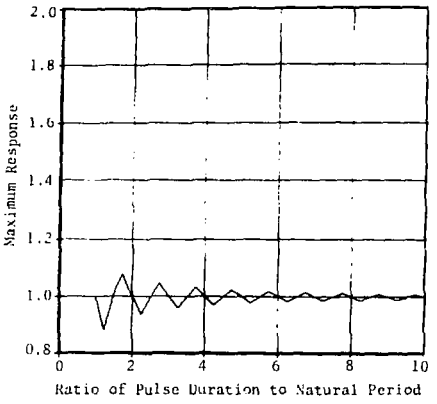

Figure IV.29. Elementary dynamic transducer model maximum response to a unit terminal peak sawtooth pulse

Figure IV.30 illustrates the response predicted by the elementary transducer model to a Dirac delta or single unit impulse acceleration forcing function. Figure IV.31 illustrates the response predicted for this model to two unit impulses where the second impulse occurs at a later time than the first. The system is linear; therefore, superposition holds and the net response is simply the sum of the individual impulse responses. Dependent upon the time of occurrence, these responses can add in phase or out of phase. Figure IV.32 portrays the response to three unit impulses which occur in time so that the results they produce add in phase.

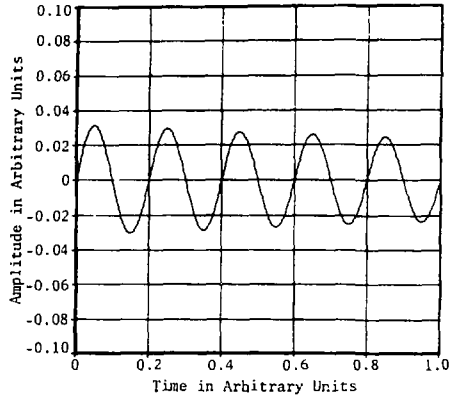

Figure IV.30. Elementary dynamic transducer model response to a unit impulse

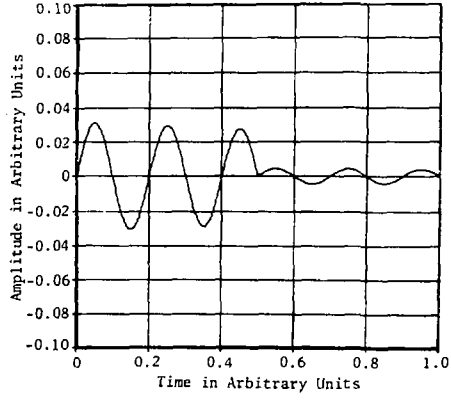

Figure IV.31. Elementary dynamic transducer model response to two unit impulses adding out of phase

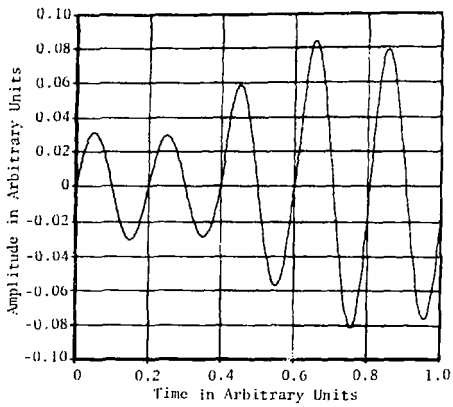

Figure IV.32. Elementary dynamic transducer model response to three unit impulses adding in phase

The common feature of the preceding three figures appears to be the uncertainty in their resultant amplitude. The signal attributable to this impulse chain during material response, in the case of an accelerometer, is superimposed on the later occurring signal which is attributable to the structural response. It is impossible to predict what linear amplitude range an instrumentation channel would need to keep from being overdriven.

Figure IV.33 simulates reflected blast pressure loading to a structure with pressure transducer response superimposed. Figure IV.34 illustrates an identical reflected blast loading with the exception that the second reflection occurs at time 0.20 instead of time 0.21 as in Figure IV.33. The amplitude of the transducer response is more than doubled from that of the previous figure. Again, it is impossible to

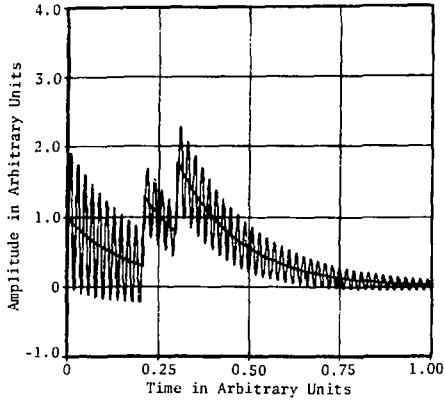

Figure IV.33. Elementary dynamic transducer model response to reflected blast pressures occurring at times 0.21 and 0.30

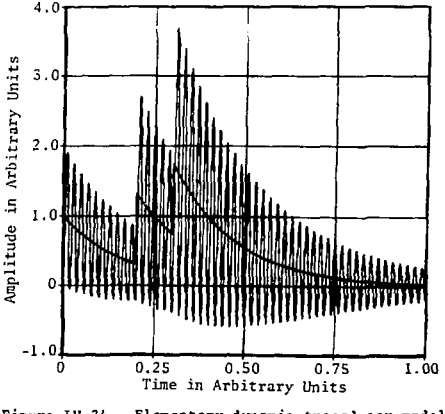

Figure IV.34. Elementary dynamic transducer model response to reflected blast pressures occurring at times 0.20 and 0.30

predict over what linear amplitude range an instrumentation channel would have to be calibrated to prevent it from being overdriven.

Although the degree of uncertainty when using resonant transducers has not been reported in the cited references, distortion produced by their transfer function has been reported and previous work on the problem performed. This previous work will now be described.

It was commented earlier that measurement references almost universally present a dynamic model for force, pressure, and acceleration transducers that is consistent with Figure IV.1. Manufacturer's specifications, frequently formulated around technical societies' recommended practices or guides, encourage the use of this model by specifying only a single resonant frequency in their literature.

The introduction to this chapter demonstrated in detail that the elementary model of Figure IV.1, while conceptually simple, did not dynamically well characterize actual transducers. The elementary model was used in this chapter only to illustrate the potential for problems which exists when using resonant devices to measure structural dynamics in transient loading environments. It was indicated that complete characterization of the transfer function of most real resonant transducers is not attainable. Subsequent chapters will document why this characterization cannot be accomplished. A dynamic model for a transducer based on those characteristics which can be determined will later be described.

The limitations discussed in the previous paragraph are generally not acknowledged in the literature. When they are acknowledged, their application to the problem of interest is not made apparent. As a result, the tendency has been to categorize the measurement difficulties

encountered when using resonant transducers as solvable through an inverse problem.

References 13 through 16, 29, and 57 describe past work performed respectively at Iowa State University, The University of New Mexico, Technion-Israel Institute of Technology, Indian Institute of Technology, Bombay, The University of Houston, and the Boeing Company in Seattle, Washington. The solution technique which has been advocated to account for distortion in the signal from resonant transducers is to perform the inverse operation on their transfer function. This technique has been proposed both in the form of analog compensation during data acquisition[13,15,16,29] and computer compensation during data reduction.[14,15,57] The computer compensation methods for data reduction have ignored the analytic unpredictability of the transducer's response which frequently prevents the distorted signal from being initially recorded. In addition, all previous work has been dependent upon one of two assumptions. These assumptions are:

1. an adequate experimental characterization of the dynamic response of the transducer is available, or
2. the transducer is adequately characterized by the elementary dynamic models of Figure IV.1.

The application of the advocated solution technique has generally been to data whose frequency content is much lower than that of the data which will be considered in the next chapter. Only reference 29 has applied this technique to high frequency data, such as are encountered in shock tubes, and limitations in an analog compensator's transfer characteristics are acknowledged. In a similar application, reference 58 notes the inadequacy of the assumption of an elementary single degree of

freedom transducer model when deconvolving acoustic-emission signals. The two preceding assumptions upon which past work has been dependent are not necessary and often times are not practical when measuring structural dynamics. In addition, the problem of analytically unpredictable signal amplitude has not been observed in previous publications.

Summary and Conclusions

1. Transducers intended to define structural dynamics must be characterized by a continuous system model.
2. When resonant transducers are used to define structural dynamics under severe transient loading, it is not practical to analytically predict the linear range an instrumentation channel must possess to prevent it from being overdriven.
3. Previous work concerning measurement difficulties encountered when using resonant transducers has treated these difficulties as being solvable as an inverse problem. Solution techniques proposed have been in the form of analog compensation during data acquisition or digital compensation during data reduction. Unwarranted assumptions associated with these techniques are:
   a. an adequate experimental characterization of the dynamic response of the transducer is available, or
   b. the transducer is adequately characterized by the elementary dynamic model of Figure IV.1.

CHAPTER V

PROBLEM ILLUSTRATION USING ACTUAL TEST DATA

Chapter IV indicated that analytically unpredictable and distorted signals can result when using resonant transducers to measure the dynamic characteristics of structural systems. The present chapter illustrates these effects using experimental data from tests on actual structures. These data were acquired during nuclear weapon effects testing.

The Introduction to this work contains a test record which, based upon the facts presented, appears to contain valid data. It was noted that such a record would provide a basis for the establishment of component test specifications and to permit comparison with and modification of a dynamic analytical model of the structure tested. In this chapter, it will be demonstrated that this test record actually contains invalid data.

As was noted previously, a decaying exponential function approximates the static overpressure experienced in a free field blast environment. Figure V.1 illustrates a typical record from such an environment. This record was produced during a test in an explosively driven shock tube used to simulate nuclear blast effects. The measuring pressure transducer was a flush diaphragm resistance bridge device with a manufacturer's specified fundamental resonant frequency of 75 kHz and a range of 300 psig (1 psi = 6.895 kPa). The shock was propagated in air at 12 psia. The importance of this example will be to illustrate that while resonant pressure transducers are adequate in working with structural dynamics they cannot resolve the shock front associated with a propagating blast wave.

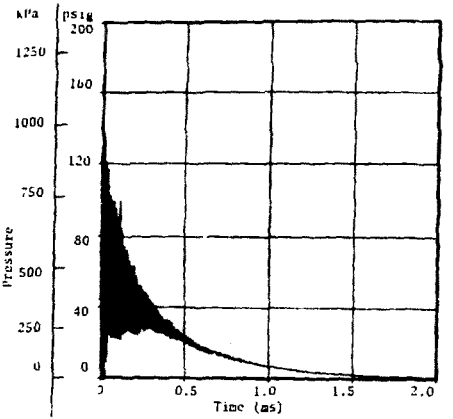

Figure V.1. Static overpressure record from explosively driven shock tube test

Figure V.2 is a diagram of the instrumentation system used to record and digitize the transducer response. The assistance of a data reduction group was necessary in "code cracking" to provide compatibility between the DEC digital tape with 12 bit words and the Control Data Corporation scientific computer with 60 bit words used for data analysis. The Biomation Transient Recorder, an analog-to-digital converter with a recirculating memory, was operated in a pretrigger mode with 1024 samples of the transducer response digitized to eight bit resolution over a two-millisecond interval. This corresponded to a sampling interval of $T = (0.002/1024)$ seconds and a Nyquist frequency of $1/2T$ or 256 kHz.

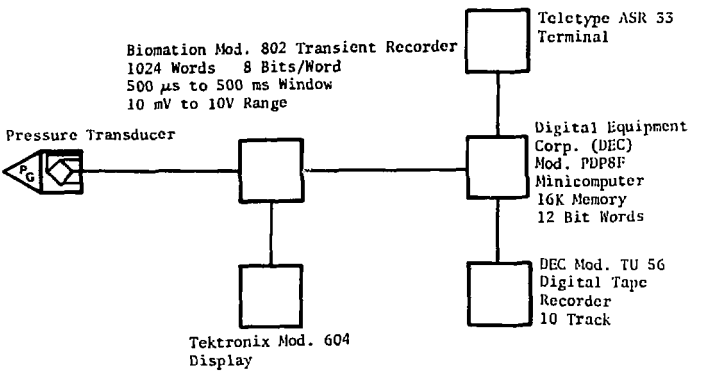

Figure V.2. Instrumentation system used to record and digitize pressure transducer response

To analyze both the data illustrated in Figure V.1 and succeeding examples, digital signal processing techniques are employed. These techniques are described in Reference 17. In all examples presented, analog reconstruction is by straight line approximation between the data points. The high data sampling rate on all records which will be analyzed avoids the need for more sophisticated techniques.

Before proceeding with analysis of the data illustrated in Figure V.1, a few points will be noted regarding discrete (DFT) and fast (FFT) Fourier transforms since they will be used repeatedly. The DFT can be expressed as:

$$\bar{F}_m = \sum_{n=0}^{N-1} f_n e^{-j(2\pi mn/N)}; \; m = 0, 1, \ldots, N-1 \qquad (V.1)$$

for

$$\omega = \frac{2\pi m}{NT}$$

where f_n is a sample of the set which represents the input function f(t) starting at time equal zero, N is the total number of samples, T is the sample interval, and $\bar{F}_m$ is the discrete transform corresponding to each value of ω. Actually, there are two parts to $\bar{F}_m$ corresponding to each of N values since $\bar{F}_m$ is complex. Equation (V.1) illustrates that N^2 complex products are required for DFT computation. Since some of the records examined will have N as large as 4096, this computation becomes lengthy in terms of computer time. The FFT is an algorithm which eliminates redundancy in the DFT and computes the DFT by expressing it as a linear combination of smaller DFTs. Figure V.3 lists the particular FFT algorithm utilized throughout this section; this algorithm is modified only slightly from that given in Appendix B of Reference 17. The algorithm requires 2^K input data points where K is an integer. The advantage of the FFT is that it reduces computation time compared to the DFT by K/2N. It is of interest to note that both the DFT and the FFT bear the same relation to the digital system as the continuous Fourier transform bears to the analog system.

Figure V.4 is the result of applying the FFT of Figure V.3 to the data of Figure V.1. The curve is plotted though points which are 0.5 kHz apart in frequency. Phase information is not presented since the amplitude spectrum alone is sufficient to illustrate the problem. Clearly, the high frequency content of the transient required to define the shock front is "contaminated" by the resonant response of the measuring transducer which is centered at approximately 70 kHz. The low

frequency portion of this spectrum is adequate, however, to define the input forcing function applied to a structure over the range of frequencies to which the structure possesses significant response. Subsequent examples will illustrate this last point more fully.

```
 78/01/12. 17.06.14.
PROGRAM    FFT

10000 SUBROUTINE FFT(FR,FI,K,IS)
10010C
10020C FAST FOURIER TRANSFORM USING TIME DECOMPOSITION
10030C WITH INPUT BIT REVERSAL
10040C DATA IS IN FR (REAL) AND FI (IMAGINARY) ARRAYS
10050C COMPUTATION IS IN PLACE, OUTPUT REPLACES INPUT
10060C NUMBER OF POINTS MUST BE N=2**K
10070C FR(N) AND FI(N) MUST BE DIMENSIONED IN MAIN PROGRAM
10075C IS=-1 FOR FORWARD TRANSFORM, IS=+1 FOR INVERSE TRANSFORM
10080C
10090 DIMENSION FR(1),FI(1)
10100 N=2**K
10110 MR=0
10120 NN=N-1
10130 DO 2 M=1,NN
10140 L=N
10150 1 L=L/2
10160 IF(MR+L.GT.NN)GO TO 1
10170 MR=MOD(MR,L)+L
10180 IF(MR.LE.M)GO TO 2
10190 TR=FR(M+1)
10200 FR(M+1)=FR(MR+1)
10210 FR(MR+1)=TR
10220 TI=FI(M+1)
10230 FI(M+1)=FI(MR+1)
10240 FI(MR+1)=TI
10250 2 CONTINUE
10260 L=1
10270 3 IF(L.GE.N)RETURN
10280 ISTEP=2*L
10290 EL=L
10300 DO 4 M=1,L
10310 A=3.14159265359*FLOAT(IS*(M-1))/EL
10320 WR=COS(A)
10330 WI=SIN(A)
10340 DO 4 I=M,N,ISTEP
10350 J=I+L
10360 TR=WR*FR(J)-WI*FI(J)
10370 TI=WR*FI(J)+WI*FR(J)
10380 FR(J)=FR(I)-TR
10390 FI(J)=FI(I)-TI
10400 FR(I)=FR(I)+TR
10410 4 FI(I)=FI(I)+TI
10420 L=ISTEP
10430 GO TO 3
10440 RETURN
10450 END
READY.
```

Figure V.3. Fast Fourier transform subroutine

The second set of data records to be analyzed are those for channels A4 and A6 which were recorded from accelerometers mounted in close proximity to the accelerometer of channel A5, the record presented

in the Introduction of this work. These signals were recorded from accelerometers mounted inside the shell of a reentry vehicle which was subjected to explosive loading on the shell's outer surface. The records from this location should contain the highest frequency content of any of the accelerometers recorded during this particular test. This is because numerous joints and different materials tend to attenuate the high frequencies that would excite interior components of the reentry vehicle, whereas only the thin shell wall separates accelerometers recorded as A4, A5, and A6 from impulsive explosive loading.

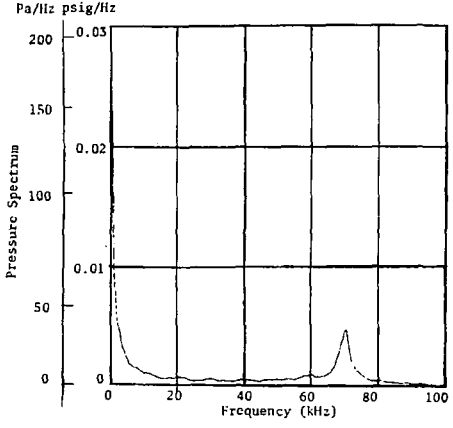

Figure V.4. Magnitude of Fourier transform of static overpressure record from explosive shock tube test

Figure V.5 diagrams the instrumentation system for recording and digitizing these acceleration channels. The Disk Recording System was a combination of commercial equipment and equipment developed at Sandia

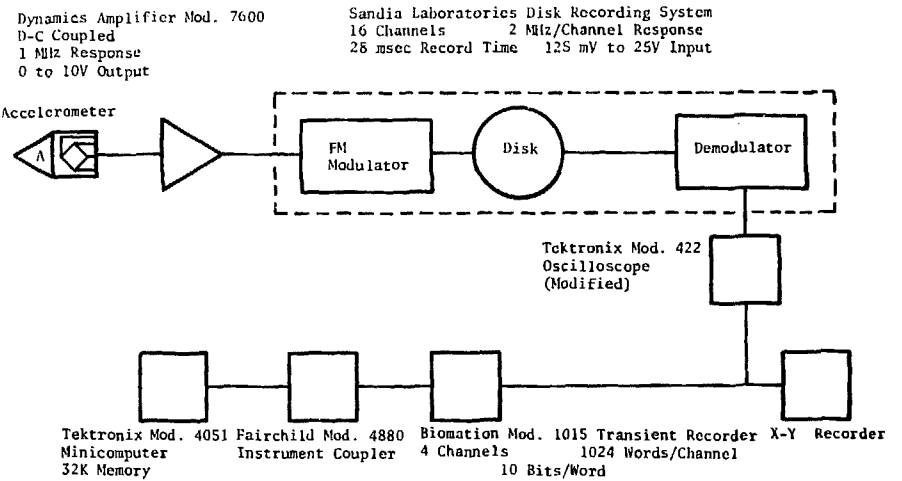

Figure V.5. Instrumentation system for recording and digitizing acceleration data channels A4, A5, and A6

Laboratories, Albuquerque, New Mexico. The FM modulator on each channel operated at 4.5 MHz and deviated from 3 to 6 MHz. The demodulator was a pulse-averaging discriminator. Frequency response of the data recording electronics was limited by the 1-MHz response of the dc differential input instrumentation amplifiers.

Four channels in the Model 1015 Biomation Transient Recorder were connected in series so that the 1024 words/channel could be combined to permit 4096 samples of accelerometer response over five milliseconds. The Tektronix Model 422 oscilloscope was modified to make available the ramp signal controlling its horizontal sweep time. A sampler on this ramp signal gated and effectively time-expanded successive portions of the recorded signal so that the frequency responses of the X-Y recorder and the Biomation recorder were compatible with the high frequencies recorded on the Disk Recorder. In this manner, the five millisecond window was expanded on playback to 82 seconds.

Data output from the Biomation recorder was interfaced into a Tektronix Model 4051 Minicomputer. With a digital tape and an acoustic coupler, digitized data were then transmitted by telephone from a remote test area to the same Control Data Corporation scientific computer used to analyze the earlier shock tube blast pressure record.

The nominal fundamental resonant frequency of the accelerometers to be recorded on channels A4, A5, and A6 had been determined to be 50 kHz. To accommodate noise on the channel, it was desired to have at least ten samples/cycle at 50 kHz since the spectrum analysis performed would extend slightly above this frequency.

In digitizing signals such as were recorded on channels A4 and A6, it was difficult to tell exactly where data began because of electrical noise which occurred at time zero. This noise resulted from the discharge of capacitor banks to initiate the explosive. A greater judgment problem involved when to stop the digitization process since the structure response does not end abruptly but decays into the channel noise level. The criteron selected for deciding when to truncate the digitization process was to choose the time when the recorded signal level had decayed to, and remained below, ten percent of the maximum initial value of the signal. The signal was first observed on an oscilloscope and it was determined that the five millisecond window would satisfy this criterion and provide 16 samples/cycle at 50 kHz. Nyquist frequency was 409 kHz when allocating the 4096 samples over this time window.

Figures V.6 and V.7 display the results of this digitization process; they represent the unfiltered acceleration time histories of these two channels. Channel range for A4 was 8,000 g or 16,000 g peak to peak, while the recorded signal was 8,000 g peak to peak. Channel range for A6 was the same as for A4, while the recorded signal was 12,000 g peak to peak. The linear specified range of the accelerometers was 10,000 g peak to peak with some overrange capability. In Figures V.8 and V.9 the first millisecond of each of the five millisecond long records of Figures V.6 and V.7 is expanded so that more resolution is achieved. The 50-kHz resonant frequency of the accelerometers is apparent superimposed on the recorded signals.

Before discussing the data recorded on channels A4 and A6, one important point should be considered. Some finite, but minimal, amount

of error will occur when analyzing these signals in the frequency domain. The error is attributable to the truncation process which occurred during digitizing. After truncation, it is a typical procedure to apply a data window to the digitized signal to round off the "sharp corners." An example is a Hanning window, which is defined as:

$$w(t) = \frac{1}{2}\left(1 - \cos\frac{2\pi t}{NT}\right) \qquad (V.2)$$

where NT is the sample interval.

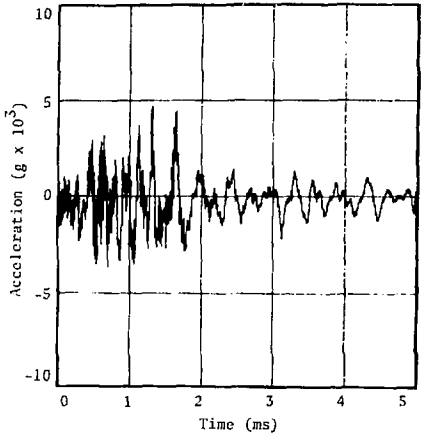

Figure V.6. Unfiltered acceleration-time history for channel A4

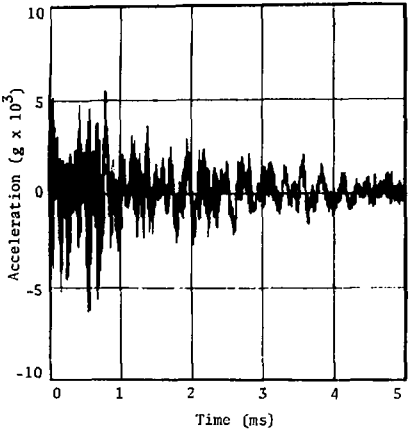

Figure V.7. Unfiltered acceleration-time history for channel A6

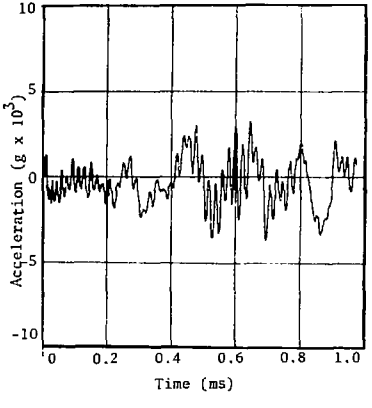

Figure V.8. Unfiltered acceleration-time history for channel A4 expanded

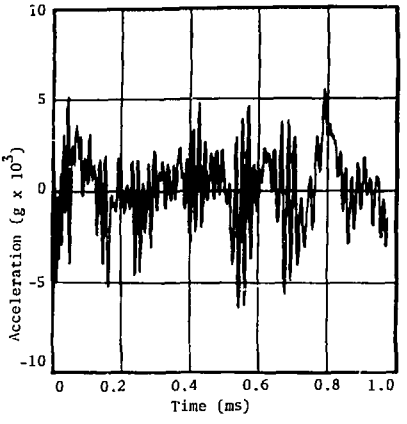

Figure V.9. Unfiltered acceleration-time history for channel A6 expanded

Other forms of data windows are available. All of them have in common the fact that they taper the amplitude of the leading and trailing edges of the data obtained during the observation period. In applying any type of data window, it is important to remember that multiplication by a window in one domain is equivalent to convolution of the Fourier transforms of the window and the data in the other domain, resulting in distortion of the transformed signal. The following two equations[18] illustrate this point. Let f(t) be the truncated signal and w(t) be the data window. The double-pointed arrow represents a Fourier transform.

$$f(t)\, w(t) \leftrightarrow \frac{1}{2\pi} \int_{-\infty}^{\infty} F(jx)\, W\left[j(\omega - x)\right] dx \qquad (V.3)$$

$$\int_{-\infty}^{\infty} f(\tau)\, w(t-\tau)\, d\tau \leftrightarrow F(j\omega)\, W(j\omega) \qquad (V.4)$$

Data windows were not imposed on the transient data digitized on channels A4 and A6 since they both contained significant amplitude near the beginning of the observation. Applying a data window to either of these transient signals would have diminished their apparent frequency content.

The motivation for instrumenting and recording channels A4 and A6 was to define the response of the structure (the reentry vehicle) at the accelerometer-mounting locations. Concentrating only on the measurement problem, the objective was to acquire and transmit a valid signal describing the structural response.

One measure of the validity of a signal transmitted through an intrumentation channel is the signal-to-noise ratio. The signal-to-noise ratio is expressed as a power ratio or a mean-squared voltage ratio. For a periodic waveform, the signal power is a time average occurring over one cycle. As the noise power increases, the validity of the transmitted signal decreases.

Considering a transient waveform to be the limiting case for a periodic waveform where the period becomes infinite, the normalized power of a transient approaches zero. The energy contained in the transient signal does, however, have a finite value. Noting this fact, the transient signals recorded can be analyzed for their energy content. It is desired to have the energy content of the signal associated solely with the problem of defining the response of the structure.

The energy (E) supplied by a voltage signal (v(t)) to a load (R) is:

$$E = \int_{-\infty}^{\infty} \frac{v^2(t)}{R}\, dt \quad . \tag{V.5}$$

For a one-ohm load, this can be written as:

$$E = \int_{-\infty}^{\infty} v^2(t)\, dt \quad . \tag{V.6}$$

Extending this concept to any signal f(t) in general, and noting for f(t) real that $f^2(t) = |f(t)|^2$, Parseval's theorem[18] states that:

$$E = \int_{-\infty}^{\infty} |f(t)|^2 dt = \frac{1}{2\pi} \int_{-\infty}^{\infty} |F(j\omega)|^2\, d\omega \quad . \tag{V.7}$$

The quantity $|F(j\omega)|^2$ was computed and the result plotted for the data recorded on channels A4 and A6. These plots are presented as Figures V.10 and V.11. Frequency resolution is 0.2 kHz.

Figures V.10 and V.11 may be considered as a plot of the energy spectrum, in g^2/Hz^2, of the recorded acceleration signal. The areas under the curves in these plots have units of g^2/Hz. The concept of considering $(acceleration)^2/Hz$ or g^2/Hz as energy is not abstract. A given acceleration level can be equated to an equivalent signal level in volts. $(Acceleration)^2/Hz$ is then proportional to $(volts)^2/Hz$ which, when normalized to a one-ohm load, will be in units of energy.

Some very important observations are possible based upon these last two figures. Figure V.10 illustrates that for channel A4 most of the energy of the signal is devoted toward defining the response of the structure, which is occurring below 6 kHz. Some lesser structural responses exists at 10 kHz. It is also possible to note that the

remainder of the energy of the signal is concentrated betwen 45 and 50 kHz. This energy is at the resonant frequency of the accelerometer and is not defining structural response but is associated with the characteristics of the measuring transducer.

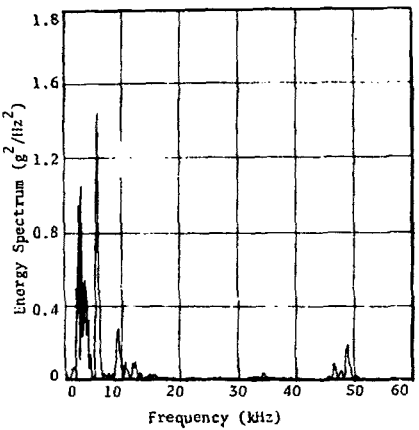

Figure V.10. Signal energy spectrum versus frequency for channel A4

Figure V.11 portrays the same type of analysis for channel A6. The energy in the signal associated with the structure is concentrated below 10 kHz. In the signal, a large quantity of energy associated with the transducer is centered around 55 kHz. Since total signal energy is proportional to the area under the curve in this plot, it is apparent that approximately as much of the energy in this signal is associated with the resonant characteristics of the accelerometer as is associated with the structure's response.

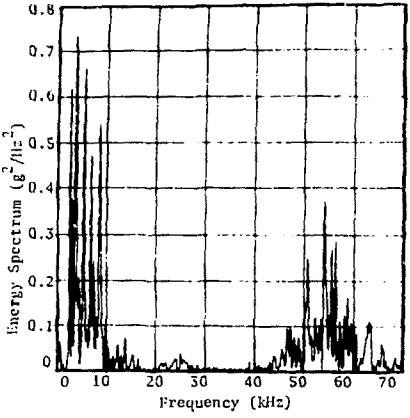

Figure V.11. Signal energy spectrum versus frequency for channel A6

These findings are consistent with the time histories of Figure V.6 through V.9. These earlier figures show channel A6 contains much more high frequency response associated with the accelerometer resonance than does channel A4. The key point to note in Figures V.10 and V.11 is that because the energies are in two distinct frequency bands the response of the structure is separable from the resonant characteristics of the accelerometer. This was not readily apparent in Figure V.6 through V.9. The acquisition of meaningful data from channels A4 and A6 then becomes a "data separation" problem in the frequency domain.

Before performing this separation, one last point should be made. The energy spectrum associated with the signal is plotted as the ordinate in Figures V.10 and V.11. In the frequency domain, acceleration can be converted to velocity if it is multiplied by $1/j\omega$. The ordinate

plotted is the square of the magnitude of the acceleration spectrum. The kinetic energy of the structure is proportional to velocity squared. Thus, if it were of interest to determine the energy spectrum associated with the structure, as opposed to the energy spectrum of the signal defining the structure, the ordinate of Figures V.10 and V.11 would have to be multiplied by $1/(\text{frequency})^2$ over that frequency region containing the structural response. If the response measured were velocity, as opposed to acceleration, this point of confusion would not arise. Acceleration is measured because accelerometers are small inertial devices not requiring a fixed reference point.

The final analysis performed on data channels A4 and A6 will separate the structure response from the accelerometer resonance in both the time and frequency domains. This operation is accomplished by filtering.

Since the data for channels A4 and A6 are available in digital form, this filtering can be performed through use of a digital algorithm. A nonrecursive filter was designed where each output data sample, g_m, was computed as a linear function of the input sampled data set $[f_m]$ so that

$$g_m = \sum_{n=-N}^{N} b_n f_{m-n} \quad . \tag{V.8}$$

A low pass filter was designed with zero phase shift by using the algorithm

$$g_m = \sum_{n=-N}^{N} b_n x_n f_{m-n} \tag{V.9}$$

with transfer function

$$\overline{H}(j\omega) = b_0 + 2\sum_{n=1}^{N} b_n x_n \cos n\omega T \qquad \text{(V.10)}$$

where

$$b_n x_n = \frac{\left[1 + \cos (n\pi/N)\right] \sin (n\omega_c T)}{2n\pi} \; ; \; -N \leq n \leq N \qquad \text{(V.11)}$$

The effect of $x_n = 1 + \cos (n\pi/N)$ was to eliminate errors that were attributable to Gibbs phenomenon[18] causing a ripple in the passband of the filter. The specific filter designed used $N = 100, \omega_c = 24000\pi$, and $T = 0.005/4096$. Its transfer function is illustrated in Figure V.12. Its -3 dB point is approximately 10 kHz, and its roll off is greater than 40 dB/octave.

When the unfiltered records of Figures V.6 and V.7 are passed through the filter illustrated by Figure V.12, the results are as plotted in Figures V.13 and V.14. These two figures represent the true response of the structure. The maximum peak-to-peak acceleration response for channel A4 is 6500 g, which represents 81 percent of the peak-to-peak amplitude of its recorded unfiltered signal. The maximum peak-to-peak response for channel A6 is 5,500 g, which represents 46 percent of the peak-to-peak amplitude of its recorded unfiltered signal. The fact that the filtered outputs shown in Figures V.13 and V.14 are not equal to zero at time zero is attributable to the starting transient associated with the filter. For this particular filter, the output started at time equal to -0.000122 second.

The preceding analysis completed, it is now possible to conclude that the test data recorded on channel A5 are inadequate both for

defining the response of the structure and for generating test specifications. The following paragraphs will provide justification to support this conclusion.

The channel range for A5 was only slightly greater than for channels A4 and A6, being 10,000 g or 20,000 g peak to peak. The measuring accelerometer was the same type used to acquire the data recorded on channels A4 and A6. The unfiltered acceleration time record is presented in Figure V.15. The peak-to-peak recorded acceleration range was 28,000 g.

Several observations are possible based upon Figure V.15. The accelerometer has been overranged by a factor of three and is probably

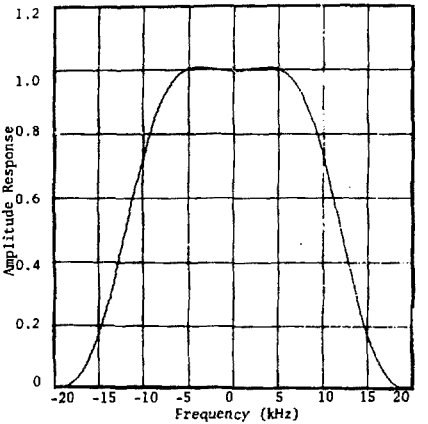

Figure V.12. Magnitude of transfer function of non-recursive low pass filter with zero phase shift

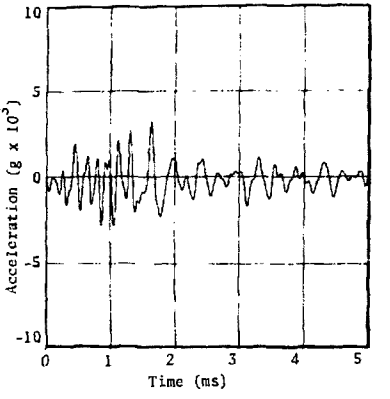

Figure V.13. Filtered acceleration-time history for channel A4 (compare with Figure V.6)

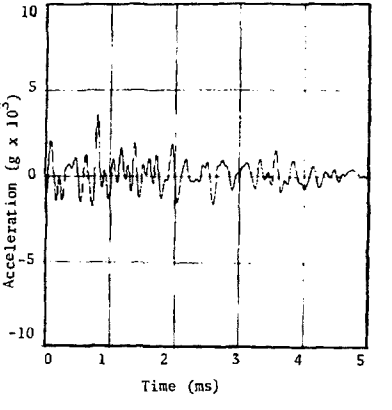

Figure V.14. Filtered acceleration-time history for channel A6 (compare with Figure V.7)

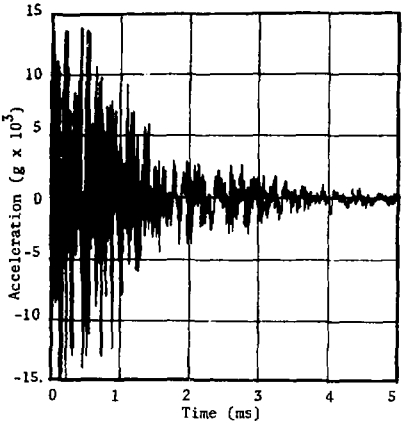

Figure V.15. Unfiltered acceleration-time history for channel A5

highly nonlinear at this magnitude of response. The signal range of the recording channel electronics has been exceeded, resulting in additional nonlinearities. Evidence of these latter nonlinearities can be seen in the truncation of the signal, which is occurring over the first millisecond of the record for the positive going acceleration peaks.

Chapter III explained the importance of a linear measuring system to prevent distortion when recording dynamic data. It is to be expected that the data recorded on channel A5 will contain "created" frequencies attributable to the nonlinearities noted in the preceding paragraph.

Figure V.16 illustrates the signal energy spectrum computed for channel A5 containing these "created" frequencies. It is apparent that the response of the structure is not separable from that of the measuring transducer. Since this measurement was made at a location on

the shell in close proximity to the accelerometers recorded on channels A4 and A6, which indicated structural response only below 10 kHz, structural response occurring only below 10 kHz would be expected on channel A5. Meaningful definition of structural response from channel A5, however, is not achievable through a filtering process or any other known technique. Figure V.17 illustrates the frequency content of the record presented as A5 in the Introduction. Clearly, more than structural response information is contained in this record.

Fortunately, in this example an unfiltered record in the form of Figure V.15 was available upon which to base the conclusion that the data intended to define structural response at the location of the accelerometer recorded on channel A5 were invalid. The obvious question is, could valid data have been recorded on channel A5? The answer is yes.

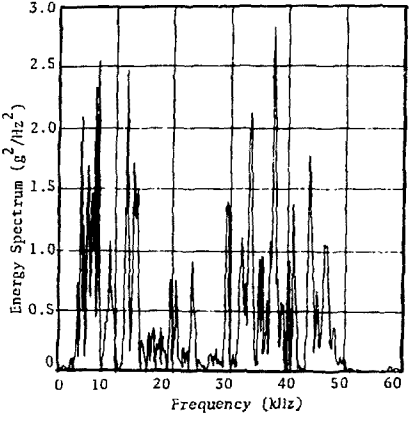

Figure V.16. Signal energy spectrum versus frequency for channel A5

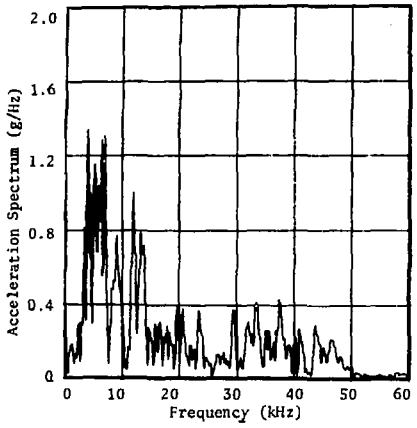

Figure V.17. Magnitude of Fourier transform of test record presented as A5 in Introduction

An accelerometer with a peak-to-peak specified linear range of 10,000 g probably would be a reasonable selection if consideration were based only on predictions resulting from the analysis of the structural model. A problem arises in these predictions. Because of the nature of the model, only an estimate of the peak-to-peak range of the structure, and not that of the signal, is provided. The range of the signal which must be recorded is dominated by uncertainties attributable to the resonant transducer's response to the sudden acceleration impulses during the structure's material response. This portion of the transducer's response will be superimposed upon that portion of the signal defining the structural response. If the measuring accelerometer utilized on channel A5 had possessed a linear peak-to-peak range of

30,000 g, and if the linear range of the electronics had been compatible with the recorded signal, valid data could have been obtained.

Based on the previous analysis, one might conclude that if the resonant transducer and the recording electronics always remained within their linear operating range, and if the transducer's fundamental resonant frequency was always high enough to be separable in the frequency domain from those lower frequencies to which the structure possesses significant response, meaningful data could be recovered. This oversimplification ignores the very real presence of electrical noise in all instrumentation systems. Electrical noise, in the present context, implies "spontaneous fluctuations" often requiring statistical data treatment. All records analyzed thus far have been relatively free of this type of noise consideration, primarily because of the very close proximity between signal sources and record electronics.

The final set of data records to be analyzed will illustrate both the presence and effect of electrical noise. These records are identified as track 5 and track 6 and are acceleration channels recorded from a reentry vehicle subjected to an underground nuclear test. Acceleration data are again used because these particular records possess significant electrical noise. Of principal importance are the observations that resonant measuring transducers encountered a high frequency transient loading, that both the resonant transducer and the recording electronics remained within their linear range, yet meaningful information concerning the structure was still not acquired.

These records were recovered from an FM magnetic tape. The record identification originates from the tape track number on which the data were recorded. The analog tape was processed, and a digital binary tape

was created. Information contained on this tape was transferred into permanent disk files accessible by the Control Data Corporation scientific computer for analysis. A great deal of flexibility was possible in selecting sample rate and time window size during digitization. A total of 4096 samples was taken on both tracks, with a time window of 8.192 milliseconds for track 5 and 4.096 milliseconds for track 6. This corresponded to Nyquist frequencies of 250 kHz and 500 kHz, respectively. This high sampling rate again permitted reconstruction of the waveforms by straight line approximation since the fundamental resonant frequency of the traneducers was only 40 kHz. Figure V.18 illustrates pertinent details of a typical instrumentation channel which recorded data. The low pass filter used when demodulating the recorded FM signal had a -3 dB frequency of 60 kHz and a roll-off characteristic of 36 dB/octave.

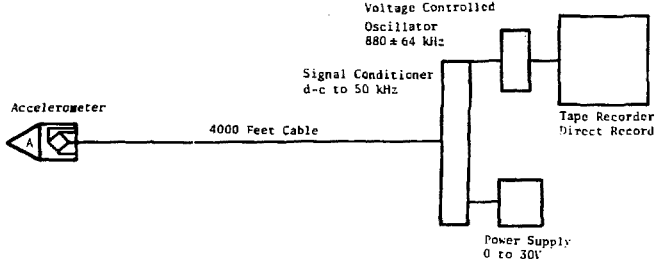

Figure V.18. Typical instrumentation channel used to record acceleration data on tape tracks 5 and 6

Both instrumentation channels were adjusted for operation over ranges of 10,000 g peak to peak, with both accelerometers capable of

operation over this same range. This acceleration range corresponded to a 189-millivolt peak-to-peak signal from the accelerometer recorded on track 5 and a 250-millivolt peak-to-peak signal from that recorded on track 6. Figure V.18 shows that these signals must travel over 4000 feet of cable before amplification can be provided.

Figures V.19 and V.20 illustrate the acceleration time histories recorded on tape tracks 5 and 6. Enough overrange capability existed on both channels so that it is assured that all of the recorded signal which could be attributed to the accelerometer response is linear. The high frequency ringing on both channels is attributable to the 40 kHz resonant frequency of each of the accelerometers.

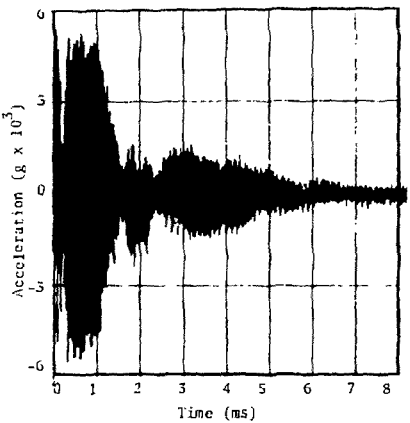

Figure V.19. Unfiltered acceleration-time history for track 5

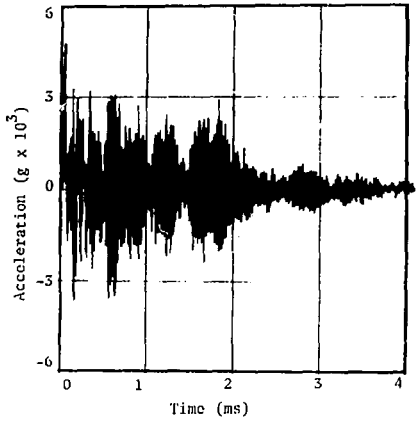

Figure V.20. Unfiltered acceleration-time history for track 6

It is desired to examine the energy spectrum of each of these two transient time histories. Figures V.21 and V.22 illustrate these spectra in the same manner as calculated for previous records. Frequency resolution is 0.122 kHz for track 5 and 0.244 kHz for track 6.

Of immediate interest is the fact that there is no separation between structural response and the resonant characteristics of the transducer. In fact, in both figures the energy in the transient signal is almost totally associated with the resonant characteristics of the transducer.

The question now arises as to whether filtering of these records, which is possible since the recorded signals have remained linear, will produce any usable information. Figures V.21 and V.22 provide no apparent indication as to the frequency at which this filtering should

occur. Since the accelerometers recorded in these figures were mounted on the inside of a reentry vehicle shell in a manner similar to the accelerometers in the previous group of data records, the same filter criteria were applied, in an attempt to acquire meaningful data.

Digital filtering was performed using the same filter algorithms presented previously in Eq. (V.8) to (V.11). The same values of N and ω_c were used, with a value of T = 0.000002 second for track 5 and 0.000001 second for track 6. The resultant filters were quite similar to Figure V.12. The filter for track 5 had its -3 dB point at 12 kHz and introduced approximately four percent attenuation in the low frequency pass band. The filter for track 6 had its -3 dB point at 10 kHz and introduced approximately two percent attenuation. Figures V.23 and V.24 illustrate the results of this filtering algorithm.

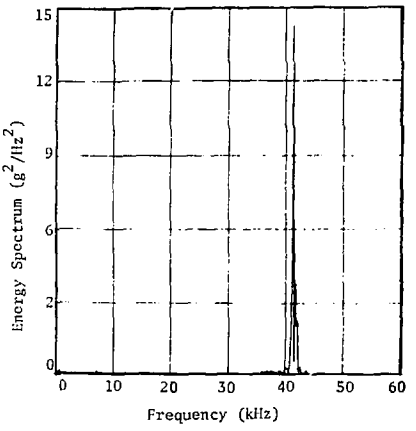

Figure V.21. Signal energy spectrum versus frequency for track 5

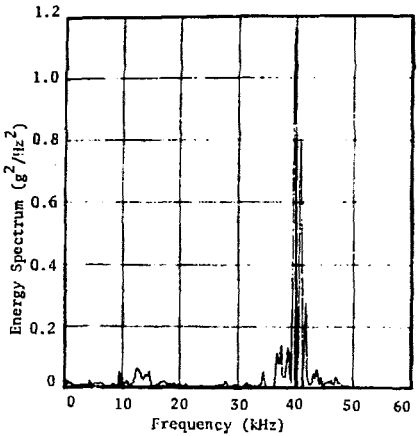

Figure V.22. Signal energy spectrum versus frequency for track 6

Evident in both figures is an initial acceleration spike of approximately 2000 g. Without proof, it will be stated that this spike is not data and it will be ignored in all subsequent discussion. Its cause is attributable to X-ray products resulting from the nuclear detonation arriving at time zero.

Maximum peak-to-peak response of the filtered data records for both tracks 5 and 6 shown in Figures V.23 and V.24 was approximately 1,000 g. This corresponded to only 10 percent of the unfiltered amplitude of the data recorded as track 5 and 15 percent of the unfiltered amplitude of the data recorded as track 6. A question then arises as to the validity of this filtered data.

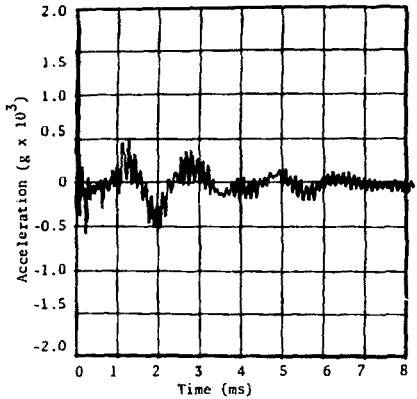

Figure V.23. Filtered acceleration time history for track 5

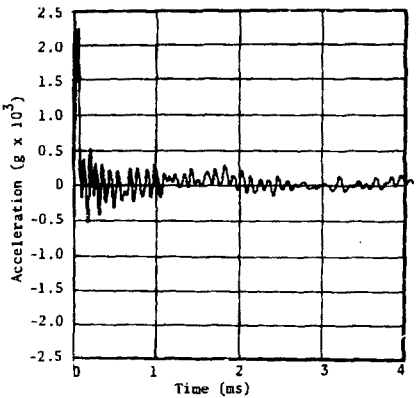

Figure V.24. Filtered acceleration time history for track 6

Figure V.25 illustrates a 4.096-millisecond sample of record baseline after the completion of the acceleration response on track 6. This represents channel noise level. The maximum magnitude of the acceleration-equivalent noise response is 850 g peak-to-peak. Note that this is essentially the same magnitude as the filtered records it is desired to treat as data! Passing this digitized noise record through the same digital filter as the acceleration signal on track 6 results in the plot of Figure V.26. The maximum peak-to-peak range of the filtered noise is 250 g. A direct comparison of Figure V.24, the filtered signal plus noise, with Figure V.26 the later time filtered noise, indicates that the acquisition of meaningful data on this or similar noisy channels is unlikely.

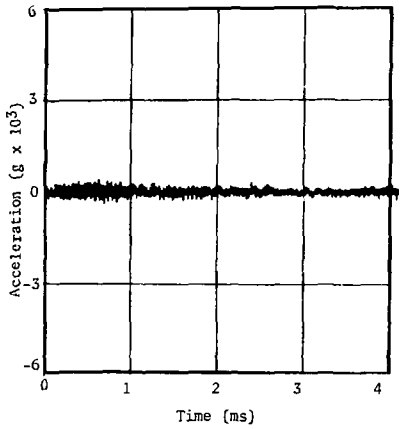

Figure V.25. Noise versus time for track 6

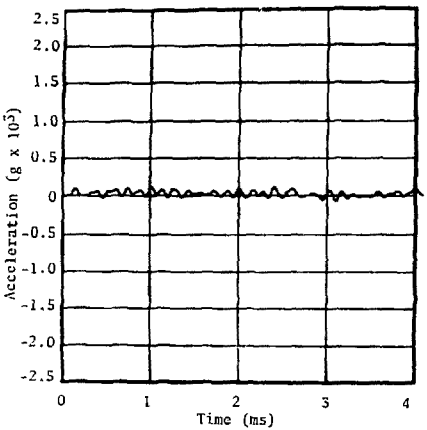

Figure V.26. Filtered noise versus time for track 6

This chapter has shown some of the consequences of an attempt to develop meaningful information for the structural dynamicist by filtering transient signals to remove distortion caused by the resonant characteristics of the measuring transducer. In these examples, all filtering occurred during data playback after a signal had been processed through the entire instrumentation system. Digital, as opposed to analog, filtering was employed primarily for convenience. The technique used a filter design intended to reject effects of the resonant characteristics of the transducer while passing without distortion the signal attributable to either the structural response or the forcing function to the structure over the range of frequencies to which it could significantly respond.

There are many classes of problems which can be analyzed through mathematical inversion techniques such as inverse Fourier transforms or deconvolution. Since both the structural forcing functions and the responses analyzed in this chapter possessed Fourier transforms, it may not be readily apparent why these techniques were not applied to this problem. Subsequent chapters will attempt to resolve this question. In addition, it will be shown that postfiltering of the data, by either digital or analog techniques, is not a good approach to solving the particular problem of interest. Instead, analog filtering must be provided within the instrumentation system before recording.

Summary and Conclusions

1. If the instrumentation channel is driven into its nonlinear range, accurate measurement definition of the structural dynamics problem is not achieved. This can be attributed to either channel nonlinearities being undefined or frequencies being created and lost in the data transmission process.
2. In the examples presented, the ratio of channel amplitude range required to linearly pass the resonant transducer response to that which would have been required to pass only that portion of the signal containing information about the structure varied from 116 to 1000 percent.
3. If energy in the signal is primarily associated with the transducer resonant characteristics, electrical noise may preclude meaningful structural dynamics measurements. This situation can occur even though the instrumentation channel operates within its linear range.
4. The resonant characteristics of the transducer must be high enough

in frequency to be separable from those frequencies to which the structure possesses significant response. This permits definition of the structural dynamics problem through "data separation" considerations in the frequency domain.

5. Actual data have illustrated the fact that resonant transducers cannot define the shock front in a blast environment because the loading excites high frequency resonances.
6. All of the data analyzed previously had been accepted as containing valid structural response information during development testing programs. (The problem is not hypothetical.)
7. It was possible to examine the validity of several test records only because of the availability of the wide bandwidth data which included that due to the resonant characteristics of the measuring transducer. If these signals had been multiplexed over narrower bandwidth channels, "cosmetically" better appearing records would have been acquired. However, these multiplexed records would have been devoid of meaningful information although that fact might not have been apparent.

CHAPTER VI

LIMITATIONS WHICH PRECLUDE INVERSE PROBLEM TREATMENT

Chapters IV and V have illustrated that both signal distortion and analytically unpredictable signal magnitude are associated with structural dynamics measurements. It was stated that the signals resulting from these measurements cannot have their inaccuracies corrected by an inverse problem treatment. Specific limitations which preclude this treatment are:

1. the inability to adequately experimentally characterize the transfer function of the measuring transducer,
2. modification of this transfer function by the technique in which the transducer is coupled to its desired stimulus, and
3. modification of the desired stimulus by the presence of the transducer.

For piezoelectric transducers, the electrical boundary conditions at the transducer output can modify crystal stiffness and therefore transducer transfer function. If all these limitations were understood, measurement systems would be better applied and improved data quality would result.

A recent report[19] issued by the National Bureau of Standards regarding measurement accuracy standards relative to the needs of U.S. industry describes these limitations. Some quotes from this report follow.

> "The system of standards and measurement techniques for dynamic force is substantially nonexistent."
>
> "Dynamic pressure measurements are without central calibration

support, as are measurements under extreme conditions of vibration, temperature, or corrosion."

"The most serious problem in measurement of vibration and shock is the general lack of applicable knowledge as to how to select the proper instrumentation, install it adequately, and interpret the results correctly."

"Significant work needs to be done to redefine the shock calibration service."

The following sections detail these limitations for acceleration, force, and pressure measurements.

Acceleration

Limitations in Defining the Transfer Function

The fundamental dynamic calibration service provided for accelerometers by the National Bureau of Standards is absolute calibration through the measurement of displacement. If a vibration exciter possesses sinusoidal uniaxial motion of low distortion, a determination of its peak displacement A, along with its frequency f, permits the calculation of peak acceleration, $4\pi^2 f^2 A$. A knowledge of the acceleration of the vibration exciter over a frequency range of interest, along with the output response of the accelerometer being calibrated, permits determination of an accelerometer's transfer function. This assumes the motion of the accelerometer to be the same as the motion of the exciter at the point where displacement is measured.

Photometric interferometry is used to determine vibration exciter peak displacement through a fringe disappearance technique over the frequency range of 1,500 to 10,000 Hz. Other optical techniques are used at lower frequencies. The calibration report issued by NBS specifies a maximum uncertainty of two percent for accelerometers calibrated to 10,000 Hz.[20] Above 10,000 Hz, NBS provides some limited calibration service although it is seldom requested and uncertainties increase by an order of magnitude over the next higher frequency octave.

For a National Bureau of Standards calibrated accelerometer to be useful, it must be possible to perform a comparison calibration to transfer its sensitivity through the calibration chain. An intermediate vibration transfer standard is typically a "piggyback" accelerometer. The "piggyback" is an accelerometer which has an inverted sensing element attached to the underside of its top mounting surface. This configuration minimizes transmissibility errors between the "piggyback" and the reference or test accelerometer coupled directly to this top mounting surface. Transmissibility errors can be created due to differences in mass and mounting surface area among accelerometers calibrated on the "piggyback." Difference of mass has been shown to produce errors of one to two percent to 10,000 Hz, while varied mounting surface area can create transmissibility errors of slightly less than one percent to 10,000 Hz.[21] These errors are in addition to uncertainties discussed previously, and are also separate from electronic instrument errors in amplifier gain, stability, etc. Problems associated with comparison calibration have not been adequately studied above 10,000 Hz.

The transfer function for an accelerometer can also be determined by transient excitation methods. Knowledge of the frequency spectrum of an input transient $I(j\omega)$, along with test accelerometer response $R(j\omega)$, can provide both amplitude frequency response and phase frequency response of a linear accelerometer. This technique has been successfully used at the Boeing Company, Seattle, Washington,[22] and the National Bureau of Standards.[23] The primary advantage of this method is that it is faster than sinusoidal vibration calibration. No improvement of input transfer function definition is obtained, however, since knowledge of $I(j\omega)$ requires a reference accelerometer such as a "piggyback" which has been calibrated on a vibration exciter. Several other transient calibration schemes which have found application will be noted. These are not, however, generally used for transfer function determination.

One technique employs Hopkinson bars and the application of elementary bar theory.[24] According to this theory, the acceleration at the bar's end is:

$$C_o \frac{\partial \epsilon_{xx}}{\partial t} \qquad \text{(VI.1)}$$

where C_o is the wave velocity and $\partial \epsilon_{xx}/\partial t$ is the time derivative of strain in the bar. One problem with this technique is the influence of the accelerometer on the bar's motion. This is discussed in the following pages when the problem of interfacing the accelerometer with its desired stimulus is considered.

Another transient calibration scheme involves impacting a test carriage or fixture on which an accelerometer is mounted and integrating the accelerometer's resultant charge or voltage-time response. The

accelerometer must operate within its linear range for this integration to provide meaningful data. The ratio of this integral to an independent measurement of test fixture velocity change can then be calculated and sensitivity determinations made.

Based upon limitations alluded to in the national systems of standards, a reasonable upper limit for the quantitative determination of the transfer function of an accelerometer is 10,000 Hz. It follows that this limitation also determines the maximum upper limit for quantitative acceleration measurements of the structural response of engineering systems.

Limitations in the Interface to the Desired Stimulus

When an accelerometer is coupled to a structure, one or both of two effects can occur:

1. the transfer function of the accelerometer determined in calibration can be modified by the coupling process, or
2. the structure's own transfer function can be modified by the presence of the accelerometer.

In considering effect 1, it is noted that information generally supplied with an accelerometer by the manufacturer includes the maximum frequency to which its amplitude response will be flat within a few percent when the optimum mounting technique is used. Typically, this mounting is by means of a threaded stud onto a flat surface of fine finish. The initial mounting torque applied must preload the accelerometer sufficiently so that it will not separate from a test structure in application. In actual practice, it may not be possible to tap a hole in a structure to attach an accelerometer, the mounting

surface afforded by the structure may not be flat, or the structure may not possess adequate thread strength when tapped. To overcome these limitations, coupling to the structure can be by means of helicoils, adhesives, interface blocks, etc. Insulated studs are used in some situations for electrical noise considerations when using piezoelectric accelerometers. All of the variations in mounting technique tend to degrade the response of the accelerometer from that specified by the manufacturer by introducing lower frequency resonances which distort the accelerometer's frequency response.

One of the most detailed experimental studies of these effects is found in Reference 25. Figure VI.1, from the referenced study, illustrates how the frequency response of an accelerometer is degraded from that achievable by using a solid stud when the accelerometer is mounted using either interface blocks of varying geometry or an insulated stud. Reference 26 details how various mounting surface finishes influence accelerometer frequency response. In general, each mounting technique must be evaluated individually to determine how it modifies the transfer function of the accelerometer as compared to that determined under its optimum mounting condition.

Effect 2 noted that the transfer function of the structure can be modified by the presence of an accelerometer. This effect can be evaluated by accounting for the mechanical impedance of the structure relative to that of the accelerometer. This analysis is useful since mechanical impedance can be thought of as a measure of the resistance of a system to motion. It is the complex ratio of sinusoidal force to sinusoidal velocity, i.e.,

$$Z = \left(\frac{F}{V}\right) e^{j\theta} \quad . \tag{VI.2}$$

For a linear elastic structure subjected to a fixed harmonic forcing function, the presence of an accelerometer will modify the structural motion such that

$$V_f = V_i\left(\frac{Zs}{Zs + Za}\right) \tag{VI.3}$$

where

V_f is the velocity experienced by the accelerometer,

V_i is the structure point velocity without the accelerometer attached,

Z_s is the mechanical impedance of the structure, and

Z_a is the mechanical impedance of the accelerometer.

Accelerometers with very light internal damping may be modeled as a pure mass to about 0.9 times their resonant frequency.[27] The mechanical impedance of an accelerometer having mass m is then:

$$Z_a = j\omega m \quad . \tag{VI.4}$$

Equation (VI.3) shows that for the structure itself to be modeled as a lumped mass, its mass must be more than nine times that of the test accelerometer to produce less than a ten percent error in measured motion.

A more realistic problem can be investigated by studying the effect of a typical accelerometer weighing eight grams on the motion of the free end of a long thin aluminum rod harmonically excited at the other end. The rod will be assumed to be made with a length to diameter ratio of 20. Calculations will be made at 0.5 times the natural frequency of

the first longitudinal rod mode. For a 30 inch (1 in. = 0.0254 m) long rod, this corresponds to a frequency of 1,677 Hz, while for the eight inch rod this corresponds to 6,289 Hz. For a given rod length, loading errors will become greater as higher frequencies are considered.

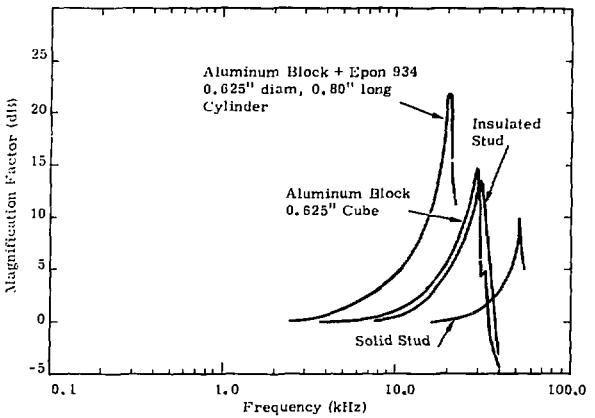

Figure VI.1. Degradation of the frequency response of an accelerometer by different mounting techniques

The partial differential equation governing rod free vibration was presented as Eq. (IV.5). Application of the boundary conditions:

$$EA \frac{\partial u(0, t)}{\partial x} = P \sin \omega t \quad \text{and} \quad EA \frac{\partial u(1, t)}{\partial x} = 0, \tag{VI.5}$$

along with separation of variables in the governing equation, leads to the solution form:

$$u(1, t) = \frac{P}{\sqrt{E\rho}\ \omega A} \frac{1}{\sin (\omega L/\sqrt{E/\rho})} \sin \omega t \, . \tag{VI.6}$$

Rod transfer impedance at the free end can be expressed as:

$$Z_s = -j\sqrt{EP}\,A \sin\left(\omega l/\sqrt{E/P}\right) \qquad \text{(VI.7)}$$

The effect the accelerometer has on the motion of the free end of the rod then becomes a function of rod length. This can be investigated using Eq. (VI.3).

Rod Length (in.)	V_f/V_i
30	1.006
15	1.046
8	1.406

Clearly, the presence of an accelerometer can modify structural motion if its impedance is significant relative to that of the structure.

Force

Limitations in Defining the Transfer Function

There are only a few applications in which the dynamic model of a force transducer fits the same dynamic model as pressure and acceleration transducers. These occur primarily in impact studies where the elasticity of the impacting mass can be ignored. This requires the stiffness of the impacting mass to be very high relative to the stiffness of the force transducer. In situations where the assumption is valid, dynamic force traceability can be achieved through mass and acceleration standards.

A vibration exciter is used to provide stimulus to calibrate the

force transducer. The impacting mass is attached to the top of the force transducer, a standard accelerometer is mounted on top of the mass, and a transfer function is derived by operating the vibration exciter over a range of frequencies at a known acceleration level which is controlled by the standard accelerometer. In assigning a sensitivity value to the force transducer, the mass of the standard accelerometer, the effective mass of the standard accelerometer's cable, and the effective mass of the force transducer must be considered. Reference 28 details a procedure to account for these effects.

Since transfer function determination for force transducers is dependent upon dynamic acceleration standards, the frequency range for force calibration is limited by the range of accelerometer calibration. Quantitative results are not currently achievable for frequencies higher than 10,000 Hz.

Limitations in the Interface to the Desired Stimulus

In other situations, which are not considered here, the force transducer cannot be modeled as a resonant device but must be considered as a part of the structural system. This situation is typically encountered in experimental determinations of mechanical impedance.

The experimental determination of mechanical impedance involves the measurement of both force input and acceleration response. The most common method of making this determination involves the direct approach of using transducers that convert force and acceleration response into electrical signals. A mechanical impedance head is a transducer with built-in force and motion measuring devices. The motion measuring device is typically an accelerometer since velocity and displacement

transducers tend to provide low signal levels at high frequencies and small amplitudes of motion.

In analyzing the structural system with the impedance head inserted, both the stiffness of the impedance head and its effective mass must be accounted for. The importance of the effective mass is evident at minimum values of impedance, while at peak values of impedance the stiffness must remain high to avoid false motion indications produced by dynamic stresses. The bolt securing the impedance head to the structure must also be considered since it becomes part of the load bearing structure.

Pressure

Limitations in Defining the Transfer Function

Dynamic pressure measurements are required in many applications in addition to those where it is desired to define the forcing function to structural systems. A few examples include the determination of internal and exhaust pressures in jet and rocket engines, cylinder pressure in internal combustion engines, pressure in air guns, and pressure in wind tunnels. Because of the large demand for dynamic pressure measurements, and because of a lack of central calibration support at the National Bureau of Standards, dozens of independent calibration schemes have evolved. The literature devoted to the dynamic calibration of pressure transducers is voluminous, repetitive, and in some instances erroneous. Fortunately, two documents condense a large portion of this information: NBS Monograph 67[29] and ANSI B88.1-1972.[30]

The transfer function of dynamic pressure transducers can also be

determined during either periodic or transient excitation. Techniques involving periodic excitation will be discussed first.

Greater problems are encountered in generating purely sinusoidal pressure than in generating sinusoidal displacement or its derivatives. When generating periodic gas pressure with a piston-in-cylinder device, the shape of the pressure wave is determined by the piston motion, the gas dynamics and acoustic factors associated with the phenomena, friction effects at the lateral boundaries and inherent in the gas, and, when the motion of the gas is forced into its nonlinear domain, shock fronts.

Present sinusoidal pressure calibration techniques do not meet the amplitude, frequency, and accuracy requirements of many applications. The word calibration is actually a misnomer since most sinusoidal dynamic pressure calibrators require a "reference" transducer. With no traceability to the National Bureau of Standards for the calibration chain for dynamic pressure, the "reference" performs a comparison function rather than a calibration function. The sinusoidal pressure generators which are most widely used can be generally categorized as acoustic resonators, variable volume generators, or variable mass generators.

Acoustic resonators operate on the principle of a driving device operating into a chamber of specific geometry containing a specific fluid. Changing the frequency of operation requires varying either or both the chamber dimensions and working fluid.

Variable volume generators use a fixed mass of working fluid which is alternately compressed and expanded within a small chamber. Assuming the gas compression to be isentropic and the chamber to be of constant

cross sectional area:[59]

$$\frac{p}{p_o} = \left(\frac{x_o}{x}\right)^k \qquad \text{(VI.8)}$$

where p_o and x_o are the pressure and piston or diaphragm position at equilibrium, k is the ratio of gas specific heats, and p and x are pressure and piston or diaphragm position at any given time. Because the displacement dependence is not linear ($k \neq 1$), a sinusoidal piston displacement will not result in a sinusoidal pressure response.

Variable-mass generators use a fixed volume chamber where the mass flow into and out of the chamber is cyclically varied. Typically, a rotating disc with holes on its periphery is used to interrupt the mass flow from the chamber, resulting in a pulsating chamber pressure.

Figure VI.2, from the ANSI B88-i 1972 document referenced earlier, summarizes the amplitude and frequency capabilities of the various periodic pressure generators studied and reported in the literature.

The transient calibration of pressure transducers is accomplished through the use of devices such as quick opening valves or pulse type generators. Determination of the transfer function of the transducer being calibrated is limited by lack of knowledge of the true time history of the pressure stimulus. The shock tube is generally accepted as the classical transient technique to qualitatively evaluate the dynamic performance of pressure transducers.

A shock tube consists essentially of a rigid tube divided into two sections by a gas-tight frangible diaphragm mounted normal to the axis. A pressure difference is applied across the diaphragm. When the diaphragm is ruptured, the pressure tends to equalize, resulting in a

shock wave traveling into the low pressure region and a rarefaction wave traveling into the high pressure region. Provided the tube is of constant cross-section, the shock wave ideally is unattenuated with distance and the pressure and particle velocity will be constant over a region behind the shock. The amount of time the pressure remains constant behind the shock front is a function of many parameters, the most important of which is the shock tube chamber lengths.

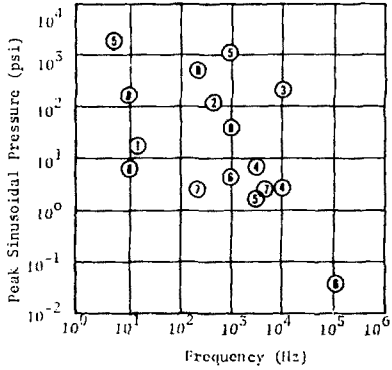

1. Rotating valve (gas)[29]
2. Electrodynamic pistonphone (liquid)[29]
3. Piezoelectric (liquid)[31]
4. Variable mass (gas)[32]
5. Hydraulic pistonphone (liquid)[31]
6. Fluidic pressure generator (gas)[33]
7. Resonant, variable frequency (gas)[34]
8. Inertial piston (liquid)[35]

Figure VI.2. Amplitude and frequency capabilities of various periodic pressure generators

A transducer mounted flush in the sidewall of the low pressure section experiences a step pressure of rise-time approximately equal to its diameter divided by the shock wave velocity. For a 0.1 inch diameter transducer measuring mach 1.5 air at ambient temperature, this rise time corresponds to approximately four microseconds. A pressure transducer mounted flush in an end plate which seals off the low preasure section of the shock tube will experience a step pressure which for weak shocks is approximately double the sidewall pressure, with a risetime on the order of nanoseconds.

The fifth illustration of Figure VI.3 portrays a situation where a useable pressure step would be impinged on a transducer mounted in the closed end plate of a shock tube. For shock tubes of dimensions compatible with a calibration laboratory (e.g., 25 feet in length), the duration of the sustained pressure step is typically a few milliseconds. Reference 36 develops most of the equations used in shock tube applications.

The advent of high speed analog to digital converters, along with advances in digital signal processing, have permitted shock tubes to be used to quantify the transfer functions of pressure transducers. The nanosecond order risetime is adequate to excite all the significant high frequency modes associated with any flush mounted pressure transducer. A significant problem may arise, however, if the transducer's starting transient response is not complete at such time as the step pressure is no longer sustained. When such a situation occurs, and it typically does, the assumption of an input frequency spectrum $1/j\omega$ associated with a pressure step to the transducer is violated.

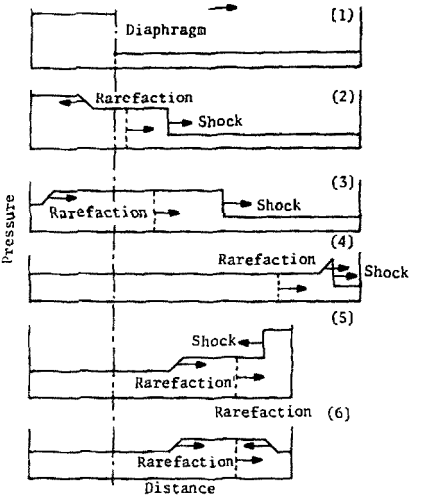

(1) Before diaphragm is burst
(2) After burst and before reflection of rarefaction
(3) After reflection of rarefaction
(4) Reflected rarefaction overtakes shock wave
(5) Shock wave reflected by closed end of tube
(6) Rarefaction wave reflected by open end of tube

Figure VI.3. Shock tube pressure at various times and for various boundary conditions

To elaborate on this last point, assume the pressure step in the shock tube is sustained for 0.002 second and that a measuring transducer will respond as a lightly damped ideal oscillator with step response approximately equal to

$$s(t) = \frac{1}{k}\left(1 - e^{-\zeta\omega_n t} \cos \omega_{nd} t\right) \qquad \text{(VI.9)}$$

where

k is the spring constant,

ω_n is the angular natural frequency = $2\pi f_n$,

ζ is the viscous damping factor, and

$\omega_{nd} = \sqrt{1 - \zeta^2}\,\omega_n$.

A reasonable value for ζ estsblished in Chapter IV is 0.01. For the transducer to settle to within ten percent of the step response in 0.002 second, it must possess a natural frequency greater than 18,000 Hz.

One method[37] used in industry to attack this problem is to force the transient response to return to the steady state step value by conditioning the transducer's signal through a low pass filter. The data are then manipulated by synthesizing a negative going pressure step function, equal in magnitude to the original positive going step function, at some time before the input step is no longer sustained. The input forcing function is treated as a rectangular pressure pulse.

Two limitations in this technique are obvious:

1. the low pass filter limits the upper frequency of analysis, and
2. the Fourier transform of a rectangular function in time is a sin x/x function in the frequency domain which has holes in the input spectrum.

The computer analysis of shock tube data shown earlier in this report used Sandia Laboratories' program TRANFUNC.[38] For the duration that the input pressure step in the shock tube remains constant, the

transducer response r(t) is approximated by connecting discrete data samples with straight line segments. The program does not depend on equal sample intervals, and it adds a factor to account for truncation of the input pressure step. Details of the procedure used by this program are included in Appendix B.

The calculation described a few paragraphs earlier noted that a viscous damping factor having a value of 0.01 in an oscillator with an 18,000 Hz natural frequency would produce a return to within ten percent of a steady state response within 0.002 second. Figure B.2 in Appendix B permits determination of the error in transfer function determination which is attributable to the magnitude alone of the truncation error in such a system. TRANFUNC should provide reasonable definition of the transfer function of the oscillator (within five percent) to 10,000 Hz.

This discussion emphasizes that the transfer function of pressure transducers, which is similar to those of accelerometers and force transducers, cannot be determined under periodic excitation at reasonable signal levels past 10,000 Hz. The step excitation available from a shock tube is an effective method for partially defining the transfer function of a pressure transducer and, depending on the duration of the pressure step behind the shock as well as transducer fundamental resonance and damping, may permit quantitative determinations past 10,000 Hz. Neither periodic nor transient techniques permit complete definition of the transducer transfer function.

Limitations in the Interface to the Desired Stimulus

Effects to be considered when interfacing a pressure transducer to a pressure environment include:

1. the transfer function of the pressure transducer determined during calibration can be modified by the coupling process, and
2. the environment can be modified by the presence of the transducer.

When modification of the environment by the presence of the transducer is of concern, it can be accounted for by impedance type concepts.

The mechanical impedance (Z) of the pressure receiver of a pressure transducer can be defined as:

$$Z = \frac{\Delta p}{\Delta V} \tag{VI.10}$$

where ΔV is the incremental change in volume of a pressure receiver due to incremental pressure change Δp. The elastic constant (K) of the pressure receiver can be defined as:

$$K = \frac{\Delta f}{\Delta x} \tag{VI.11}$$

where Δf is the incremental force applied to the pressure receiver and Δx represents receiver displacement. An effective area (A_{eff}) can then be defined such that:

$$\Delta p = \frac{\Delta f}{A_{eff}} \tag{VI.12}$$

and

$$\Delta V = A_{eff} \Delta x \quad . \tag{VI.13}$$

Combining terms results in the mechanical impedance of the pressure

receiver being redefined as:

$$\chi = \frac{K}{A_{eff}^2} \quad . \tag{VI.14}$$

When considering pressure fronts in a blast wave, except in a very small chamber, the energy absorbed by the pressure transducer is minimal, thus justifying the assumption of an infinite mechanical impedance for the pressure receiver. This assumption is not valid, however, for liquid media in chambers that are both small and rigid. In this latter situation, even when the dynamics of the transducer are good enough to give an accurate pressure measurement, the result will not represent the conditions which exist when no transducer is attached to the chamber.

In discussing modifications in the transfer function of a pressure transducer by the coupling process, it will be assumed that the transducer selected for the measurement has a fully exposed flush diaphragm such that no internal cavities are created by the transducer itself. The ideal configuration in mounting would be to position the transducer diaphragm so that no spurious resonances occur due to organ pipe or cavity effects. It may occur, however, that requirements exist to record rapidly changing pressures from a pressure tap located where a pressure transducer cannot be flush mounted. It may also be necessary to mount the pressure transducer remotely from the environment to isolate it from a high heat source. In such cases, the transducer is coupled to the environment through a length of tubing. This tubing can degrade the dynamic performance of the pressure measuring system.

The effect of tubing terminating into a flush diaphragm transducer of diameter equal to the tube diameter can be studied by investigating

longitudinal waves in a column of gas. The assumptions which follow,

1. the tube is sufficiently narrow for the displacement at any instant to be the same at all points on any cross section,
2. friction can be neglected along the sides of the tube, and
3. the process is adiabatic,

permit derivation of a linear partial differential equation governing pressure in the gas column. The result is:[40]

$$\frac{\partial^2 p}{\partial x^2} = \frac{1}{c^2}\frac{\partial^2 p}{\partial t^2} \qquad \text{(VI.15)}$$

where $c^2 = kP_o/\rho_o$. In this derivation, P_o is ambient pressure, ρ_o is ambient density, p is a small pressure variation superimposed on P_o, t is time, x is the coordinate along the axis of the gas column, and k is the ratio of gas specific heats. This equation may be investigated for the specific case where the gas column has an open end at x = L and a closed end at x = 0 (the transducer). Boundary conditions are:

$$p = 0 \quad \text{at} \quad x = L \quad \text{and} \quad u_{,t} = 0 \quad \text{at} \quad x = 0 \qquad \text{(VI.16)}$$

where u is particle motion of the gas column and $u_{,t}$ is particle velocity. Solution of the partial differential equation yields the eigenfrequencies as

$$f_n = \frac{(2n-1)\,c}{L} \text{ Hz} \quad , \quad n = 1, 2, 3 \ldots \quad . \qquad \text{(VI.17)}$$

The fundamental natural frequency of a gas column of dry air with one closed end is plotted in Figure VI.4 as a function of column length for three different gas temperatures. In some texts the L in the previous equation is taken to be the tube length summed with 0.6 times the tube radius. The fundamental natural frequency is of prime importance since

it limits the frequency response of the pressure measurement. The amplitude of pressure response at the higher natural frequencies is reduced by damping which has to be accounted for in actual systems.

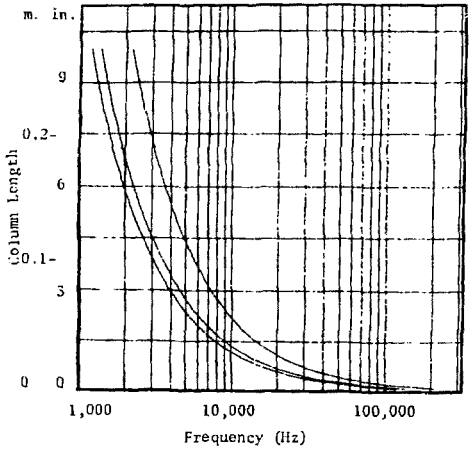

Figure VI.4. Fundamental natural frequency of a column of dry air with one closed end (upper curve is at 500°C, middle curve is at 25°C, lower curve is at -50°C)

In other mounting techniques, the flush diaphragm of the transducer is exposed to an enclosed volume (V) of gas which is connected to the environment by a smaller circular aperture of length L and area πa^2. Based on the assumption that all dimensions are much less than the wavelength of sound at the frequency at which the system is designed to operate, an analysis of this cavity as a single degree of freedom system

can be performed. The plug of gas in the circular aperture acts as a mass, and the enclosed volume acts as a spring. The Helmholtz resonator model[40] yields a natural frequency equation for this type of coupling such that:

$$f = \frac{c}{2\pi}\sqrt{\frac{\pi a^2}{V(L + 1.7a)}} \quad \text{Hz} \quad . \tag{VI.18}$$

For the Helmholtz resonator, or any gas filled tube, predictability of natural frequency is poor when the gas composition is unknown since gas density varies so greatly with gas type.

A common mistake is to fill the feed line to the transducer with liquid.[41] The ringing which occurs in this situation is attributable to the mass of the liquid and the spring rate of the transducer diaphragm. Excessive overshoot to a step input has been observed to occur with such fluid filled lines.

When measuring the forcing function applied to structural systems from reflected overpressures from a shock wave, organ pipe or cavity effects may be adequate to account for other than flush mounting of the pressure transducer. In measuring static overpressure, where the transducer's diaphragm is mounted flush and in a plane parallel to the flow velocity vector, modification of the transfer function of the pressure transducer can still occur. High frequency waves normal to the axis of the transducer diaphragm can be distored. This distortion is attributable to averaging of the high frequencies of a spacially distributed wave as it traverses over the finite area of the transducer diaphragm.

Some insight into this problem can be achieved by treating the diaphragm as an ideal integrator. This treatment bypasses the determination of strain distribution within each of the numerous types of diaphragms due to a singular load, which would lead to a more rigorous but, hopefully, not a very different result. Reference 42 follows an approach similar to the one taken here in discussing the frequency response of length averaging sensors.

Appendix C provides an analytical study of the dynamic response of a flush-mounted circular-diaphragm pressure transducer, modeled as an ideal integrator, when attempting to measure static overpressure in an air blast. Results of the study indicate that the transfer function of the transducer can be modeled as

$$\frac{\lambda}{\pi r} J_1\left(\frac{2\pi r}{\lambda}\right) \qquad \text{(VI.19)}$$

where J_1 is a first order Bessel function, r is the transducer radius, and λ is the wavelength of the harmonic frequency of interest. Figure VI.5 plots such a transfer function for flush diaphragm transducers of diameters 1.0, 0.3, and 0.1 inch. A negative response indicates a 180 degrees phase shift. The horizontal axis of the plot, multiplied by the wave velocity, yields the response in Hz at any frequency of interest. As long as the transducer diameter is less than one-fifth the wavelength of the harmonic forcing function, Figure VI.5 indicates less than a five percent resultant measurement error. Figure VI.6 indicates a situation where distortion would occur in the measured pressure time history due to the transducer's diaphragm being too large.

The analysis of Appendix C is strictly for pressure waves moving normal to the axis of the transducer diaphragm. As the angle between the

flow velocity vector and the plane of the diaphragm is decreased, the exposed diaphragm area becomes elliptical in nature. Figure VI.7 illustrates this effect. At an angle of 90 degrees, the flow velocity vector is parallel to the diaphragm axis and the dynamic characteristics of the flush mounted diaphragm will dictate transducer response. This may be rephrased to state that at normal incidence there is no spatial dependency on transducer response. At lesser angles, this spatial dependency modifies the transfer function of the transducer.

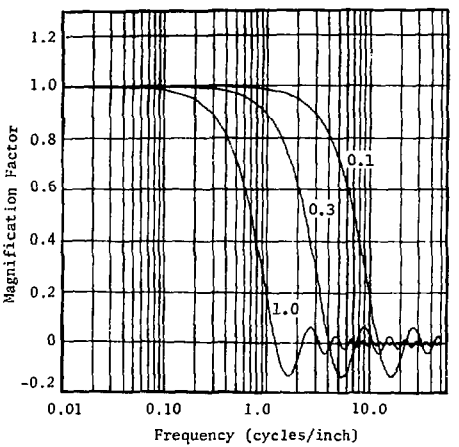

Figure VI.5. Transfer function of flush diaphragm pressure transducer when pressure wave is normal to diaphragm axis (response improves with diaphragm diameters of 1.0, 0.3, and 0.1 in.)

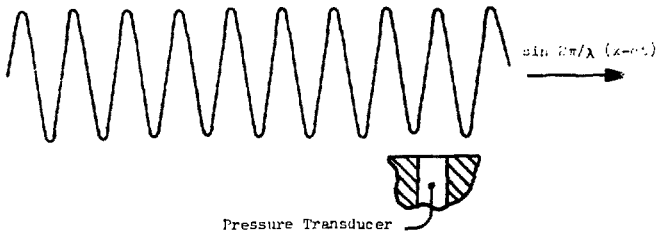

Figure VI.6. Cross section of flush-mounted circular-diaphragm pressure transducer measuring pressure wave

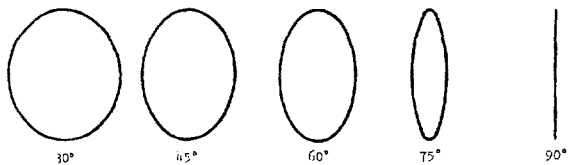

Figure VI.7. Change in effective integrating area of circular diaphragm with increasing angle of incidence of *propagating wave to plane of diaphragm*

Summary and Conclusions

1. Problems associated with generating accurately known periodic or transient accelerations, forces, and pressures generally preclude quantitative determination of a transducer's transfer function over a frequency range which includes even its fundamental resonant frequency. The upper frequency limit for quantitative assessment of the transfer function for most

accelerometers, pressure transducers, and force transducers is 10,000 Hz.

2. The inability to define completely the transfer function of the measuring transducer prohibits treating the data reduction problem of a signal recorded over a wide frequency bandwidth as an inverse problem.
3. The transfer function of the transducer may be modified by the process which couples it to the structure. In this situation, the fundamental resonant frequency which limits the measurement is no longer that of the mechanical sensing element associated with the transducer. In the case of pressure measurements, the limit can result from the fundamental resonance of a gas column between the sensing diaphragm and the location of the desired measurement. In the case of acceleration measurements, it can become the fundamental resonance of the mechanical mount securing the accelerometer to the structure.
4. Assuming the transducer is producing the desired response to the desired stimulus, maximum accuracies to be expected in defining structural response in blast, crash, and impact environments will be within three to five percent. Digitization of the measured signal to a precision in excess of eight bits, excluding sign, is unnecessary.
5. When integrated into a structure, force transducers are not characterized by a dynamic model compatible with the problem under consideration in this study. The select case of a flush-mounted pressure transducer, with a diaphragm possessing a high fundamental resonant frequency and measuring high frequency

components of static overpressure, also may not be characterized by a dynamic model compatible with the problem under consideration in this study.

6. As in all measurement situations, care must be taken to assure that the measurand is not severely modified by the presence of the transducer. This can be accounted for by impedance type concepts.

CHAPTER VII

CHARACTERIZATION OF THE MEASURING TRANSDUCER

Chapter VI described the difficulties which exist in experimentally characterizing the transfer function of measuring transducers used to determine structural forcing functions and response. It was noted in Chapter II that in structural testing there is some upper frequency limit above which structural response becomes small enough to be ignored. The majority of data requirements were observed to be in the range of 10 to 2,000 Hz, with an upper frequency limit always below 10,000 Hz. In Chapter VI, it was subsequently determined that quantitative assessment of the transfer function of the measuring transducer was possible to 10,000 Hz, indicating compatibility between verification requirements and verification capabilities.

The measurement problem of interest was developed in Chapter IV by dynamically modeling the transducer as a lightly damped oscillator. The results of the present chapter will not depend upon this elementary model. However, an understanding of the viscous damped system with governing equation:

$$\ddot{x} + 2\zeta\omega_n\dot{x} + \omega_n^2 x = F(t) \quad , \tag{VII.1}$$

coupled with the results in Chapters IV and V, should raise two questions:

1. Can the resonant characteristics of a transducer be suppressed by damping?
2. Is it possible to use a measuring transducer with an extremely high resonant frequency to increase the separation between the

structural response and the transducer resonant characteristics in the resulting signal frequency spectrum?

In this chapter, the consideration of these two questions will lead to an investigation of transducer technologies applicable to the measurement problem. Finally, those dynamic characteristics which must be known about the resonant type transducer before applying it to measurement situations of interest will be described.

Concerning the first question, the solving of Eq. (VII.1), using a viscous damping factor of 0.7 ($\zeta = 0.7$), results in the maximum flat amplitude-frequency and the phase-frequency curves of Figures VII.1 and VII.2. The abscissas are normalized to the undamped natural frequency. The amplitude response of a system represented by such an equation is reasonably flat (within five percent) and the phase response reasonably linear (within a few degrees) to 0.6 of the undamped natural frequency, ω_n. The requirement for flat frequency response and linear phase response to preclude distortion of dynamic data was established in Chapter III. The system's amplitude response, illustrated in Figure VII.1, is attenuated approximately 30 percent at the transducer's undamped natural frequency, while the elementary model used in Chapter IV assumed a 5000 percent amplification ($\zeta = 0.01$) in response at the undamped natural frequency. Thus, the addition of damping to measuring transducers is shown to be a desired improvement when they must respond to either short duration transient forcing functions or to transients containing discontinuities.

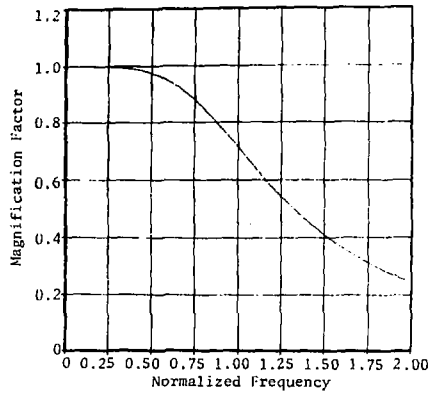

Figure VII.1. Linear second order system amplitude-frequency response with 0.7 viscous damping factor

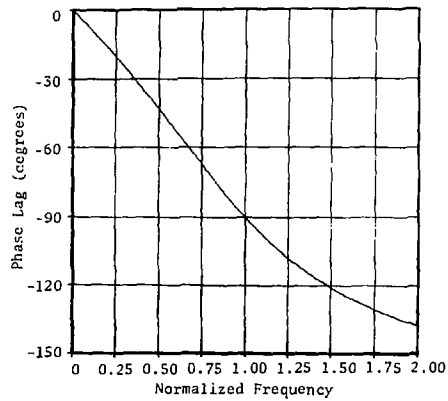

Figure VII.2. Linear second order system phase-frequency response with 0.7 viscous damping factor

The question of why transducers are not always damped, as well as the question of why extremely high resonant frequency transducers are not always used, can be considered in terms of the mechanical properties of the transducer flexure. It was earlier noted that cantilever beams and fixed edge circular plates represent two typical types of flexural elements used in transducer design. The following definitions are provided:

E = Young's modulus

L = beam length

I = beam area moment of inertia

a = plate radius

t = plate thickness

ν = Poisson's ratio

μ = mass/unit length

ρ = mass/unit area

The natural frequency (in radians/second) for the first circular mode of vibration of a fixed edge circular plate is:[44]

$$\omega_n = \frac{(1.015)^2}{a^2} \sqrt{\frac{Et^3}{12\rho(1-\nu^2)}} \quad . \tag{VII.2}$$

The natural frequency (in radians/second) for the fundamental mode of vibration of a cantilever beam is:[44]

$$\omega_n = 3.516 \sqrt{\frac{EI}{\mu L^4}} \quad . \tag{VII.3}$$

The sensitivity of a transducer of the type used to measure structural dynamics is proportional to the compliance of its flexural element. The

compliance is the flexure deflection (y) per applied load. The compliance of a cantilever beam subjected to an end load (F) is:[45]

$$\frac{Y}{F} = \frac{L^3}{3EI} = \frac{4.121}{\mu L \omega_n^2} \quad . \tag{VII.4}$$

The compliance of the center of a fixed edge circular plate to a uniform load (P) is:[45]

$$\frac{Y}{W} = \frac{3(1 - \nu^2)a^2}{16\pi E t^3} = \frac{0.236\ \rho a^2}{\pi^3 \omega_n^2} \tag{VII.5}$$

where $W = (P\pi a^2)$. The interaction between the resonant frequency and the sensitivity of a transducer can now be investigated.

The achievement of damping in mechanical systems requires energy dissipation. Energy dissipation in turn requires mass motion. A system with large compliance is the easiest to damp. In examining the preceding equations, it is found that each factor which increases the compliance of the transducer flexure also decreases its natural frequency and thus its frequency response. In addition, flexures with large compliances may be overstressed and driven into nonlinear regions by higher levels of transient force, pressure, and acceleration than those to which they properly respond. For this reason, damping transducers to suppress their resonant characteristics is possible only at low levels of the applied environment and at low frequencies. Transducers which are damped also may be objectionably large due to the requirement for this high compliance flexure. Examples of successful application of damping to transducers can be found in accelerometers operating to a few hundred g's and in condenser microphones measuring acoustic pressures.

Since damped transducers provide at most a limited solution to the problem of defining structural response, several transduction techniques which depend upon flexures of large compliance may be ignored. These sensing techniques include potentiometric, variable reluctance such as "E" core, force balance, unbonded strain gage, and linear variable differential transformer.

From the preceding discussion it is apparent that it is generally necessary to use lightly damped transducers, i.e., those possessing significant response at their fundamental resonant frequency, to define structural response or loading in severe transient environments. This is because a transducer flexure of low compliance is required in order to assure adequate frequency response and linear amplitude range. It is then appropriate to investigate transduction techniques which maximize the electrical signal associated with this low compliance fixture. This investigation leads to consideration of piezoresistive and piezoelectric technology.

A justification for the applicability of semiconductor technology to the measurement problem of interest can readily be made. The electrical resistance of a length of conductive element is:

$$R = \frac{\rho L}{A} \quad , \tag{VII.6}$$

where ρ is the resistivity of the conductor, L its length, and A its cross sectional area. A differential change in this resistance can be expressed as:

$$dR = \frac{R}{\rho} d\rho + \frac{R}{L} dL - \frac{R}{A} dA \quad . \tag{VII.7}$$

The volume change in the conductor associated with a change in resistance is:

$$dV = V_{final} - V_{initial}, \text{ or}$$

$$dV = L\ (1 + \epsilon)\ A\ (1 - \nu\epsilon)^2 - LA, \text{ or} \qquad \text{(VII.8)}$$

$$dV = AdL\ (1 - 2\nu) = AdL + LdA \ .$$

The last two lines can be written after noting that the strain ϵ is dL/L and ν is Poisson's ratio for the conductor. Terms in the last line with orders of ϵ^2 or higher have been ignored. If this last line of Eq. (VII.8) is solved for dA, dA substituted in Eq. (VII.7), and the resultant equation normalized by RL/dL, the definition of the gage factor for a strain gage will result, i.e.,:

$$1 + 2\mu + \frac{d\rho}{\rho/\epsilon} = \frac{dR/R}{dL/L} \ . \qquad \text{(VII.9)}$$

For metallic strain gages, the $d\rho/\rho/\epsilon$ term is not as important as for strain gages utilizing semiconductor elements.

The gage factor of a strain gage relates its unit change of resistance to the unit applied strain. Some typical values for metallic strain gages are:[46]

Nichrome (Ni-0.80, Cr-0.20)	+ 2.0
Advance (Ni-0.45, Cu-0.55)	+ 2.1
Iso-elastic (Ni-0.36, Cr-0.08, Fe-0.52, Mo-0.005)	+ 3.5

The metallic strain gage is usually a wire or foil ribbon mounted on some insulating backing material. The gages are then individually bonded to the transducer flexure and typically connected electrically into a

Wheatstone bridge configuration whose output is proportional to the applied environment (e.g., acceleration, force, or pressure). More sophisticated fabrication techniques than adhesive bonding utilize vacuum deposition, such as is used in the manufacture of electronic microcircuitry. The ceramic film, the metallic strain gage elements, and interconnecting leads are sequentially deposited in a high vacuum chamber directly onto the transducer flexure. This latter technique provides a measuring device with excellent stability, matched thermal coefficients, and minimal hysteresis and creep.

The basic definition of the gage factor indicates that to change from a lower to a higher resonant frequency transducer, and thus one with a flexure of lower compliance, the gage factor must be increased to maintain an equivalent electrical signal magnitude at the resulting reduced strain input. The use of semiconductor materials as the strain gage sensing element achieves a high gage factor. Whereas metals typically provide a gage factor of 2 to 5 in strain gage design, the gage factor for semiconductor materials typically varies from 50 to 200.[47] Semiconductor gages do display greater temperature dependency.

One type of semiconductor device is basically a bonded gage with doped silicon as the sensing element. Controlling the dopant in the silicon allows the gage properties to be optimized for various measurement applications. Gages are then bonded to the transducer flexure, electrically connected in a bridge network, and operated at low strain levels to avoid nonlinearities which are present in the gage factor for semiconductor materials.

Semiconductor technology also permits transducer fabrication using silicon as the basic flexural element, with diffusion of the strain

sensing elements occurring directly into the parent material. Diffusion permits use of the transverse or shear piezoresistive effect of the sensing elements as well as their longitudinal piezoresistive coefficient. Diffusion techniques also permit miniaturization, which enhances frequency response. In addition, since the modulus of elasticity for silicon is comparable to steel, and its density is only one-third that of steel, enhancement of frequency response and resonant frequency is possible due to improved material properties.

Piezoelectricity is another transduction technique capable of providing linearity over a wide range and of producing a useable signal magnitude. In addition, the modulus of elasticity of many piezoelectric crystals and ceramics is equal to or greater than that of some metals. Thus, these materials can be integrated easily into high frequency resonant systems.

Piezoelectricity is attributable to strain inducing a change in the shape of a crystal which possesses no center of charge symmetry. An electric charge results from this change in shape. Twenty-one of the 32 crystal classes lack this symmetry element, and crystals in all but one of these classes can exhibit piezoelectricity.

Any piezoelectric constant of a material expresses the amount of charge generated per unit applied force or its deflection per unit applied voltage. This is typically provided in tensor notation, such as d_{33} or d_{15}, with the first subscript identifying electrical direction and the second subscript identifying mechanical direction. A few values of two piezoelectric constants, in picocoulombs/newton, are presented to indicate why high sensitivity transducers can be fabricated utilizing these materials. Also presented is the Curie temperature for the

materials. The Curie temperature is the temperature above which a material is no longer piezoelectric.

Material	d_{33} (pC/N)	d_{15} (pC/N)	Curie temperature (°C)
PZT5A	380	595	>350
PZT8	215	335	>300
$BaTiO_3$	145	245	>115
$LiNbO_3$	6.2	70.5	>1200
SiO_2 (X cut quartz)	2.2 (d_{11})	0.85 (d_{14})	>576

Because of the many classes of piezoelectric materials, a detailed discussion of those most applicable to this measurement problem would be quite extensive. Of the 20 crystal classes which are piezoelectric, 10 possess a dipole in their unit cells and are pyroelectric. Thermal heating typically expands and contracts this dipole, thus generating an electrical charge. Ferroelectric materials are a subdivision of pyroelectric materials. Ferroelectrics are characterized by their dipoles being arranged within domains inside the crystal. Ferroelectric ceramics are polycrystalline ceramic masses of ferroelectric materials which have been processed to align all the dipole containing domains. Ferroelectric ceramics which are electrically soft, i.e., those which depolarize at low electric field levels, are not recommended for application in severe transient environments.[48]

The selection of the optimum semiconductor or piezoelectric material for a particular measurement application is best determined based on an understanding of the physics of the material and past experience with it. The important factor is that when integrated into transducers, these two types of material satisfy three key requirements

relative to measuring structural dynamics in severe environments:

1. They provide a linear response over a wide range.
2. They provide adequate signal levels so that valid data can be recorded when measuring transients possessing amplitudes which comprise only a small portion of the transducer's full range.
3. Their sensitivity is adequate to permit them to be designed into instruments with high resonant frequencies. This characteristic enhances separation of structural response from transducer resonant characteristics in the transducer's resultant signal frequency spectrum.

Transducers of the type being considered typically will display multiple resonances. These resonances may be associated with the transducer flexure and its higher modes, with the transducer housing, with the coupling technique which interfaces the transducer to the environment, or with internal components such as lead wires vibrating within the transducer. The frequencies at which these resonances occur are determinable although it is not always possible to provide similar precise information about the magnification factor associated with each resonance.

Previous discussion has identified test equipment capable of experimentally locating these resonant frequencies. Included were shock tubes, high frequency vibration exciters, and impulse excitation generators. For geometrically simple accelerometer adapter mounts, for known masses impacting force transducers, and for geometrically simple cavities for interfacing pressure transducers to their environment, location of the fundamental resonant frequency can be analytically determined with reasonable accuracy. Information regarding the resonant

characteristics of the transducer is also provided by the manufacturer. Since this latter information is controlled by design, it remains fixed for a given model of transducer within design tolerances.

The transducer should have a flat frequency response over the range of frequencies in which quantitative data are desired. Semiconductor and piezoelectric transducers capable of measuring a few pounds of force, g's, or psi are readily available with fundamental resonant frequencies in kHz. As the range of these instruments increases, this fundamental resonant frequency also increases into the tens or hundreds of thousands of Hz. These resonant frequencies are sufficiently high that, if care is taken in transducer mounting, uniform frequency response over that range in which a given structure possesses significant response can be assured.

A lightly damped resonant transducer has essentially a zero phase shift over the region where it has flat frequency response. This will be illustrated shortly by analysis and can also be noted in some of the experimentally derived transfer functions for pressure transducers which were presented in Chapter IV.

The conclusion reached from the preceding paragraphs is that a transducer which possesses flat frequency response and essentially zero phase shift over some low frequency region ultimately becomes limited by multiple resonances occuring at higher frequencies. The following two cases will cover the various combination of occurrence of these multiple resonances.

The initial case to be considered is the most common. This case treats the situation where the first resonance limiting the transfer function of the transducer is either the major resonance of the

transducer or its mount. In a properly designed and optimally mounted transducer, this first resonance could be associated with the fundamental mode of the flexure. Higher resonances, of lesser amplitude, could be associated with higher modes of this flexure or modes associated with the transducer housing. This first major resonance could also be associated with the mounting adapter that couples the transducer to the environment. Resonances occurring at higher frequencies would then be associated with both the transducer and the higher modes of this mounting.

Figure VII.3 illustrates this initial case with the simplifying assumption that there are only two resonances of concern. If m_1 is associated with the transducer flexure, then m_2 can be associated with a higher flexure, transducer housing, or mounting adapter mode. If m_1 is associated with the transducer adapter, then m_2 can be associated with a flexure, transducer housing, or higher mounting adapter mode.

The system of Figure VII.3 is described by two linear second order differential equations having constant coefficients. One equation is homogeneous, and the other is not. Since the equations are linear, solution forms

$$x_1 = Ae^{j\omega t} \qquad \text{(VII.10)}$$

and

$$x_2 = Be^{j\omega t} \quad ,$$

are justified. The desired transfer function for analysis is $A/(F/k_1)$. Substitution of the preceding values of x_1 and x_2 into these equations, along with cancellation of common factors and application of Cramer's

rule, produces the following results.

$$|\text{transfer function}| = \frac{\sqrt{RN^2 + IN^2}}{\sqrt{RD^2 + ID^2}}$$

$$\text{phase angle} = \tan^{-1}\left[\frac{(IN)(RD) - (ID)(RN)}{(RN)(RD) + (IN)(ID)}\right] . \qquad \text{(VII.11)}$$

The following definitions permit computation of these results.

$$RN = \left(\omega_{n2}^2 - \omega^2\right)$$

$$IN = 2\zeta_2\omega_{n2}\omega$$

$$RD = \frac{\omega^4}{\omega_{n1}^2} - \omega^2\left(1 + \frac{k_2}{k_1} + 4\zeta_1\zeta_2\frac{\omega_{n2}}{\omega_{n1}} + \frac{\omega_{n2}^2}{\omega_{n1}^2}\right) + \omega_{n2}^2$$

$$ID = \omega\left(-\omega^2\left(\frac{2\zeta_1}{\omega_{n1}} + \frac{c_2}{k_2} + \frac{2\zeta_2\omega_{n2}}{\omega_{n1}^2}\right) + \frac{2\zeta_1\omega_{n2}^2}{\omega_{n1}} + 2\zeta_2\omega_{n2}\right)$$

$$\omega_{n2}^2 = \frac{k_2}{m_2}$$

$$\omega_{n1}^2 = \frac{k_1}{m_1}$$

$$2\zeta_1\omega_{n1} = \frac{c_1}{m_1}$$

$$2\zeta_2\omega_{n2} = \frac{c_2}{m_2}$$

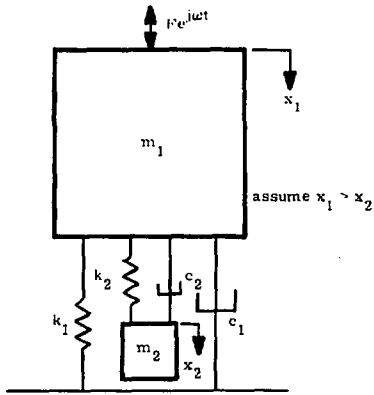

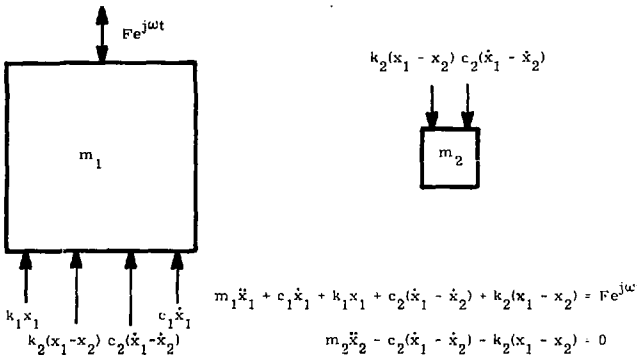

Figure VII.3. Two degree of freedom linear damped system

Figure VII.4 plots the magnitude of the transfer function for the situation $m_1 = m_2$, $\omega_{n2} = 3\omega_{n1}$, and $\zeta_1 = \zeta_2 = 0.01$. These are provided as

reasonable values of parameters with which to investigate this initial case. The frequency scale in this plot is normalized to ω_{n1}. Figure VII.5 shows the phase lag between output and input on this same frequency scale.

Each resonance, and the corresponding antiresonance, produces phase shifts of 180 degrees. It is obvious that a transient with significant frequency components on either side of a resonance is likely to be badly distorted. This fact is further complicated by the fact that actual systems may possess more than two significant resonances that must be considered. Conservative practice dictates that such resonant transducers can be relied upon to reproduce faithfully only those transients whose frequency content is below the lowest major resonant frequency. The important point is to locate this lowest major resonance.

It was stated that two cases could cover all combinations of occurrence for multiple resonant frequencies which occur in transducers. The second case considers one or more minor resonances occurring lower in frequency than that of the major resonance. An example of this situation could occur in a properly mounted transducer which has an internal component with a vibrating frequency below the fundamental resonance of the flexure. The system of Figure VII.3 can again describe this situation if only two resonances are considered. Reasonable parameters for investigating this situation are $m_1 = 10m_2$, $\omega_{n1} = 3\omega_{n2}$, and $\zeta_1 = \zeta_2 = 0.01$. Figures VII.6 and VII.7 show plots of the magnitude of the transfer function and the phase lag versus frequency, with frequency again normalized to ω_{n1}. It is interesting to note that this minor resonance causes only a temporary, small perturbation in the phase response.

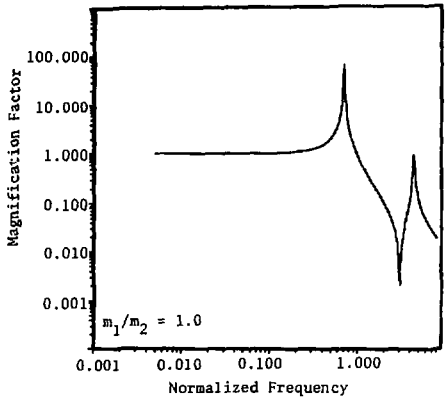

Figure VII.4. Two degree of freedom system amplitude-frequency response (second resonance occurs above major resonance)

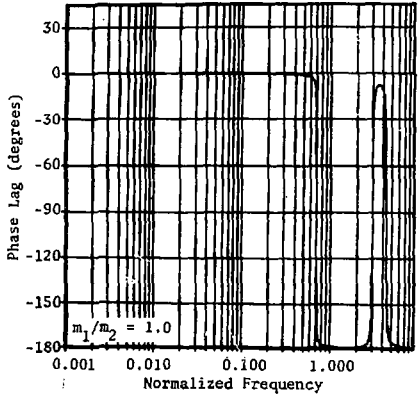

Figure VII.5. Two degree of freedom system phase-frequency response (second resonance occurs above major resonance)

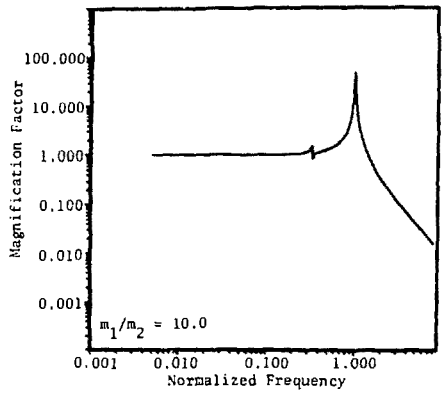

Figure VII.6. Two degree of freedom system amplitude-frequency response (second resonance occurs below major resonance)

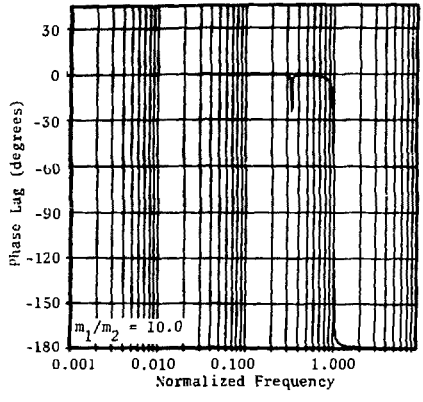

Figure VII.7. Two degree of freedom system phase-frequency response (second resonance occurs below major resonance)

The next section will present design criteria for optimizing the instrumentation system. These criteria will depend upon knowing the frequency of the major resonance of the transducer/mount combination. A conservative practice would be to treat any early-occurring minor resonance as the lowest major resonance and base design criteria on it. This practice could place unnecessary restrictions on the frequency response of a measuring system. Criteria developed in the next section also will discuss the question concerning what magnitude a minor resonance, which occurs before the major resonance, must have before its effect on the data has to be considered.

Summary and Conclusions

1. The inclusion of damping in transducers is only a limited solution to the problems associated with defining structural response in severe transient environments.
2. The transduction techniques applicable to many of the measurement problems of interest are piezoresistive (semiconductor) and piezoelectric. Their unique properties are:
   a. linearity over a wide range,
   b. adequate electrical signal magnitude, and
   c. the ability to be integrated into high resonant frequency systems to enhance the data separation problem illustrated in Chapter V.
3. To permit consideration to be directed towards optimizing the instrumentation system, two facts concerning the dynamic characteristics of the measuring transducer must be known. They are:

a. the transducer's frequency response should be flat and, as a by-product, its phase shift essentially zero over the frequency range of measurement interest, and

b. the location of the first major resonance of the transducer/mount combination must be identified.

4. Criteria for assessing the importance of minor resonances occurring before the first major resonance, if they exist, will be developed in the next chapter.

CHAPTER VIII

INSTRUMENTATION SYSTEM CONSIDERATIONS FOR PROBLEM SOLUTION

This chapter deals exclusively with signal conditioning considerations relating to the measurement of the dynamic characteristics of structural systems. The objective is to provide a practical solution to the problem associated with acquiring meaningful data when using resonant type measuring transducers to define structural dynamics.

With a wide variety of signal conditioning modules and multiplexing techniques available, as well as differing requirements between data users, optimizing instrument channel design is a significant challenge. Emphasis in this chapter is to assure that the transmission of a signal, which defines the structure, is properly conveyed through the instrumentation system.

In Chapter V, filtering of the data on playback was proven to be partially successful in determining structural response. In Chapter VI, it was demonstrated that inverse Fourier transforms or deconvolution techniques were not appropriate alternative solutions for this class of problem. Other methods of problem solution can still be considered.

One approach might be to use a logarithmic signal conditioner with antilogarithmic receiving or data reduction equipment. This technique would compress the amplitude of the data before the data progressed through the instrumentation channel. Unpredictably high signal amplitudes, attributable to the resonant characteristics of the measuring transducer, could more easily be accommodated. Greater gain would be provided to the lower amplitude portion of the signal defining

the structural response or forcing function. This higher gain would enhance the channel's signal to noise ratio.

Previously, in this work, it has been noted that most of the measuring transducers being considered possess fundamental resonant frequencies in the range above ten thousand Hz. Nonlinearities attributable to the logarithmic signal conditioner would greatly increase the frequency content of the signal being transmitted. The amount of additional bandwith required, being unpredictable, would depend both on the frequency content of the input signal as well as its amplitude. If all of this information were known regarding the input signal, the signal itself would be determined. There would be no need to measure it. If a portion of this frequency content were lost during data transmission, the antilogarithmic receiver would introduce further distortion. Compression of data by use of a nonlinear signal conditioner this is not a practical solution.

A second method which could be considered might involve automatic gain control in the signal conditioner. Amplifier gain would be frequently stepped to accommodate the output signal of the resonant transducer. Such a technique could in theory keep the signal within a predetermined linear range and also improve the signal to noise ratio of the channel.

The wildly varying signals illustrated in Chapter V indicate that this method is also impractical. The signal would be lost during gain changes, and these gain changes could not begin to keep up with the high frequency oscillations present. In addition, a second channel of information has to accompany each signal channel to provide information about the current value of gain. From a communications standpoint, this

is undesirable since two channels of information must be transmitted to define one. Loss of gain information renders both channels useless.

Including a filter at some point in the measuring system to eliminate signal frequency components nonessential to structural response then appears to be the best solution to the problem. Remaining questions to be considered are:

1. Does additional justification for filtering exist?
2. At what location in the measurement system is a filter most effective?
3. Can criteria for filter selection be developed?

The first two questions will be discussed concurrently.

Based on experience and the analysis of the structural dynamicist, an estimate can be made for each instrumented station of the structure as to the magnitude of structural loading and response to expect. If only this loading or response had to be considered, confidence factors could be applied to each estimate and meaningful channel calibration levels fixed. It should be recalled, however, that these estimates do not account for the superimposed resonant characteristics of the measuring transducer. The data analyzed in Chapter V indicated that even if these estimates were accurate the range of channel amplitude required to handle the signals without distortion would have to be anywhere from 116 to 1000 percent higher than that predicted. This uncertainty, coupled with other uncertainties in the initial estimate, make it highly likely that the instrumentation channel will exceed its linear recording limits.

Typically, a signal successively passes through a multiplexer, summing amplifier, transmitter, receiver, recorder, and various other

amplifiers before separation and demodulation of the subcarriers. When any of these devices is overdriven into its nonlinear region, new frequency components are generated related to harmonics, sums, differences, and higher order cross products of the input frequencies. In fact, the number of spurious frequency components which can be generated in an overdriven 10-channel multiplex system is so great that the resulting noise background can be treated as wideband random noise.[40]

Meaningful channel calibration levels can be fixed only if the effect of the resonant characteristics of the transducer can be eliminated by placing a filter at the transducer output. Passive* filters, those which use only passive components (resistors, capacitors, and inductors), have almost unlimited dynamic range. Active* filters, which use operational amplifiers in conjunction with resistors and capacitors, can be procured in premium quality where dynamic range is of key importance. It is then possible to select a filter whose linear range can accomodate the signal expected and, by attenuating the resonant characteristics of the transducer, also prevent the remainder of the instrumentation channel from being overdriven.

Another justification for filtering, and for locating the filter immediately after the transducer output, is based on the economics of multiplexing. In aerospace vehicles, mechanical shock is a major cause

*In this context, passive and active refer respectively to the self-generating and nonself-generating response associated with Figure III.1.

of failure for both vehicles and contained equipment. Information concerning shock is typically transmitted by means of a radio frequency data link. The basic communications concern, aside from the suppression of noise on the channel to the extent possible, is to transmit the maximum number of simultaneous signals. Multiplexing permits simultaneous multiple transmission to occur over the radio frequency link. Usually, shock information on aerospace vehicles is frequency modulated (FM) and then transmitted as FM/FM telemetry. A wider data bandwidth is available using FM/FM transmission than with other double multiplexing schemes.

The most extensive work in standarization of radio telemetry has been undertaken by the Inter-Range Instrumentation Group (IRIG). The IRIG specifications are created by, and are mandatory at, the national test ranges and are also used by NATO countries. Since these facilities are the predominant users of radio telemetry and associated equipment, the IRIG standards largely shape the practice in industry.

In frequency division multiplexing, each data channel makes use of a separate subcarrier using a defined position and bandwidth in the modulation baseband of the RF carrier. Two types of FM subcarrier formats are usually used; the data bandwidth of one type is proportional to the center frequency of the subcarrier, while the bandwidth of the other type is constant, regardless of subcarrier frequency.

Tables VIII.I and VIII.II, taken from IRIG document 106 as revised July 1975, detail the IRIG standard for FM subcarrier channels. The frequency of the proportional bandwidth channels is deviated either ±7.5 or ±15 percent about the center frequency. Deviations of less than ±20 percent are typically required in order to maintain a linear phase

relationship and still provide the necessary amplitude attentuation when bandpass filtering the subcarrier channels before demodulation.

To advise the IRIG regarding the telemetry data users' present and future requirments, a representative group of dynamicists was organized under the Society of Automotive Engineers (SAE) in the summer of 1965. Subcommittee G-5.9 on Telemetry Requirements, under SAE Committee G-5 on Aerospace Shock and Vibration, was composed primarily of dynamicists who use telemetry for flight shock, vibration, and acoustic measurements. Also included were consultants to assist in defining joint dynamics-telemetry problems. The needs described by this committee were published[50] primarily because IRIG was updating its standards for the subcarrier channels. These needs indicated requirements for 20 to 30 channels/flight of structural data with occasional requirements for 200 channels/flight. The "normal" requirement for data handling frequency capability was 10 to 2,000 Hz, with one "normal" requirement to 4,000 Hz. Occasionally requirements extended to 5,000 to 10,000 Hz.

The specifications in Tables VIII.I and VIII.II illustrate that the current IRIG standards fulfill a significant portion of these frequency bandwidth requirements. The maximum frequency response listed in the tables is based on a deviation ratio of one. This deviation ratio is one-half the channel deviation bandwidth divided by the cutoff frequency of the discriminator output filter. The difference between a deviation ratio of five and a ratio of one represents a severe degradation (approximately 11:1) in channel signal to noise ratio. This degradation is caused by increased intermodulation products between channels.

If an unfiltered signal from a resonant transducer was telemetered, these standard IRIG channel bandwidth allotments would be inadequate by more than an order of magnitude. By prefiltering the data, the data frequency content is made compatible with the frequency response of the subcarrier channels, and the available number of channels per radio frequency link can be greatly increased.

It should be noted that all data emitted from an FM channel are limited in frequency content by the subcarrier oscillator and its output bandpass filter. If signal conditioning modules located before the oscillator are overdriven, this fact can be "cosmetically" disguised due to this frequency limitation. Prefiltering the signal, if properly performed at the transducer output, eliminates this problem

An alternative to multiplexing a signal in the frequency domain is to multiplex it in the time domain. A technique such as pulse code modulation (PCM) is one of the more common pulse modulation techniques used to accomplish this time multiplexing. An advantage of PCM for recording transient signals, depending on bit word size, can be its wide dynamic range. Whether multiplexing in the time domain or simply time sampling an analog signal for subsequent digital analysis, filtering of the signal typically occurs.

Shannon's theorem[51] states that if the Fourier transform of a given signal exists and is band limited to some highest frequency spectral component, samples of the signal determined at uniform intervals and taken at a rate of twice this frequency component uniquely determine the signal and permit its reconstruction without distortion. Signals encountered in real physical systems typically contain an infinite band

Table VIII.1

Proportional-Bandwidth FM Subcarrier Channels

±7.5% CHANNELS

Channel	Center Frequencies (Hz)	Lower Deviation Limit* (Hz)	Upper Deviation Limit* (Hz)	Nominal Frequency Response (Hz)	Nominal Rise Time (ms)	Maximum Frequency Response** (Hz)*	Minimum Rise Time** (ms)
1	400	370	430	6	58	30	11.7
2	560	518	602	8	42	42	8.33
3	730	675	785	11	32	55	6.40
4	960	886	1,032	14	42	72	4.86
5	1,300	1,202	1,398	20	18	98	3.60
6	1,700	1,572	1,828	25	14	128	2.74
7	2,300	2,127	2,473	35	10	173	2.03
8	3,000	2,775	3,225	45	7.8	225	1.56
9	3,900	3,607	4,193	59	6.0	293	1.20
10	5,400	4,995	5,805	81	4.3	405	.864
11	7,350	6,799	7,901	110	3.2	551	.635
12	10,500	9,712	11,288	160	2.2	788	.444
13	14,500	13,412	15,588	220	1.6	1,088	.322
See Sec. 3-4							
14	22,000	20,350	23,650	330	1.1	1,650	.212
15	30,000	27,750	32,250	450	.78	2,250	.156
16	40,000	37,000	43,000	600	.58	3,000	.117
17	52,500	48,562	56,438	790	.44	3,938	.089
18	70,000	64,750	75,250	1050	.33	5,250	.067
19	93,000	86,025	99,975	1395	.25	6,975	.050
See Sec. 3-5							
20	124,000	114,700	133,300	1860	.19	9,300	.038
21	165,000	152,624	177,375	2475	.14	12,375	.029

±15% CHANNELS***

A	22,000	18,700	25,300	660	.53	3,330	.106
B	30,000	25,500	34,500	900	.39	4,500	.078
C	40,000	34,000	46,000	1200	.29	6,000	.058
D	52,500	44,625	60,375	1575	.22	7,875	.044
E	70,000	59,500	80,500	2100	.17	10,500	.033
F	93,000	79,050	106,950	2790	.13	13,950	.025
G	124,000	105,400	142,600	3720	.09	18,600	.018
H	165,000	140,250	189,750	4950	.07	24,750	.014

* Rounded off to nearest Hz.

** The indicated maximum data frequency response and minimum rise time is based upon the the maximum theoretical response that can be obtained in a bandwidth between the upper and lower frequency limits specified for the channels. (See Chapter 3, Sec. II and referenced discussion in Appendix B for determining possible accuracy versus response tradeoffs.)

*** Channels A through H may be used by omitting adjacent lettered and numbered channels. Channels 13 and A may be used together with some increase in adjacent channel interference.

Table VIII.II

Constant-Bandwidth FM Subcarrier Channels

A CHANNELS		B CHANNELS		C CHANNELS	
Deviation limits = ±2 KHz Nominal frequency response = 0.4 KHz Maximum frequency response = 2 KHz*		Deviation limits = ±4 KHz Nominal frequency response = 0.8 KHz Maximum frequency response = 4 KHz*		Deviation limits = ±8 KHz Nominal frequency response = 1.6 KHz Maximum frequency response = 8 KHz	
Channel	Center Frequency (KHz)	Channel	Center Frequency (KHz)	Channel	Center Frequency (KHz)
1A	16				
2A	24				
3A	32	3B	32	3C	32
4A	40				
5A	48	5B	48		
6A	56				
7A	64	7B	64	7C	64
8A	72				
9A	80	9B	80		
10A	88				
11A	96	11B	96	11C	96
12A	104				
13A	112	13B	112		
14A	120				
15A	128	15B	128	15C	128
16A	136				
17A	144	17B	144		
18A	152				
19A	160	19B	160	19C	160
20A	168				
21A	176	21B	176		

*The indicated maximum frequency is based upon the maximum theoretical response that can be obtained in a bandwidth between deviation limits specified for the channel. (See discussion in Appendix B for determining practical accuracy versus response tradeoffs.)

of frequencies. To account for this fact, terminology might be modified to state that the given signal must be bandlimited to some highest spectral component of significant amplitude. In the present context,

this highest spectral component would be based on the maximum frequency to which the structure possesses significant response. Filtering must occur to assure that no significant noise components are included above this highest spectral component. If sample rates were based on the frequency response of the structure, and the signal was not prefiltered to eliminate the high frequency resonant characteristics of the transducer, these resonant characteristics would overlap or alias the structural data in the frequency domain. The effect of this aliasing would be to create errors in the recorded signal. A detailed discussion on aliasing or folding can be found in any standard text on communication theory or digital signal processing.

When time division multiplexing is used, the signal must be filtered before going to the multiplexer, as demonstrated in the preceding discussion. As indicated previously, locating this analog filter at the transducer output also prevents the signal conditioner in front of the multiplexer from being overdriven.

It is interesting to note that all structural dynamics data are filtered either during recording or analysis. The question being dealt with is where in the instrumentation system is the optimum position for performing this filtering. The following argument adds conclusive credibility to the selection of the transducer output as the most desirable location for this filtering.

Any received signal should readily be distinguishable from its noise background. Every physical transmission path will attenuate a signal by an amount that increases with path length. This last statement is true whether or not the transmission path is a radio frequency link or wire cable.

A potential solution to this problem would be to raise the signal to such a high level that it cannot be distorted by noise. If the signal is filtered before passing through any signal conditioner, the first stage of the signal conditioner can provide the gain necessary to achieve this high signal level. If the unfiltered signal from the transducer had to pass through this first stage of the signal conditioning, the gain of this stage would have to remain low to keep it from being overdriven. Amplification would then have to be provided in subsequent signal conditioning modules after filtering had occurred. If amplification is to be provided, the optimum location is in the initial signal conditioning module. This requires immediate filtering at the transducer output. Justification of the importance of the first stage gain in influencing an instrumentation channel's signal to noise ratio follows.

The rms noise and signal are amplified by the same amount in passing through the various gain stages of an instrumentation system. A constant signal to noise ratio is impossible to maintain, and it progressively attenuates in passing through a system. Among other devices, transistors and resistors attenuate this signal to noise ratio through the addition of shot and thermal noise.

The noise figure (F) defines signal to noise ratio at the system input to the system output:

$$F = \frac{(S/N)_i}{(S/N)_o} \quad . \qquad \text{(VIII.1)}$$

The available power gain (G) of an arbitrary linear network is:

$$G = \frac{S_o}{S_i} \quad , \qquad \text{(VIII.2)}$$

which is a ratio of signal output power to signal input power. It is possible to determine the overall noise figure F of two successive stages of gain with respective F_1, G_1 and F_2, G_2. Results are:[52]

$$F = F_1 + \frac{F_2 - 1}{G_1} \quad . \tag{VIII.3}$$

Additional stages of gain modify the preceding equation but not its conclusion. A high value for G_1, the gain of the first stage of the signal conditioning, maximizes the system signal to noise ratio.

Previously it had been concluded that if the instrumentation channel can be operated within its linear range, and if the portion of the signal containing structural data is distinguishable from channel background noise, transient loads to, and responses of, structures can be determined through data separation (filtering) in the frequency domain. This chapter has demonstrated that the optimum location for this filtering is at the transducer output because of the following reasons:

1. It reduces the tendency for subsequent signal components to be overdriven and distort the transient signal.
2. It enchances the signal to noise ratio.
3. It minimizes the frequency spectrum occupied by the data being transmitted.
4. It increases the effectiveness with which the information capacity of the instrumention system is utilized.

The assumption that the transducer and the analog filter remain linear was inherent in all of the previous considerations. Justification for this assumption was based on the fact that both of these devices can be acquired with linear dynamic ranges many times that of the remainder of the instrumentation system. If additional bandwidth is available, it

is always desirable to verify this linearity assumption through concurrent recording of the unfiltered transducer output. In actual measurement situations involving large numbers of channels, this bandwidth usually is not available.

A final consideration, before developing criteria for filter selection, concerns the ease with which transducers using piezoresistive (semiconductor) and piezoelectric technology can be interfaced to filters. Piezoresistive transducers possess low impedance outputs (less than 1000 ohms) and can be readily interfaced to filter circuits. Piezoelectric devices possess very high impedance outputs, typically 10^9 to 10^{12} ohms, and the ease with which they can be interfaced is not so apparent. The inclusion of a field effect transistor within the piezoelectric transducer transforms the high impedance device into one with low impedance output while still maintaining an instrument with wide dynamic range. Filtering can then be introduced before subsequent stages of gain. For applications where piezoelectric transducers interface into charge amplifiers, passive components can be inserted between the transducer and the first stage charge converter of the amplifier to design filtering into the circuit.

Criteria for the selection of filters to be used in performing structural dynamics measurements will now be developed. The subject of signal filtering is interesting in that, while it appears to be simple in concept and easily understood qualitatively, its application to signal processing systems requires a sophisticated appreciation of such disciplines as Fourier spectrum analysis, information theory, and the time-domain characteristics of complex networks. For the purpose of definition, a filter will be considered to be any component of the

measuring system having both input and output terminals. This definition emphasizes the fact that filtering can enter the instrumentation system in locations other than that desired. Any transmission line, attenuator, amplifier, or other signal transmission element acts as a filter.

Attention will be focused on low-pass filters since they possess the desired property of passing information regarding the low frequency response modes of a structure while attenuating the high frequency resonant characteristics of the measuring transducer. Every filter will have associated with it a transfer function ($H(j\omega)$) which is a complex quantity. For actual filters, the cutoff frequency will be defined as that frequency at which the response $|H(j\omega)|$ is attenuated -3dB. The roll off rate of an actual filter is the assymptotic slope of $|(H(j\omega)|$ above the cutoff frequency. The roll off rate is usually expressed in dB/octave.

Filters can be classified as being either analog or digital, lumped parameter or distributed parameter, and active or passive. This discussion will be concerned only with analog lumped parameter filters of either the active or passive type. The decision as to whether to use active or passive filtering in a given application can be based upon several different considerations. Advantages to be found in passive filtering are very low noise, no power supply requirements, and practically no signal amplitude limitations. Advantages to be found in active filtering are no bulky inductors, no insertion losses (power gain is available), no impedance matching problems, and low susceptibility to magnetic fields.

Whether utilizing active or passive filters, filter selection involves conflicting requirements. Communications engineers, being very

aware of aliasing problems when time division multiplexing, tend to specify filters with steep roll offs. Filters with steep roll offs possess the most nonlinear phase-frequency characteristics and can severely distort transient signals. Measurement engineers, being very aware of the requirement for linear phase response when recording transients, usually specify linear phase filters when recording this type of signal. Linear phase filters possess the slowest roll offs and are therefore the least desirable based on aliasing considerations. Neither criterion is optimum.

The following discussion centers around all pole filters. These are ones which possess no finite zeros in their transfer function. The relationship between filter input and output voltage in the s plane can be represented as:

$$\frac{e_{out}}{e_{in}} = \frac{1}{F(s)} \qquad \text{(VIII.4)}$$

where F(s) is a polynominal in s which is usually factored into first and second order sections. The s plane is a two-dimensional set of coordinates where variables which take on complex as well as real values are plotted. A filter described by a sixth order polynomial (six-pole filter) can be fabricated by cascading three second order sections. Hurwitz polynominals are those which possess no right half plane nor multiple $j\omega$ zeros. For a filter to be realizable, F(s) must fit this category of polynomial.

Some of the more common low pass, all pole filters of interest include Butterworth, 0.1dB Chebyshev, and Bessel. In the frequency domain the Butterworth filter provides a maximally flat approximation of the magnitude of an ideal filter (described in the next paragraph). Its

form, normalized so that $\omega = 1$ corresponds to its cutoff frequency, is:

$$|H(j\omega)|^2 = \left(1 + \omega^{2n}\right)^{-1} \quad , \tag{VIII.5}$$

where n is the order of the filter. The realizable poles of transmission are on a semicircle in the left hand s plane. The Chebyshev filter is one in which the error of approximating the flat magnitude of the ideal filter is distributed through the passband in an oscillating manner. Its form is:

$$|H(j\omega)|^2 = \left[1 + \epsilon^2 C_n^2(\omega)\right]^{-1} \quad , \tag{VIII.6}$$

where $\epsilon < 1$ is a real constant which determines the magnitude of the ripple, $\omega = 1$ is the cutoff frequency, and

$$\begin{aligned} C_n &= \cos\left(n \cos^{-1}\omega\right) \quad 0 \le \omega < 1 \\ C_n &= \cosh\left(n \cosh^{-1}\omega\right) \quad \omega > 1 \quad . \end{aligned} \tag{VIII.7}$$

The filter order is represented by n. The Chebyshev filter produces a sharper "knee" in the frequency domain than does the Butterworth filter. Its realizable poles of transmission are on an ellipse in the left hand s plane. The Bessel filter is characterized by a constantly increasing phase error with frequency. The phase error is very small, however, for frequencies below the filter cutoff frequency. This type of filter places all the constraints on phase linearity at zero frequency. The Bessel polynomial approximates the ideal normalized function e^{-s}.

An ideal low pass filter would have a transfer function

$$\begin{aligned} H_i(j\omega) &= Ke^{-j\omega T} \qquad |\omega| < \omega_c \\ H_i(j\omega) &= 0 \qquad\qquad |\omega| > \omega_c \end{aligned} \tag{VIII.8}$$

where K and T are constants. Such a filter would uniformly pass all frequencies up to ω_c with only a linear phase shift or an equivalent constant time delay T. The ideal filter is not physically realizable since an inverse Fourier transform of its transfer function indicates an impulse response starting before time zero. It does, however, provide a standard against which to compare actual filters.

The establishment of optimum filter criteria depends upon the type of analysis to be performed on the resultant signal. The data must be analyzed as resulting either from a deterministic or nondeterministic (random) process. Deterministic data are those which can be described by an exact or explicit mathematical relationship. Nondeterministic data are random in character and must be described in terms of probability statements and statistical averages. Reference 53 is an excellent text covering random data and may be consulted for the definition of any standard terminology in the following discussion which proves unfamiliar.

An example of a random forcing function can be found in an impact wrench exciting a structure with an irregular sequence of transients. The practicality of most situations involves treating the data acquired in such random environments as being stationary (statistically time invariant).

Perhaps the single most important characteristic of stationary random data is its power spectral density function. This function defines the frequency composition of the data. For linear physical systems, the output power spectrum is equal to the input power spectrum multiplied by the square of the magnitude of the system transfer function, i.e.,

$$S_o(\omega) = |H(j\omega)|^2 S_i(\omega) \quad . \qquad \text{(VIII.9)}$$

Thus, power spectra measurements can yield information concerning the dynamic characteristics of the system. The total area under the power spectrum curve is equal to the mean square power. The mean square value of the data in any frequency range of concern is determined by the area under the power spectrum bounded by the limits of that frequency range.

For deterministic data, the relationship between input and output for a linear system is:

$$O(j\omega) = H(j\omega)\, I(j\omega) \quad , \qquad \text{(VIII.10)}$$

where $O(j\omega)$ is the Fourier transform of the system output and $I(j\omega)$ is the Fourier transform of the system input. Recall that multiplication in the frequency domain corresponds to convolution of the system input with the system impulse response in the time domain. Note that $H(j\omega)$ must be nonzero over the entire frequency range of interest to have frequency components present in the input represented in the output.

Based on the preceding discussion, and using the ideal low pass filter for a standard, error equations can be established for filters over the data frequency range of interest. For a nondeterministic process the magnitude of the power spectrum error is:

$$|E_p(\omega)| = \left| |H_a(j\omega)|^2 - |H_i(j\omega)|^2 \right| \quad . \qquad \text{(VIII.11)}$$

For a deterministic process, the magnitude of the Fourier spectrum error is:

$$|E_f(j\omega)| = |H_a(j\omega) - H_i(j\omega)| \quad . \qquad \text{(VIII.12)}$$

$H_a(j\omega)$ is the transfer function of an actual filter, while $H_i(j\omega$

remains the transfer function of the ideal low pass filter. These equations illustrate that for a deterministic process, distortion of the output can be attributed to both amplitude response deviation from flatness and phase response deviation from linearity. For a nondeterministic process, phase nonlinearities do not contributed to the error, as verified by Eq. (VIII.11) which shows this error to be dependent on the difference between two real numbers.

An additional error calculation can intercompare low pass filters based on their roll off rate above the data frequency range of interest. If white noise is assumed at the input of a linear filter, with noise spectral density $N_o/2$, the output noise power is:

$$\left(N_o/2\right)\int_{-\infty}^{\infty} |H_a(j\omega)|^2 \, df \quad . \tag{VIII.13}$$

Using this equation, the noise power from an ideal filter of bandwidth B and unity amplitude gain is:

$$N_o B \quad . \tag{VIII.14}$$

The noise equivalent bandwidth of an actual filter is then:

$$B = \int_o^{\infty} |H_a(j\omega)|^2 \, df. \tag{VIII.15}$$

This computation is essentially equivalent to replacing the actual filter by an equivalent ideal low pass filter of bandwidth B. The output noise power is proportional to the bandwidth. Thus, for two filters introducing equal errors over the low pass data frequency range of interest, the one with the lowest noise equivalent bandwidth is preferred.

With these error criteria established, the remaining consideration

is to translate the discussion, theory, and results of this and preceding chapters into some practical design guidelines. The first requirement is to identify the frequency location of the major resonance of the transducer/mount combination. It will be shown that the filter selected must provide attenuation of at least 68 dB by this major resonance.

Two different approaches can be used to justify this 68 dB attenuation figure. The data spectra analyzed in Chapter V were selected as being representative of those encountered in applying resonant type transducers to define structural response and loading. These data identified a worst case ratio between amplitude of response at the major resonant frequency of the measuring transducer and amplitude of response over the structure's frequency range of interest to be 10:1. In Chapter VI, it was concluded that the maximum accuracy to be expected when acquiring measurements to define structural dynamics was three to five percent. It was also suggested in Chapter VI that digitization precision greater than eight bits, excluding sign, was excessive for structural data. In order to prevent aliasing errors attributable to signal output at the major resonant frequency from degrading system accuracy by more than one count (one part in 256), and considering the 10:1 worst case response ratio, channel amplitude response must be attenuated to less than 1/2560 its dc value at this major resonant frequency. This is equivalent to at least 68 dB attenuation.

A second approach to justifying this 68 dB attenuation criteria considers the expressed needs of the structural dynamicist as presented in Reference 50. For stationary nondeterministic data, these needs were for a dynamic signal range of 31 to 41 dB. For this type of data,

dynamic signal range was defined to be:

$$DR = 20 \log \left(2x_b / \sigma_y\right) \quad . \tag{VIII.16}$$

This equation defines $2x_b$ as the bandedge to bandedge data amplitude and σ_y as the rms white noise value. The expressed needs of the dynamicist for transient data, possessing less than 2 kHz frequency content, were for 20 to 42 dB dynamic range. If a transient possessed frequency content above 2 kHz, these dynamic range requirements were increased to 26 to 54 dB. For transient data, dynamic signal range was defined as:

$$DR = 20 \log \left(2Mx_p / \sigma_y\right) \quad , \tag{VIII.17}$$

where x_p is the anticipated signal peak and M is a channel calibration safety factor. Providing 68 dB or more attenuation at the transducer major resonant frequency allots up to 20 dB to account for the 10:1 worst case response ratio, with a minimum of 48 dB to attenuate the remaining transducer resonant response below the structural dynamics data. This degree of attenuation appears compatible with the previous expressed dynamic signal range requirements.

Two computer programs were developed to determine the suitability of various filters for incorporation into instrumentation systems intended to provide measurement definition of structural dynamics. One program considered the situation where the recorded signal is treated as nondeterministic data. A second program considered the situation where the recorded signal is treated as deterministic data. The earlier mentioned Butterworth, 0.1 dB Chebyshev, and Bessel low pass filters were evaluated with 2, 4, 6, and 8 poles apiece. The effect of minor resonances at 0.2, 0.4, 0.6 and 0.8 of the frequency (FN) of the major

resonance of the transducer/mount combination was investigated. Requirements for a useable frequency range from zero hertz extending to discrete values between 0.002 and 0.3 FN were considered.

Appendices D and E contain the results of this evaluation in tabular form. Included in the appendices are examples which indicate how these tables might be used.

The computer program, which treats the situation where the resulting signal is nondeterministic performs the following calculations for each filter.

1. Locate, through an iteration process, the ratio of the maximum filter cutoff (-3 dB) frequency to FN which will exactly produce 68 dB attenuation at FN.
2. Locate those frequency ranges extending up to between 0.002 and 0.3 FN which possess an error in $|H(j\omega)|^2$ of less than five percent. This error is that between an actual filter with the cutoff frequency of step 1 and the ideal low pass filter.
3. For each frequency range located in step 2, iterate the filter cutoff frequency until the maximum error in $|H(j\omega)|^2$ is exactly five percent. Identify this cutoff frequency and calculate the filter noise equivalent bandwith.
4. Normalize the computed value of noise equivalent bandwidth to the maximum value obtained for any of the filters evaluated.
5. Evaluate the effect of minor resonances at 0.2, 0.4, 0.6 and 0.8 FN. If the filter possesses more than 68 dB attenuation at a minor resonance, its effects are ignored. If the attenuation is between 48 and 68 dB, compute the maximum ratio of the amplitude of the minor resonance to the amplitude of the major

resonance for which the minor resonance can be ignored. If the attenuation is less than 48 dB, treat any minor resonance occurring as the major resonance and redesign around it.

The second program, which considers the situation where the resulting signal is deterministic, performs the following calculations for each filter.

1. Same as step 1 of nondeterministic data program.
2. Identify the filter initial phase-frequency slope.
3. Locate those frequency ranges extending up to between 0.002 and 0.3 FN which possess both an error in $|H(j\omega)|$ of less than five percent and a phase nonlinearity of less than five degrees referenced to the initial phase slope. This error is that between an actual filter with the cutoff frequency of step 1 and the ideal low pass filter.
4. For each frequency range located in step 2, iterate the filter cutoff frequency until either the maximum error in $|H(j\omega)|$ is exactly five percent or the phase nonlinearity is exactly five degrees.
5. Same as step 4 of nondeterministic data program.
6. Same as step 5 of nondeterministic data program.

Results of the preceeding programs indicate that for nondeterministic data the 0.1 dB Chebyshev filter is preferred. Appendix D permits determination of the amount of compromise involved in applying a filter other than the optimum selection from the tables. For deterministic data, program results indicate the Butterworth filter is preferred. This last conclusion may be somewhat surprising to those expecting the linear phase Bessel filter to be optimum for deterministic

data. For Bessel and Butterworth filters with identical cutoff frequencies and the same number of poles, the Bessel filter produces only amplitude distortion while approaching its cutoff frequency, while the Butterworth filter produces distortion in both amplitude and phase. The point to keep in mind for the class of problems considered, however, is that in the band of frequencies between the highest frequency to which the structure significantly responds and the resonant characteristics of the transducer there is very little or essentially no signal response. Neither nonlinear phase nor amplitude attentuation occurring over this frequency band will distort the data of interest. The reputation for poor transient response associated with a Butterworth filter is based on published data regarding its step response characteristics. The frequency requirements for recording structural data are considerably different from frequency requirements for reproducing a step response. The Butterworth filter, based on both its ability to better truncate the high frequency resonant modes and its lower noise equivalent bandwidth, is then superior if its cutoff frequency is carefully located. Similar to Appendix D, Appendix E permits determination of the amount of compromise involved in alternate filter selection.

Summary and Conclusions

1. Instrumentation channels intended to measure structural dynamics require the inclusion of filtering between the measuring transducer output and the input of the first stage gain of the signal conditioning. This filtering accomplishes several purposes:

a. It reduces the tendency for subsequent signal conditioning components to be overdriven and distort the transient signal.

b. It enhances the data signal to noise ratio.

c. It minimizes the frequency spectrum occupied by the data being transmitted.

d. It increases the effectiveness with which the information capacity of the instrumentation system is utilized.

2. Filter selection for measuring structural dynamics should not be dictated solely by antialiasing requirements (steep roll off of the filter) nor by transient reproduction requirements (linear phase) but rather by a compromise between the two considerations. The noise minimization capabilities of a filter should be also considered. The Chebyshev filter, with 0.1 dB ripple in its pass band, is an effective filter for nondeterministic structural dynamics data. The Butterworth filter, with its cutoff frequency judiciously selected, is an effective filter for deterministic structural dynamics data. Appendices D and E contain tabular data to optimize this filter selection process.

CHAPTER IX

GENERAL SUMMARY AND CONCLUSION

This work has demonstrated that measuring the dynamic characteristics of structural systems presents a significant challenge to the engineer. In severe environments, the structural loading was observed to be impulsive in nature, characterized by discontinuities, and complicated by reflections. The structure's material response to these environments included discontinuites in particle velocities with corresponding sudden acceleration impulses. Test records illustrated that signals from resonant transducers attempting to measure structural loading and response became both distorted and analytically unpredictable because of multiple peaks in the transducer's transfer function. These test records also showed that erroneous data could appear to be valid if the transfer characteristics of the instrumentation obscured the presence of distortion in the transducer's output.

While signal distortion has been noted in previous studies, the analytic unpredictability of signal amplitudes has not been previously treated. Attempts by previous researchers to correct distortion in the signal from resonant transducers have been dependent on one of two assumptions, i.e.,

1. an adequate experimental characterization of the dynamic response of the measuring transducer is available, or
2. an adequate characterization of the transducer by a linear second order constant coefficient differential equation.

The solution technique advocated by these researchers has been to perform the inverse operation on the measuring transducer's transfer function.

The present work has demonstrated that the assumptions of the earlier researchers were both not necessary and not practical when measuring structural dynamics. It has been shown that calibration limitations in the national system of standards prevent the transfer function of the measuring transducers from being completely characterized. In addition, the transducer's transfer function can be modified by the technique used to interface it to its stimulus and, over certain frequency ranges, the stimulus being measured can be modified by the presence of the transducer.

Even though measurement difficulties encountered when using resonant transducers are not generally treatable by the inverse operations advocated by the previous researchers, procedures are described in this work which can be applied on a frequency selective basis to acquire valid data. These procedures necessitate analog filtering of the measuring transducer's signal. The optimum location for this filtering has been identified to be between the measuring transducer and the first stage gain of the signal conditioner. Filter design criteria have been developed to effect a compromise between antialiasing requirements (steep roll off of the filter) and transient reproduction requirements (linear phase) in signal recording. These criteria have considered whether the recorded data is treated as resulting from either a deterministic or nondeterministic (random) process. The criteria have been applied to the Bessel, Butterworth, and 0.1 dB Chebyshev filters of two, four, six, and eight pole design

resulting in the filter selection tables and the application examples presenced in Appendices D and E.

In any structural testing, particularly in the adverse environments which have been considered, there is always some potential for measurement error. The results of the present work, however, should significantly increase the likelihood of the structural dynamicist receiving valid data against which to compare his analytical model and generate test specifications. The design criteria of Appendices D and E are presently being applied by the agency which sponsored this research and have been found to be convenient to use and practical to implement in structural testing.

Additional productive research on this subject might involve applying the selection criteria developed in Chapter VIII to other filter types with differing numbers of poles from those considered in Appendices D and E. The most productive research, however, would be directed towards improving the capability to dynamically characterize the measuring transducers. As noted in Chapter VI, the system of standards for dynamic force and pressure transducers is almost nonexistent.

Generally, the individual topics of stress wave propagation, structural dynamics, modal analysis digital signal processing, communication theory, and electrical filter theory are not commonly viewed as mutually related engineering disciplines. Solution of the problem introduced in this study has demonstrated, however, that all these disciplines must be applied if valid structural measurements are to be acquired.

BIBLIOGRAPHY

1. Ecker, W., "Reproduction of Pulsed Forces by Force Detectors with Different Dynamic Properties," Werkstattstechnik, 62, 673-677 (1972).

2. Glasstone, S., The Effects of Nuclear Weapons, United States Atomic Energy Commission, ch.1, 8 (1962).

3. Graham, R.A. and Ingram, G.E., "Piezoelectric Current from x-Cut Quartz Subjected to Short-Duration Shock-Wave Loading," Journal of Applied Physics, 43(3), 826-835 (Mar. 1972).

4. Ungar, E.E., "The Status of Engineering Knowledge Concerning the Damping of Built-Up Structures," Journal of Sound and Vibration, 26(1),141-154 (Jan. 1973).

5. Harris, C.M. and Crede, C.E., Shock and Vibration Handbook, McGraw-Hill Book Company, New York, NY, ch. 43, 43-13 (1976).

6. Ramboz, J.D., private communication, Vibrations Section, Mechanics Division, National Bureau of Standards, Washington, DC (Nov. 1977).

7. Stein, P.K., "A New Conceptual and Mathematical Transducer Model-Application to Impedance-Based Transducers Such as Strain Gages," VDI Bericht Nr. 176, Dusseldorf, Germany, 221-236 (1972).

8. Stein, P.K., "A New Conceptual Model for Components in Measurement/Control Systems - Practical Applications to Thermocouples," Proceedings Fifth Symposium on Temperature, Instrument Society of America, 1991-2007 (1973).

9. Stein, P.K., "Traceability - The Golden Calf," Measurements and Data, 2(4), 97-105 (July-Aug. 1968).

10. Vigliante, R., "Dynamic Calibration of Spherical Copper Crushers," APG DPS1045, Aberdeen Proving Ground, MD. (Nov. 1963).

11. Stein, P.K., "The Response of Transducers to Their Environment - The Problem of Signal and Noise," Shock and Vibration Bul., 40(7), 1-15 (Dec. 1969).

12. Stein, P.K., "A Unified Approach to Handling of Noise in Measurements Systems," AGARD/NATO Lecture Series 50 on Flight Test Instrumentation, 5-1 to 5-11 (Sept.-Oct. 1972).

13. McConnell, K.G., "Active Notch Filters for Extending Frequency Response of Accelerometers," Experimental Mechanics, 12(5), 223-228 (May 1972).

14. Schulz, G.L. and Baker, W.E., "A Dynamic Data Compensation Technique for Seismic Transducers," Shock and Vibration Bul., 40(7), 123-132 (Dec. 1969).

15. Braun, S., "Dynamic Errors and Their Compensation in Seismic Low-Tuned Transducers," Journal of Sound and Vibration, 44(2), 223-236 (1976).

16. Sarma, G.K. and Bapat, Y.N., "Extending the Range of Seismic Transducers," Instruments and Control Systems, 45(2), 111-112 (Feb. 1972).

17. Stearns, S.D., Digital Signal Analysis, Hayden Book Company, Rochelle Park, NJ, ch. 5-8 (1975).

18. Chirlian, P.M., Signals, Systems, and the Computer, Intext Educational Publishers, New York, NY, ch. 2, 73-79 (1973).

19. Sangster, R.C., "Final Summary Report Study of the National Measurement System," NBSIR75-925, National Bureau of Standards, Boulder, CO (Dec. 1976).

20. National Bureau of Standards Report of Calibration, Lab. No. 213.04/215040, Sandia Laboratories, Albuquerque, NM (July 1976).

21. Koyanagi, R.S. and Ramboz, J.D., "A Systematic Study of Vibration Transfer Standards - Mass Loading Characteristics," Report 10955, National Bureau of Standards, Washington, DC (Nov. 1972).

22. Favour, J.D., "Accelerometer Calibration by Impulse Excitation Techniques," Preprint Number P13-1-PHYMMID-67, Proceedings of the 22nd Annual Instrument Society of America Conference (Sept. 1967).

23. Federman, C., Ramboz, J.D. and Walston, W.H., "Shock Calibration of Accelerometers," Eighth Transducer Workshop, Secretariat Range Commander's Council, White Sands Missile Range, NM (Apr. 1975).

24. Brown, W.G., "Accelerometer Calibration with the Hopkinson Pressure Bar," Preprint Number 49.3.63, Proceedings of the 18th Annual Instrument Society of America Conference (Sept. 1963).

25. Rasanen, G.K. and Wigle, B.M., "Accelerometer Mounting and Data Integrity," Sound and Vibration, 1(11), 8-15 (Nov. 1967).

26. Mangolds, B., "Effect of Mounting-Variables on Accelerometer Performance," Shock and Vibration Bul., 33(3), 1-12 (Mar. 1964).

27. Pennington, D., Piezoelectric Accelerometer Manual, Endevco Corporation, Pasadena, CA, ch. 4, 65-66 (1965).

28. Bouche, R.R., "Instruments and Methods for Measuring Mechanical Impedance," Shock and Vibration Bul., 30(2), 18-29 (Jan. 1962).

29. Schweppe, J.L., Eichenberger, L.C., Muster, D.F., Michaels, E.L. and Paskusz, G.F., "Methods for the Dynamic Calibration of Pressure Transducers," NBS Monograph 67, National Bureau of Standards, Washington, DC (Dec. 1963).

30. "A Guide for the Dynamic Calibration of Pressure Transducers," American National Standards Institute Subcommittee B88-1, The American Society of Mechanical Engineers, New York, NY (1972).

31. Morefield, R.I., "Dynamic Comparison Calibrator for High Range Pressure Transducers," Institute of Environmental Sciences 1965 Annual Technical Meeting Proceedings, 511-515 (Apr. 1965).

32. Layton, J.P. and Thomas, J.P., "Final Summary Technical Report on Transient Pressure Measuring Methods Research," Princeton University Aeronautical Engineering Report No. 595t, Princeton University, Princeton, NJ (Mar. 1967).

33. Simpson, J.P. and Gatley, W.L., "Dynamic Calibration of Pressure Measuring Systems," Instrumentation in the Aerospace Industry-Volume 16, Instrument Society of America (May 1970).

34. Nyland, T.W., "Sinusoidal Pressure Generator for Testing Pressure Probes," Proceedings of the 25th Annual Instrument Society of America Conference, 25(2), 621-670 (Oct. 1970).

35. Kistler Instrument Co. Data Sheet 210-2/671, Division of Sundstrand Data Control, Inc., Overlake Industrial Park, Redmond, WA.

36. Wright, J.K., Shock Tubes, Spottiswoode, Ballantyne & Co. Ltd., London & Colchester, ch. 3 (1961).

37. Favour, J.D. and Steward, R., "Primary Calibration of Pressure Transducers to 10,000 Hz," Instrumentation in the Aerospace Industry-Volume 15, 89-96 (May 1969).

38. Darsey, D.M., "System Calibration by Dynamic Response Analysis," SC-DR-69-816, Sandia Laboratories, Albuquerque, NM (Apr. 1970).

39. Chirlian, P.M., Signals, Systems, and the Computer, Intext Educational Publishers, New York, NY, ch. 2, 67-72 (1973).

40. Morse, P.M., Vibration and Sound, McGraw-Hill Book Co., New York, NY, ch. 22, 221-235 (1948).

41. Thomson, T.B., "The Effect of Tubing on Dynamic Pressure Recording," Technical Report No. 61-3, Rocketdyne Division of North American Aviation, Inc., Canoga Park, CA (Feb. 1961).

42. Stein, P.K., Measurement Engineering, Stein Engineering Services, Inc., Phoenix, AZ, ch. 14, 533-534 (1964).

43. Handbook of Mathematical Functions, National Bureau of Standards Applied Mathematic Series 55, United States Government Printing Office, 360 (June 1964).

44. Meirovitch, L., Analytical Methods in Vibrations, The Macmillan Co., New York, NY, 163 and 187 (1967).

45. Roark, R.J., Formulas for Stress and Strain, McGraw-Hill Book Co., New York, NY, ch. 8, 104 and ch. 10, 217 (1965).

46. Perry, C.C. and Lissner, H.R., The Strain Gage Primer, McGraw-Hill Book Co., New York, NY, ch. 2, 19 (1962).

47. Semiconductor Strain Gage Handbook, BLH Electronics, Inc., Waltham, Mass., Product Data 107, sec. 1 (Dec. 1973).

48. Plumlee, R.H., "Zero Shift in Piezoelectric Accelerometers," SC-RR-70-755, Sandia Laboratories, Albuquerque, NM (Mar. 1971).

49. Gruenberg, E.L., Handbook of Telemetry and Remote Control, McGraw-Hill Book Co., New York, NY, ch. 6, 15 (1967).

50. Himelblau, H., "Desired Telemetry System Characteristics for Shock, Vibration, and Acoustic Measurements," Subcommittee G-5.9 on Telemetry Requirements, SAE Committee G-5 on Aerospace Shock and Vibration, Proceedings International Telemetering Conference, vol. 2, 232-253 (Oct. 1966).

51. Shannon, C.E., "Communications in the Presence of Noise," Proceedings of the I.R.E., 37, 10-21 (Jan. 1949).

52. Schwartz, M., Information Transmission, Modulation, and Noise, McGraw-Hill Book Co., New York, NY, ch. 7, 358-565 (1970).

53. Bendat, J.S. and Piersol, A.G., Measurement and Analysis of Random Data, John Wiley and Sons, Inc., New York, NY, ch. 1-6 (1966).

54. Kolsky, H., Stress Waves in Solids, Dover Publications, Inc., New York, NY, ch. 2, 3, 5, 7 (1963).

55. Zel'dovich, Ya. B. and Raizer, Yu. P., Physics of Shock Waves and High-Temperature Phenomena, Academic Press, New York, NY, ch. 2, 49-50 (1966.)

56. Bradley, J.N., Shock Waves in Chemistry and Physics, John Wiley and Sons, Inc., New York, NY, 332-333 (1962).

57. Favour, J.D., "Transient Data Distortion Compensation," Shock and Vibration Bul., 35(4), 231-238 (Feb. 1966).

58. Houghton, J.R., Townsend, M.A. and Packman, P.F., "The Application of a Time-domain Deconvolution Technique for Identificatinn of Experimental Acoustic-emission Signals," Experimental Mechanics, 18(6), 233-239 (June 1978).

59. Marks, L.S. and Baumeister, T., Standard Handbook for Mechanical Engineers, McGraw-Hill Book Co., New York, NY, 4-25 (1967).

60. Instrument Society of America, 530 William Penn Place, Pittsburgh, PA.

APPENDIX A

MEASUREMENT TECHNIQUES FOR STUDYING WAVE PROPAGATION

Investigation of the wave propagation problem, i.e., providing definition of either material response or the pressure front associated with a blast wave, requires measuring transducers which are characterized in terms of their own wave propagation properties. Examples of some of the transducer types applied in wave propagation studies are discussed below.

Shock wave propagation can be investigated by using the electrical response of shock loaded solids. These shock waves can depole ferroelectrics, demagnetize ferromagnets, cause resistivity changes in metals, and generate currents in piezoelectric materials.

In the "Sandia quartz gage" a proportionality is established between the instantaneous short circuit current output of an X-cut quartz disk and the instantaneous stress at the interface between the specimen and the gage. The gage is designed with a large diameter to thickness ratio to maintain its electroded center portion (working area) in a condition of one-dimensional strain and a peripheral guard ring is provided to avoid electrical fringe distortion. Measurements are acquired over that portion of the shock loaded disk where both mechanical and electrical fields are one-dimensional. This gage records stress pulses to more than 25 kilobars with typical recording durations of one to four microseconds.

Equations governing the operation of the quartz gage follow.[3]

Let

K = piezoelectric constant of quartz

P = constant pressure during passage of wave through gage

A = working area of the circular disk

q = charge

c = dilational wave velocity which is constant for X-cut quartz at 5.72 mm/microsecond

h = thickness of the quartz disk

s = distance dilational wave has propagated into the quartz disk = ct at time t;

then:

$$q = KPA$$

$$q = KPAs/h \text{ (at time t)}$$

$$dq = KPAcdt/h$$

and the short circuit current is:

$$i = KPAc/h \quad \text{for} \quad 0 < t \leq h/c \quad . \tag{A.1}$$

This current is typically measured through a 50 ohm resistor.

The rise time of the pressure front in a reflected blast wave can be measured by devices such as pressure bars. If a long, slender, homogeneous, elastic rod experiences a pressure transient at one end, elementary bar theory states that a corresponding compressive stress pulse will be transmitted down the rod without dispersion. If the rod's front surface is loaded by a very low acoustic impedance medium such as a gas and its rear surface is bounded by a medium of insignificant acoustic impedance such as a low density encapsulating foam, the front surface will remain in equilibrium with the environment. A piezoelectric

crystal, whose transit time is short compared to the rise time of the pressure front, can be attached to the rod's front surface If the crystal's acoustic impedance is matched to that of the rod, the crystal can produce an electrical signal to define the leading edge of the pressure wave front. The signal is valid until dispersion in the rod begins to deteriorate pressure bar performance.

The requirement for matching the acoustic impedance (Z) of the rod and crystal will be presented. Let σ_A be a compressive stress wave propagating in a rod of material A, σ_B a compressive stress wave generated at the interface of materials A and B attributable to $_A$ reaching this point, and $\sigma_{A/B}$ the magnitude of the reflected stress relative to the incident stress in material A. Assume that $Z_B > Z_A$. Figure A.1 illustrates this situation.

Continuity of stress and particle velocity (V) at this interface requires that

$$\sigma_A + \sigma_{A/B} = \sigma_B$$

and $$V_A - V_{A/B} = V_B$$

Defining $Z = \sigma/V$ and substituting in the second of these equations yields:

$$\sigma_A/Z_A - \sigma_{A/B}/Z_A = \sigma_B/Z_B \quad .$$

Solving for $\sigma_{A/B}$ in the previous equation and substituting into the first equation yields an identity for σ_B as:

$$\sigma_B = \frac{2\sigma_A}{(1 + Z_A/Z_B)} \quad . \qquad (A.2)$$

Thus, if the acoustic impedance of the crystal matches that of the bar the transmitted stress σ_B is the same as the incident stress σ_A and no

reflections occur at the interface. A thin quartz crystal on the front surface of an aluminum rod is an example of an impedance match.

This discussion concerning the application of transducers capable of monitoring wave propagation problems considered the wave propagation characteristics of the transducers themselves. Similarly, in considering the application of transducers to structural response problems, it will be necessary to consider the structural characteristics of these devices.

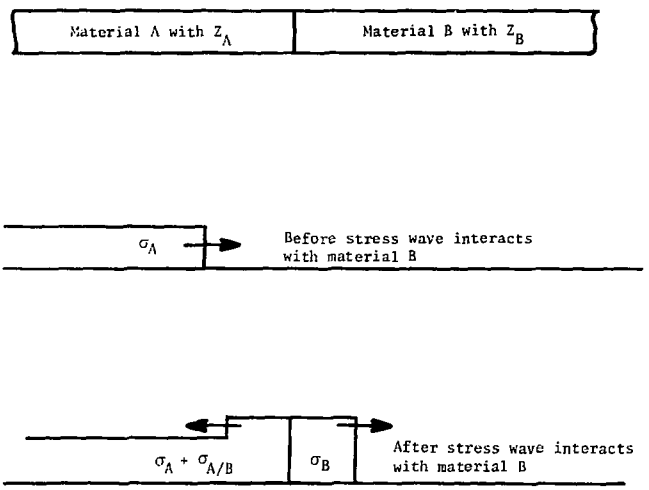

Figure A.1. Stress wave reflection at interface for $Z_B > Z_A$

APPENDIX B

TRANFUNC

The determination of a transfer function for a physical system is sometimes accomplished by evaluating the response of the system to a step excitation. A simple numerical method for transforming the time domain response to a step excitation to a corresponding frequency domain transfer function has been described by Darsey.[38] This method is used in computer code TRANFUNC.

The analysis technique used by TRANFUNC is particularly applicable to any resonant transducer whose starting transient response approaches its steady state step response in an oscillatory manner. In shock tube testing of pressure transducers, the step excitation cannot generally be maintained for a time period long enough for a transducer to achieve its steady state response. The computer code accounts for the fact that the specific step response is known only for some initial time interval.

The following equations summarize the analysis performed by the computer code. In this development, $r(t)$ is the physical system step response, $g(t)$ is an approximation of $r(t)$ by straight line segments, $u(t)$ is the unit step function, and $G(j\omega)$ the Fourier transform of $g(t)$.

Assume that an analog signal $r(t)$ is sampled, resulting in y_1, y_2, ..., y_{npts} at time t_1, t_2, ..., t_{npts}. The slope of the line joining the n and n+1 point is:

$$m_n = \frac{y_{n+1} - y_n}{t_{n+1} - t_n}$$

which permits the smooth function $r(t)$ to be approximated by a function comprised of straight line segments so that:

$$r(t) \approx g(t) = \sum_{n=1}^{npts-1} \left[m_n (t - t_n) + y_n \right] \left[u(t - t_n) - u(t - t_{n+1}) \right] .$$

After adding a step function at $t = t_{npts}$ of amplitude A such that A represents the steady state amplitude averaged over the oscillations, this approximation becomes:

$$g(t) = \sum_{n=1}^{npts-1} m_n (t - t_n)\, u(t - t_n) - \sum_{n=1}^{npts-1} m_n (t - t_{n+1})\, u(t - t_{n+1})$$

$$- \sum_{n=1}^{npts-1} y_n\, u(t - t_{n+1}) + \sum_{n=1}^{npts-1} y_n\, u(t - t_n) + A u(t - t_{npts}) .$$

Utilization of the time shift and time differentiation theorems[39] as they apply to Fourier transform theory yields:

$$G(j\omega) = \sum_{n=1}^{npts-1} m_n \frac{e^{-j\omega t_n}}{(j\omega)^2} - \sum_{n=1}^{npts-1} m_n \frac{e^{-j\omega t_{n+1}}}{(j\omega)^2} - \sum_{n=1}^{npts-1} y_n \frac{e^{-j\omega t_{n+1}}}{j\omega}$$

$$+ \sum_{n=1}^{npts-1} y_n \frac{e^{-j\omega t_n}}{j\omega} + A \frac{e^{-j\omega t_{npts}}}{j\omega} . \qquad (B.1)$$

The Fourier transform of the step excitation is $A/j\omega$. Knowledge of this transform, along with $G(j\omega)$ of the approximate physical system response, allows transfer function determination.

Investigation of the effect of truncation of r(t) on the transfer function computed by TRANFUNC was performed[38] by truncating the synthesized oscillatory response of an ideal lightly damped second order system of known transfer function to a unit step input after it had decayed to within ten percent of a steady state value. Figures B.1 and B.2 from Reference 38 illustrate input to the program and the error in the resultant transfer function attributable to truncation. A noise free signal is assumed, and a very high digitization rate is utilized to minimize errors attributable to other sources. The magnitude of error described in Figure B.2 is representative of the magnitude of error contained in Figures IV.15 and IV.17. Frequencies at which errors occur are scaled by the ratios of the resonant frequencies.

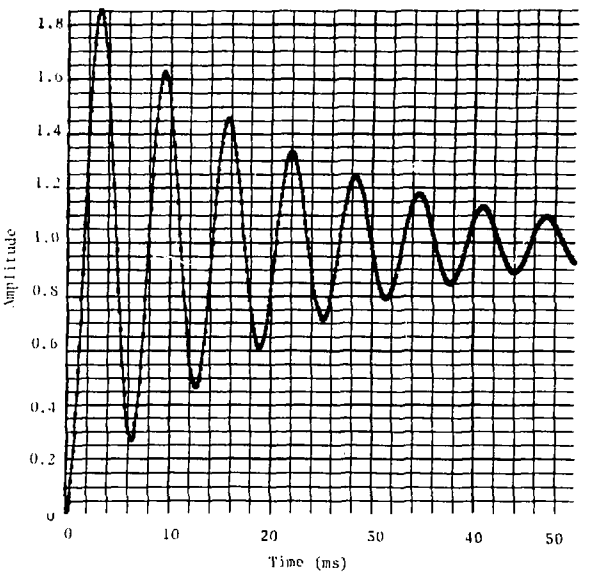

Figure B.1. Truncation of lightly damped oscillator response within ten percent of unit step input

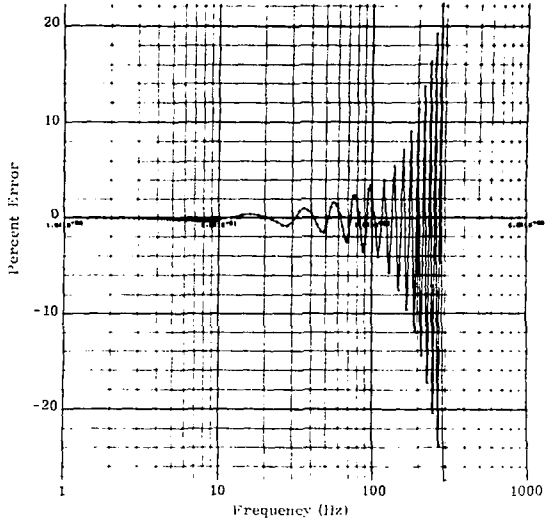

Figure B.2. Error in magnitude of transfer function attributable to truncation of Fig. B.1 (resonant frequency is 160 Hz)

APPENDIX C

CONSIDERATION OF A FLUSH MOUNTED CIRCULAR DIAPHRAGM PRESSURE TRANSDUCER AS AN IDEAL INTEGRATOR

Assume:

1. the transducer is a linear system, and

2. the circular transducer diaphragm behaves as an ideal integrator. Let $\sin 2\pi/\lambda(x - ct)$ be a right traveling pressure wave superimposed on top of some positive bias pressure P_0 (for a linear system, the effect of P_0 can be ignored) where:

c = velocity of propagation (inches/second),

t = time,

x = spatial variable, and

λ = wavelength (inches).

Station the pressure transducer at x = o, y = o.

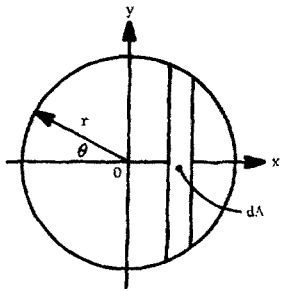

$$dA = 2y\,dx$$

$$A = 2\int_{-r}^{r} y\,dx$$

$$y = r\sin\theta$$

$$x = -r\cos\theta$$

so $$A = 2r^2\int_0^{\pi} \sin^2\theta\,d\theta$$

Call P_i the spatially integrated pressure.

$$P_i = \frac{1}{A}\int_A P(x,t)\,dA$$

$$\frac{1}{A}\int_A \left[\sin\frac{2\pi}{\lambda}(x - ct)\right] dA$$

$$\frac{1}{\pi r^2}\int_0^{\pi} 2r^2 \sin\frac{2\pi}{\lambda}(x - ct)\,\sin^2\theta\,d\theta$$

$$\frac{2}{\pi}\int_0^{\pi} \sin\frac{2\pi}{\lambda}(x - ct)\,\sin^2\theta\,d\theta$$

Recall the trigonometric identity $\sin(\alpha - \gamma) = \sin\alpha\cos\gamma - \cos\alpha\sin\gamma$. The previous relation becomes:

$$P_i = \frac{2}{\pi}\left[\cos\left(\frac{2\pi ct}{\lambda}\right)\int_0^{\pi} \sin\frac{2\pi x}{\lambda}\sin^2\theta\,d\theta - \sin\left(\frac{2\pi ct}{\lambda}\right)\int_0^{\pi} \cos\frac{2\pi x}{\lambda}\sin^2\theta\,d\theta\right].$$

Next substitute $x = -r\cos\theta$.

$$P_i = \frac{2}{\pi}\left[\cos\left(\frac{2\pi ct}{\lambda}\right)\int_0^{\pi} \sin\left(\frac{-2\pi r}{\lambda}\cos\theta\right)\sin^2\theta\,d\theta\right.$$

$$\left. - \sin\left(\frac{2\pi ct}{\lambda}\right)\int_0^{\pi} \cos\left(\frac{-2\pi r}{\lambda}\cos\theta\right)\sin^2\theta\,d\theta\right].$$

The first integral in the previous expression is equal to zero. This can be seen by noting that $\sin^2\theta$ is an even function about $\pi/2$ in the interval 0 to π and $-\cos\theta$ is an odd function about $\pi/2$, implying that $\sin(-2\pi r/\lambda\cos\theta)$ also is an odd function in the interval 0 to π about $\pi/2$. The expression for P_i now simplifies to:

$$P_i = \frac{-2}{\pi} \sin\left(\frac{2\pi ct}{\lambda}\right) \int_0^{\pi} \cos\left(\frac{-2\pi r}{\lambda} \cos\theta\right) \sin^2\theta \, d\theta \ .$$

Recall the trigonometric identities $\sin(-\Phi) = -\sin\Phi$ and $\cos(-\Phi) = \cos\Phi$

$$P_i = \sin\left(\frac{-2\pi ct}{\lambda}\right)\left[\frac{2}{\pi} \int_0^{\pi} \cos\left(\frac{2\pi r}{\lambda} \cos\theta\right) \sin^2\theta \, d\theta\right] . \qquad (C.1)$$

Now evaluate the integral in the brackets. Let $z = 2\pi r/\lambda$ so that the bracketed quantity is:

$$\frac{2}{\pi} \int_0^{\pi} \cos(z \cos\theta) \sin^2\theta \, d\theta \ .$$

Recall the identity that:

$$\cos(z \cos\theta) = J_0(z) + 2 \sum_{k=1}^{\infty} (-1)^k J_{2k}(z) \cos 2k\theta$$

where J_{2k} is a Bessel function of the first kind of order 2k. From this identity and orthogonality and recurrence relations, the following expression arises:[43]

$$J_1(z) = \frac{(z/2)}{\sqrt{\pi}\ \Gamma(3/2)} \int_0^{\pi} \cos(z \cos\theta) \sin^2\theta \, d\theta \ ,$$

and note

$$\Gamma(3/2) = \sqrt{\pi}/2 \ .$$

The solution to the integral of interest is then:

$$\frac{2}{\pi}\int_0^{\pi} \cos(z\cos\theta)\sin^2\theta\, d\theta = \frac{2}{z}J_1(z) \quad . \tag{C.2}$$

Substituting the results of Eq. (C.2) into Eq. (C.1) indicates the spatially integrated pressure to be equal to:

$$P_i = -\sin\left(\frac{2\pi ct}{\lambda}\right)\left[\frac{\lambda}{\pi r}J_1\left(\frac{2\pi r}{\lambda}\right)\right] .$$

The presumed pressure input was:

$$P(x,t) = \sin\frac{2\pi}{\lambda}(x - ct) \quad .$$

One expression for the transfer function is the ratio of the sinusoidal output to the corresponding sinusoidal input to a transducer; thus,

$$\frac{P_i}{P(x,t)} = \frac{\frac{\lambda}{\pi r}J_1\left(\frac{2\pi r}{\lambda}\right)\sin\left(\frac{2\pi ct}{\lambda}\right)}{\sin\frac{2\pi}{\lambda}(x - ct)} .$$

Since the transducer was located at $x = 0$, the transfer function becomes:

$$\frac{P_i}{P(0,t)} = \frac{\lambda}{\pi r}J_1\left(\frac{2\pi r}{\lambda}\right) \quad . \tag{C.3}$$

This expression permits investigation of the effect on transducer response of varying the wavelength λ of the particular sinusoidal forcing function.

APPENDIX D

NONDETERMINISTIC STATIONARY DATA FILTER CRITERIA

Application Example

Figure D.1 is the transfer function of an accelerometer/mount combination. This transfer function possesses two minor resonances below the major resonance. For application to the tables in this appendix, the frequency of this major resonance (32,000 Hz) is identified as FN. For illustration, Figure D.1 can be viewed as a typical transfer function of any resonant measuring transducer.

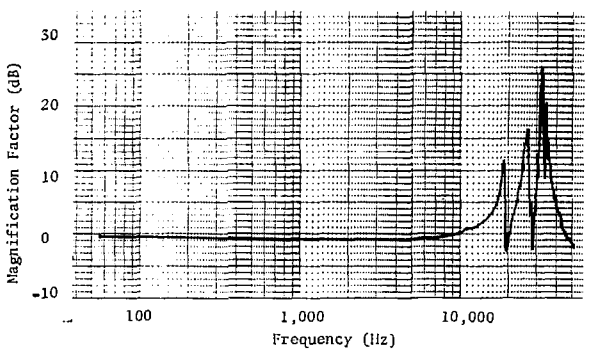

Figure D.1. Magnitude of transfer function of accelerometer/mount combination

Assume first that it is desired to acquire quantitative structural response data to 0.1 FN. Note that the transfer function possesses a flat amplitude response to about 0.19 FN. This response is compatible

with the data frequency range of interest. Assume next that because of a prior knowledge about the environment the recorded signal can be treated as nondeterministic stationary data so that this appendix becomes the applicable one to use. Since the amplification factor at the major resonance is approximately 23:1, it is not surprising that it should be desired to minimize its effect through filtering.

The first minor resonance occurs at 0.59 FN and has an amplitude approximately 0.18 that of the major resonance. The second minor resonance occurs at 0.83 FN and has an amplitude approximately 0.33 that of the major resonance.

In the filter selection tables of this appendix (Tables D.I through D.XII), a data range of 0.1 FN (left column) illustrates that none of the two-pole filters are suitable since no design criteria are listed. This is because these filters cannot maintain the error in $|H(j\omega)|^2$ within bounds and still accomplish 68 dB attenuation by FN. Considering next the four-pole filters, only the Chebyshev is adequate. This determination of adequacy is also based on the filter's ability to attenuate a minor resonance of amplitude up to 0.73 times that of the major resonance at 0.6 FN and any minor resonance occurring at 0.8 FN. Looking last at six-pole and eight-pole filter designs, both the Butterworth and Chebyshev are adequate. The Bessel filters of the number of poles considered in these tables never do become satisfactory for this application because of their slow roll off.

The minimum noise equivalent bandwidth (0.292 normalized value), and thus optimum filtering, is associated with the eight pole Chebyshev. The cutoff frequency of this particular filter is 0.1041 FN. The eight-pole Butterworth, with a cutoff frequency at 0.1202 FN, does produce

equivalent maximum errors in $|H(j\omega)|^2$ over the data range. Its 0.333 normalized noise equivalent bandwidth, however, is 14 percent larger than that for the eight-pole Chebyshev. In fact, on the basis of design criteria in this appendix, the four-pole Chebyshev provides filtering equivalent to the eight-pole Butterworth for this application.

TABLE D.I

RANDOM STATIONARY DATA FILTER CRITERIA

Maximum Error in $|H(j\omega)|^2$ is 5% Over Data Range

Filter Type Bessel Number of Poles 2

Data Range (Times FN)	-3dB Filter Frequency (Times FN)	Magl/Mag2 at Various Locations Before its Effects Cannot be Ignored				Normalized Noise Equivalent Bandwidth
		0.2 FN	0.4 FN	0.6 FN	0.8 FN	
0.002	0.0070	0.20	0.80	I	I	0.022
0.004	0.0140		0.20	0.45	0.80	0.044
0.006						
0.010						
0.020						
0.030						
0.040						
0.050						
0.060						
0.080						
0.100						
0.120						
0.140						
0.160						
0.180						
0.200						
0.250						
0.300						

Magl/Mag2 = ratio minor resonance to major resonance
FN = major resonance of transducer and mount combination
I = any minor resonance can be ignored

TABLE D.II

RANDOM STATIONARY DATA FILTER CRITERIA

Maximum Error in $|H(j\omega)|^2$ is 5% Over Data Range

Filter Type Butterworth Number of Poles 2

Data Range (Times FN)	-3dB Filter Frequency (Times FN)	Magl/Mag2 at Various Locations Before its Effects Cannot be Ignored				Normalized Noise Equivalent Bandwidth
		0.2 FN	0.4 FN	0.6 FN	0.8 FN	
0.002	0.0041	0.95	I	I	I	0.012
0.004	0.0083	0.23	0.92	I	I	0.025
0.006	0.0125		0.41	0.92	I	0.038
0.010						
0.020						
0.030						
0.040						
0.050						
0.060						
0.080						
0.100						
0.120						
0.140						
0.160						
0.180						
0.200						
0.250						
0.300						

Magl/Mag2 = ratio minor resonance to major resonance
FN = major resonance of transducer and mount combination
I = any minor resonance can be ignored

TABLE D.III

RANDOM STATIONARY DATA FILTER CRITERIA

Maximum Error in $|H(j\omega)|^2$ is 5% Over Data Range

Filter Type Chebyshev .1dB Number of Poles 2

Data Range (Times FN)	-3dB Filter Frequency (Times FN)	Magl/Mag2 at Various Locations Before its Effects Cannot be Ignored				Normalized Noise Equivalent Bandwidth
		0.2 FN	0.4 FN	0.6 FN	0.8 FN	
0.002	0.0033	I	I	I	I	0.010
0.004	0.0066	0.42	I	I	I	0.020
0.006	0.0099	0.19	0.76	I	I	0.030
0.010	0.0165		0.27	0.61	I	0.051
0.020						
0.030						
0.040						
0.050						
0.060						
0.080						
0.100						
0.120						
0.140						
0.160						
0.180						
0.200						
0.250						
0.300						

Magl/Mag2 = ratio minor resonance to major resonance
FN = major resonance of transducer and mount combination
I = any minor resonance can be ignored

TABLE D. IV

RANDOM STATIONARY DATA FILTER CRITERIA

Maximum Error in $|H(j\omega)|^2$ is 5% Over Data Range

Filter Type Bessel Number of Poles 4

Data Range (Times FN)	-3dB Filter Frequency (Times FN)	Magl/Mag2 at Various Locations Before its Effects Cannot be Ignored				Normalized Noise Equivalent Bandwidth
		0.2 FN	0.4 FN	0.6 FN	0.8 FN	
0.002	0.0070	I	I	I	I	0.020
0.004	0.0141	I	I	I	I	0.041
0.006	0.0212	0.61	I	I	I	0.061
0.010	0.0353		I	I	I	0.102
0.020	0.0707			0.40	I	0.204
0.030						
0.040						
0.050						
0.060						
0.080						
0.100						
0.120						
0.140						
0.160						
0.180						
0.200						
0.250						
0.300						

Magl/Mag2 = ratio minor resonance to major resonance
FN = major resonance of transducer and mount combination
I = any minor resonance can be ignored

TABLE D.V

RANDOM STATIONARY DATA FILTER CRITERIA

Maximum Error in $|H(j\omega)|^2$ is 5% Over Data Range

Filter Type Butterworth Number of Poles 4

Data Range (Times FN)	-3dB Filter Frequency (Times FN)	Magl/Mag2 at Various Locations Before its Effects Cannot be Ignored				Normalized Noise Equivalent Bandwidth
		0.2 FN	0.4 FN	0.6 FN	0.8 FN	
0.002	0.0028	I	I	I	I	0.008
0.004	0.0057	I	I	I	I	0.016
0.006	0.0086	I	I	I	I	0.024
0.010	0.0144	I	I	I	I	0.041
0.020	0.0288	0.92	I	I	I	0.081
0.030	0.0433	0.18	I	I	I	0.122
0.040	0.0577		0.92	I	I	0.163
0.050	0.0722		0.37	I	I	0.204
0.060	0.0866		0.18	0.92	I	0.245
0.080	0.1155			0.29	0.92	0.326
0.100						
0.120						
0.140						
0.160						
0.180						
0.200						
0.250						
0.300						

Magl/Mag2 = ratio minor resonance to major resonance
FN = major resonance of transducer and mount combination
I = any minor resonance can be ignored

TABLE D.VI

RANDOM STATIONARY DATA FILTER CRITERIA

Maximum Error in $|H(j\omega)|^2$ is 5% Over Data Range

Filter Type Chebyshev .1dB Number of Poles 4

Data Range (Times FN)	-3dB Filter Frequency (Times FN)	Magl/Mag2 at Various Locations Before its Effects Cannot be Ignored				Normalized Noise Equivalent Bandwidth
		0.2 FN	0.4 FN	0.6 FN	0.8 FN	
0.002	0.0023	I	I	I	I	0.006
0.004	0.0046	I	I	I	I	0.013
0.006	0.0069	I	I	I	I	0.020
0.010	0.0116	I	I	I	I	0.033
0.020	0.0232	I	I	I	I	0.066
0.030	0.0349	I	I	I	I	0.100
0.040	0.0465	0.35	I	I	I	0.133
0.050	0.0581	0.14	I	I	I	0.166
0.060	0.0698		I	I	I	0.199
0.080	0.0931		0.35	I	I	0.266
0.100	0.1163		0.14	0.73	I	0.332
0.120	0.1396			0.35	I	0.398
0.140	0.1629			0.18	0.60	0.465
0.160						
0.180						
0.200						
0.250						
0.300						

Magl/Mag2 = ratio minor resonance to major resonance
FN = major resonance of transducer and mount combination
I = any minor resonance can be ignored

TABLE D.VII

RANDOM STATIONARY DATA FILTER CRITERIA

Maximum Error in $|H(j\omega)|^2$ is 5% Over Data Range

Filter Type Bessel Number of Poles 6

Data Range (Times FN)	-3dB Filter Frequency (Times FN)	Magl/Mag2 at Various Locations Before its Effects Cannot be Ignored				Normalized Noise Equivalent Bandwidth
		0.2 FN	0.4 FN	0.6 FN	0.8 FN	
0.002	0.0072	I	I	I	I	0.021
0.004	0.0144	I	I	I	I	0.041
0.006	0.0216	I	I	I	I	0.062
0.010	0.0360	0.46	I	I	I	0.103
0.020	0.0720		0.46	I	I	0.206
0.030	0.1081			0.46	I	0.309
0.040	0.1441				0.46	0.412
0.050						
0.060						
0.080						
0.100						
0.120						
0.140						
0.160						
0.180						
0.200						
0.250						
0.300						

Magl/Mag2 = ratio minor resonance to major resonance
FN = major resonance of transducer and mount combination
I = any minor resonance can be ignored

TABLE D.VIII

RANDOM STATIONARY DATA FILTER CRITERIA

Maximum Error in $|H(j\omega)|^2$ is 5% Over Data Range

Filter Type Butterworth Number of Poles 6

Data Range (Times FN)	-3dB Filter Frequency (Times FN)	Magl/Mag2 at Various Locations Before its Effects Cannot be Ignored				Normalized Noise Equivalent Bandwidth
		0.2 FN	0.4 FN	0.6 FN	0.8 FN	
0.002	0.0025	I	I	I	I	0.007
0.004	0.0051	I	I	I	I	0.014
0.006	0.0076	I	I	I	I	0.021
0.010	0.0127	I	I	I	I	0.035
.020	0.0255	I	I	I	I	0.071
.030	0.0383	I	I	I	I	0.107
.040	0.0511	I	I	I	I	0.142
0.050	0.0639	0.37	I	I	I	0.178
0.060	0.0766	0.13	I	I	I	0.213
.080	0.1022		I	I	I	0.285
.100	0.1278		0.37	I	I	0.356
0.120	0.1533		0.13	I	I	0.427
0.140	0.1789			0.57	I	0.499
0.160	0.2044			0.26	I	0.570
0.180	0.2300			0.13	0.70	0.641
0.200	0.2556				0.37	0.712
0.250						
0.300						

Magl/Mag2 = ratio minor resonance to major resonance
FN = major resonance of transducer and mount combination
I = any minor resonance can be ignored

TABLE D.IX

RANDOM STATIONARY DATA FILTER CRITERIA

Maximum Error in $|H(j\omega)|^2$ is 5% Over Data Range

Filter Type Chebyshev .1dB Number of Poles 6

Data Range (Times FN)	-3dB Filter Frequency (Times FN)	Magl/Mag2 at Various Locations Before its Effects Cannot be Ignored				Normalized Noise Equivalent Bandwidth
		0.2 FN	0.4 FN	0.6 FN	0.8 FN	
0.002	0.0021	I	I	I	I	0.006
0.004	0.0043	I	I	I	I	0.012
0.006	0.0064	I	I	I	I	0.018
0.010	0.0107	I	I	I	I	0.030
0.020	0.0214	I	I	I	I	0.060
0.030	0.0321	I	I	I	I	0.090
0.040	0.0429	I	I	I	I	0.121
0.050	0.0536	I	I	I	I	0.151
0.060	0.0643	I	I	I	I	0.181
0.080	0.0858	0.41	I	I	I	0.242
0.100	0.1072		I	I	I	0.302
0.120	0.1287		I	I	I	0.362
0.140	0.1502		0.98	I	I	0.423
0.160	0.1716		0.41	I	I	0.483
0.180	0.1931		0.19	I	I	0.544
0.200	0.2145			I	I	0.604
0.250	0.2682			0.32	I	0.755
0.300	0.3218				0.63	0.906

Magl/Mag2 = ratio minor resonance to major resonance
FN = major resonance of transducer and mount combination
I = any minor resonance can be ignored

TABLE D.X

RANDOM STATIONARY DATA FILTER CRITERIA

Maximum Error in $|H(j\omega)|^2$ is 5% Over Data Range

Filter Type Bessel Number of Poles 8

Data Range (Times FN)	-3dB Filter Frequency (Times FN)	Magl/Mag2 at Various Locations Before its Effects Cannot be Ignored				Normalized Noise Equivalent Bandwidth
		0.2 FN	0.4 FN	0.6 FN	0.8 FN	
0.002	0.0072	I	I	I	I	0.021
0.004	0.0145	I	I	I	I	0.042
0.006	0.0217	I	I	I	I	0.062
0.010	0.0362	I	I	I	I	0.104
0.020	0.0725		I	I	I	0.208
0.030	0.1088			I	I	0.313
0.040	0.1451			0.20	I	0.417
0.050	0.1814				0.33	0.522
0.060						
0.080						
0.100						
0.120						
0.140						
0.160						
0.180						
0.200						
0.250						
0.300						

Magl/Mag2 = ratio minor resonance to major resonance
FN = major resonance of transducer and mount combination
I = any minor resonance can be ignored

TABLE D.XI

RANDOM STATIONARY DATA FILTER CRITERIA

Maximum Error in $|H(j\omega)|^2$ is 5% Over Data Range

Filter Type Butterworth Number of Poles 8

Data Range (Times FN)	-3dB Filter Frequency (Times FN)	Magl/Mag2 at Various Locations Before its Effects Cannot be Ignored				Normalized Noise Equivalent Bandwidth
		0.2 FN	0.4 FN	0.6 FN	0.8 FN	
0.002	0.0024	I	I	I	I	0.007
0.004	0.0048	I	I	II	I	0.013
0.006	0.0072	I	I	I	I	0.020
0.010	0.0120	I	I	I	I	0.033
0.020	0.0240	I	I	I	I	0.066
[illegible]	0.0360	I	I	I	I	0.100
0.040	0.0480	I	I	I	I	0.133
0.050	0.0601	I	I	I	I	0.167
0.060	0.0721	I	I	I	I	0.200
0.080	0.0961	0.14	I	I	I	0.266
0.100	0.1202		I	I	I	0.333
0.120	0.1442		I	I	I	0.400
0.140	0.1682		0.41	I	I	0.466
0.160	0.1923		0.14	I	I	0.533
0.180	0.2163			I	I	0.600
0.200	0.2404			0.60	I	0.667
0.250	0.3005				I	0.833
0.300	0.3606				0.23	1.000

Magl/Mag2 = ratio minor resonance to major resonance
FN = major resonance of transducer and mount combination
I = any minor resonance can be ignored

TABLE D.XII

RANDOM STATIONARY DATA FILTER CRITERIA

Maximum Error in $|H(j\omega)|^2$ is 5% Over Data Range

Filter Type Chebyshev .1dB Number of Poles 8

Data Range (Times FN)	-3dB Filter Frequency (Times FN)	Magl/Mag2 at Various Locations Before its Effects Cannot be Ignored				Normalized Noise Equivalent Bandwidth
		0.2 FN	0.4 FN	0.6 FN	0.8 FN	
0.002	0.0021	I	I	I	I	0.005
0.004	0.0042	I	I	I	I	0.011
0.006	0.0062	I	I	I	I	0.017
0.010	0.0104	I	I	I	I	0.029
0.020	0.0208	I	I	I	I	0.058
0.030	0.0312	I	I	I	I	0.087
0.040	0.0416	I	I	I	I	0.116
0.050	0.0520	I	I	I	I	0.146
0.060	0.0624	I	I	I	I	0.175
0.080	0.0833	I	I	I	I	0.233
0.100	0.1041	I	I	I	I	0.292
0.120	0.1249	0.22	I	I	I	0.350
0.140	0.1457		I	I	I	0.408
0.160	0.1666		I	I	I	0.467
0.180	0.1874		I	I	I	0.525
0.200	0.2082		I	I	I	0.584
0.250	0.2603		0.15	I	I	0.730
0.300	0.3123			I	I	0.875

Magl/Mag2 = ratio minor resonance to major resonance
FN = major resonance of transducer and mount combination
I = any minor resonance can be ignored

APPENDIX E

DETERMINISTIC DATA FILTER CRITERIA

Application Example

Figure E.1 shows the approximate transfer function of a particular flush-mounted circular-diaphragm pressure transducer. The frequency of the major resonance (282,000 Hz) will be denoted as FN. The amplification factor at resonance is approximately 46:1. No minor resonances precede this major resonance. Appendix D provides an example where minor resonances occur before the major resonance.

Figure E.1 is typical of many situations experienced in practice. A properly designed and optimally mounted transducer will display only one major resonant frequency. Additional resonances associated with the transducer and its mounting should be designed to occur only above this major resonance so that they do not degrade transducer performance. Once an instrument of this type is characterized adequately, special transfer functions are not needed for each test application. Nonstandard techniques of coupling the instrument to the environment which introduce system resonances below the transducer's fundamental resonance do require characterization of the transducer as it will be used.

For the purpose of discussion, assume it is desired to acquire deterministic data up to 0.018 FN (5000 Hz) to define the blast loading of a structure. The closest data range in the design tables of this appendix is 0.02 FN.

Locating this value in the left column of the filter selection tables of this appendix (Tables E.I through E.XII), it is found that none of the two-pole filters are suitable since no design criteria are

listed. This is because these filters are not capable of maintaining phase linearity within 5 degrees and amplitude response flat within 5 percent over the data range while still accomplishing 68 dB attenuation by FN. All of the tabulated filters with a higher number of poles, however, are capable of maintaining errors within these maximum bounds while providing adequate attenuation by FN.

Since no minor resonances are present before the major resonance, these are not a design consideration. The minimum noise equivalent bandwidth (0.072 normalized value), and thus optimum filter, is a four-pole Butterworth with cutoff frequency at 0.0348 FN (9800 Hz). A Butterworth filter with more than four poles becomes less satisfactory since the error in amplitude response is minimized at the expense of a more nonlinear phase, resulting in a larger noise equivalent bandwidth.

Suppose only an eight-pole Bessel filter is available and it is desired to ascertain what compromise is involved in its selection. The Bessel filter maintains a linear phase response, but to achieve a data range of 0.020 FN with less than a 5 percent error in amplitude response requires a cutoff frequency of 0.0513 FN (14,500 Hz). This results in a normalized noise equivalent bandwidth of 0.109 or 51 percent higher than that for the optimum four-pole Butterworth.

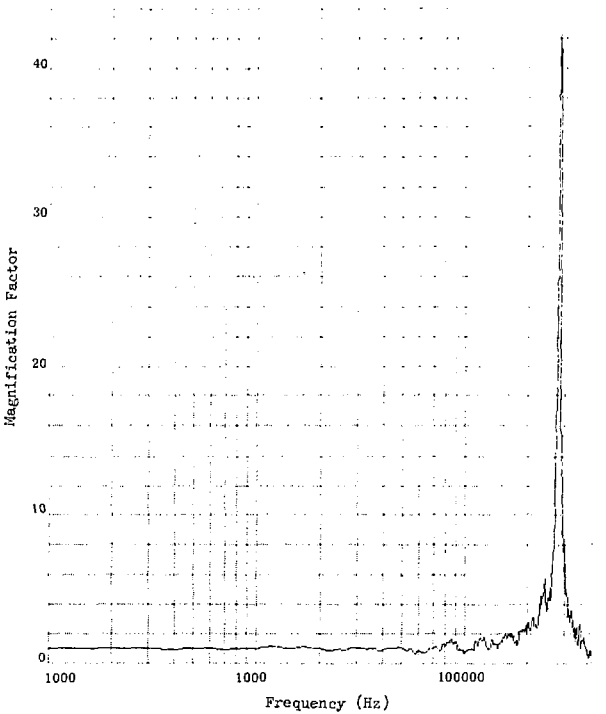

Figure E.1. Magnitude of transfer function of flush-mounted circular-diaphragm pressure transducer

TABLE E.I

DETERMINISTIC DATA FILTER CRITERIA

Maximum Error in $|H(j_0)|$ is 5% and Maximum Phase Nonlinearity is 5 Degrees Over Data Range

Filter Type Bessel Number of Poles 2

Data Range (Times FN)	-3dB Filter Frequency (Times FN)	Mag1/Mag2 at Various Locations Before its Effects Cannot be Ignored				Normalized Noise Equivalent Bandwidth
		0.2 FN	0.4 FN	0.6 FN	0.8 FN	
0.002	0.0050	0.40	I	I	I	0.012
0.004	0.0100		0.40	0.89	I	0.023
0.006	0.0150		0.18	0.40	0.70	0.035
0.010						
0.020						
0.030						
0.040						
0.050						
0.060						
0.080						
0.100						
0.120						
0.140						
0.160						
0.180						
0.200						
0.250						
0.300						

Mag1/Mag2 = ratio minor resonance to major resonance
FN = major resonance of transducer and mount combination
I = any minor resonance can be ignored

TABLE E.II
DETERMINISTIC DATA FILTER CRITERIA

Maximum Error in $|H(j\omega)|$ is 5% and Maximum Phase Nonlinearity is 5 Degrees Over Data Range

Filter Type Butterworth Number of Poles 2

Data Range (Times FN)	-3dB Filter Frequency (Times FN)	Magl/Mag2 at Various Locations Before its Effects Cannot be Ignored				Normalized Noise Equivalent Bandwidth
		0.2 FN	0.4 FN	0.6 FN	0.8 FN	
0.002	0.0034	I	I	I	I	0.008
0.004	0.0069	0.33	I	I	I	0.015
0.006	0.0104	0.15	0.59	I	I	0.023
0.010	0.0174		0.21	0.47	0.84	0.039
0.020						
0.030						
0.040						
0.050						
0.060						
0.080						
0.100						
0.120						
0.140						
0.160						
0.180						
0.200						
0.250						
0.300						

Magl/Mag2 = ratio minor resonance to major resonance
FN = major resonance of transducer and mount combination
I = any minor resonance can be ignored

TABLE E.III
DETERMINISTIC DATA FILTER CRITERIA

Maximum Error in $|H(j\omega)|$ is 5% and Maximum Phase Nonlinearity is 5 Degrees Over Data Range

Filter Type Chebyshev .1dB Number of Poles 2

Data Range (Times FN)	-3dB Filter Frequency (Times FN)	Mag1/Mag2 at Various Locations Before its Effects Cannot be Ignored				Normalized Noise Equivalent Bandwidth
		0.2 FN	0.4 FN	0.6 FN	0.8 FN	
0.002	0.0038	I	I	I	I	0.009
0.004	0.0076	0.32	I	I	I	0.017
0.006	0.0114	0.14	0.57	I	I	0.026
0.010	0.0191		0.20	0.46	0.81	0.043
0.020						
0.030						
0.040						
0.050						
0.060						
0.080						
0.100						
0.120						
0.140						
0.160						
0.180						
0.200						
0.250						
0.300						

Mag1/Mag2 = ratio minor resonance to major resonance
FN = major resonance of transducer and mount combination
I = any minor resonance can be ignored

TABLE E.IV
DETERMINISTIC DATA FILTER CRITERIA

Maximum Error in $|H(j_W)|$ is 5% and Maximum Phase Nonlinearity is 5 Degrees Over Data Range

Filter Type Bessel Number of Poles 4

Data Range (Times FN)	-3dB Filter Frequency (Times FN)	Magl/Mag2 at Various Locations Before its Effects Cannot be Ignored				Normalized Noise Equivalent Bandwidth
		0.2 FN	0.4 FN	0.6 FN	0.8 FN	
0.002	0.0050	I	I	I	I	0.011
0.004	0.0100	I	I	I	I	0.021
0.006	0.0150	I	I	I	I	0.032
0.010	0.0250	0.32	I	I	I	0.053
0.020	0.0501		0.32	I	I	0.106
0.030	0.0752			0.32	0.98	0.160
0.040						
0.050						
0.060						
0.080						
0.100						
0.120						
0.140						
0.160						
0.180						
0.200						
0.250						
0.300						

Magl/Mag2 = ratio minor resonance to major resonance
FN = major resonance of transducer and mount combination
I = any minor resonance can be ignored

TABLE E.V
DETERMINISTIC DATA FILTER CRITERIA

Maximum Error in $|H(j\omega)|$ is 5% and Maximum Phase Nonlinearity is 5 Degrees Over Data Range

Filter Type Butterworth Number of Poles 4

Data Range (Times FN)	-3dB Filter Frequency (Times FN)	Mag1/Mag2 at Various Locations Before its Effects Cannot be Ignored				Normalized Noise Equivalent Bandwidth
		0.2 FN	0.4 FN	0.6 FN	0.8 FN	
0.002	0.0034	I	I	I	I	0.007
0.004	0.0069	I	I	I	I	0.014
0.006	0.0104	I	I	I	I	0.022
0.010	0.0174	I	I	I	I	0.036
0.020	0.0348	0.43	I	I	I	0.072
0.030	0.0522		I	I	I	0.109
0.040	0.0696		0.43	I	I	0.145
0.050	0.0870		0.18	0.90	I	0.181
0.060	0.1044			0.43	I	0.217
0.080	0.1393			0.14	0.43	0.290
0.100						
0.120						
0.140						
0.160						
0.180						
0.200						
0.250						
0.300						

Mag1/Mag2 = ratio minor resonance to major resonance
FN = major resonance of transducer and mount combination
I = any minor resonance can be ignored

TABLE E.VI
DETERMINISTIC DATA FILTER CRITERIA

Maximum Error in $|H(j\omega)|$ is 5% and Maximum Phase Nonlinearity is 5 Degrees Over Data Range

Filter Type Chebyshev .1dB Number of Poles 4

Data Range (Times FN)	-3dB Filter Frequency (Times FN)	Magl/Mag2 at Various Locations Before its Effects Cannot be Ignored				Normalized Noise Equivalent Bandwidth
		0.2 FN	0.4 FN	0.6 FN	0.8 FN	
0.002	0.0040	I	I	I	I	0.008
0.004	0.0081	I	I	I	I	0.017
0.006	0.0122	I	I	I	I	0.026
0.010	0.0204	I	I	I	I	0.043
0.020	0.0409	0.59	I	I	I	0.086
0.030	0.0613	0.11	I	I	I	0.129
0.040	0.0818		0.59	I	I	0.172
0.050	0.1022		0.23	I	I	0.215
0.060	0.1227		0.11	0.59	I	0.258
0.080	0.1636			0.16	0.59	0.344
0.100						
0.120						
0.140						
0.160						
0.180						
0.200						
0.250						
0.300						

Magl/Mag2 = ratio minor resonance to major resonance
FN = major resonance of transducer and mount combination
I = any minor resonance can be ignored

TABLE E.VII
DETERMINISTIC DATA FILTER CRITERIA

Maximum Error in $|H(j\omega)|$ is 5% and Maximum Phase Nonlinearity is 5 Degrees Over Data Range

Filter Type Bessel Number of Poles 6

Data Range (Times FN)	-3dB Filter Frequency (Times FN)	Mag1/Mag2 at Various Locations Before its Effects Cannot be Ignored				Normalized Noise Equivalent Bandwidth
		0.2 FN	0.4 FN	0.6 FN	0.8 FN	
0.002	0.0051	I	I	I	I	0.011
0.004	0.0102	I	I	I	I	0.021
0.006	0.0153	I	I	I	I	0.032
0.010	0.0255	I	I	I	I	0.054
0.020	0.0510		I	I	I	0.107
[illegible]	0.0765		0.32	I	I	0.161
0.040	0.1020			0.65	I	0.215
0.050	0.1276			0.17	0.94	0.269
0.060	0.1531				0.32	0.323
0.080						
0.100						
0.120						
0.140						
0.160						
0.180						
0.200						
0.250						
0.300						

Mag1/Mag2 = ratio minor resonance to major resonance
FN = major resonance of transducer and mount combination
I = any minor resonance can be ignored

TABLE E.VIII
DETERMINISTIC DATA FILTER CRITERIA

Maximum Error in $|H(j\omega)|$ is 5% and Maximum Phase Nonlinearity is 5 Degrees Over Data Range

Filter Type Butterworth Number of Poles 6

Data Range (Times FN)	-3dB Filter Frequency (Times FN)	Magl/Mag2 at Various Locations Before its Effects Cannot be Ignored				Normalized Noise Equivalent Bandwidth
		0.2 FN	0.4 FN	0.6 FN	0.8 FN	
0.002	0.0036	I	I	I	I	0.007
0.004	0.0073	I	I	I	I	0.015
0.006	0.0110	I	I	I	I	0.022
0.010	0.0184	I	I	I	I	0.038
0.020	0.0369	I	I	I	I	0.076
0.030	0.0554	0.88	I	I	I	0.114
0.040	0.0739	0.16	I	I	I	0.152
0.050	0.0923		I	I	I	0.189
0.060	0.1108		0.88	I	I	0.227
0.080	0.1478		0.16	I	I	0.303
0.100	0.1847			0.47	I	0.379
0.120	0.2217			0.16	0.88	0.455
0.140	0.2586				0.35	0.531
0.160						
0.180						
0.200						
0.250						
0.300						

Magl/Mag2 = ratio minor resonance to major resonance
FN = major resonance of transducer and mount combination
I = any minor resonance can be ignored

TABLE E.IX
DETERMINISTIC DATA FILTER CRITERIA

Maximum Error in $|H(j\omega)|$ is 5% and Maximum Phase Nonlinearity is 5 Degrees Over Data Range

Filter Type Chebyshev .1 dB Number of Poles 6

Data Range (Times FN)	-3dB Filter Frequency (Times FN)	Mag1/Mag2 at Various Locations Before its Effects Cannot be Ignored				Normalized Noise Equivalent Bandwidth
		0.2 FN	0.4 FN	0.6 FN	0.8 FN	
0.002	0.0047	I	I	I	I	0.010
0.004	0.0095	I	I	I	I	0.020
0.006	0.0143	I	I	I	I	0.030
0.010	0.0239	I	I	I	I	0.050
0.020	0.0479	I	I	I	I	0.099
0.030	0.0718	I	I	I	I	0.149
0.040	0.0958	0.20	I	I	I	0.199
0.050	0.1197		I	I	I	0.248
0.060	0.1437		I	I	I	0.298
0.080	0.1916		0.20	I	I	0.398
0.100	0.2395			0.66	I	0.497
0.120	0.2874			0.20	I	0.596
0.140	0.3353				0.48	0.696
0.160						
0.180						
0.200						
0.250						
0.300						

Mag1/Mag2 = ratio minor resonance to major resonance
FN = major resonance of transducer and mount combination
I = any minor resonance can be ignored

TABLE E.X
DETERMINISTIC DATA FILTER CRITERIA

Maximum Error in $|H(j\omega)|$ is 5% and Maximum Phase Nonlinearity is 5 Degrees Over Data Range

Filter Type Bessel Number of Poles 8

Data Range (Times FN)	-3dB Filter Frequency (Times FN)	Magl/Mag2 at Various Locations Before its Effects Cannot be Ignored				Normalized Noise Equivalent Bandwidth
		0.2 FN	0.4 FN	0.6 FN	0.8 FN	
0.002	0.0051	I	I	I	I	0.011
0.004	0.0102	I	I	I	I	0.022
0.006	0.0154	I	I	I	I	0.033
0.010	0.0256	I	I	I	I	0.054
0.020	0.0513	0.13	I	I	I	0.109
0.030	0.0770		I	I	I	0.163
0.040	0.1027		0.13	I	I	0.218
0.050	0.1284			0.51	I	0.272
0.060	0.1541			0.13	I	0.327
0.080						
0.100						
0.120						
0.140						
0.160						
0.180						
0.200						
0.250						
0.300						

Magl/Mag2 = ratio minor resonance to major resonance
FN = major resonance of transducer and mount combination
I = any minor resonance can be ignored

TABLE E.XI
DETERMINISTIC DATA FILTER CRITERIA

Maximum Error in $|H(j\omega)|$ is 5% and Maximum Phase Nonlinearity is 5 Degrees Over Data Range

Filter Type Butterworth Number of Poles 8

Data Range (Times FN)	-3dB Filter Frequency (Times FN)	Magl/Mag2 at Various Locations Before its Effects Cannot be Ignored				Normalized Noise Equivalent Bandwidth
		0.2 FN	0.4 FN	0.6 FN	0.8 FN	
0.002	0.0039	I	I	I	I	0.008
0.004	0.0079	I	I	I	I	0.016
0.006	0.0118	I	I	I	I	0.024
0.010	0.0197	I	I	I	I	0.040
0.020	0.0395	I	I	I	I	0.081
0.030	0.0592	I	I	I	I	0.121
0.040	0.0790	0.67	I	I	I	0.161
0.050	0.0988	0.11	I	I	I	0.202
0.060	0.1185		I	I	I	0.242
0.080	0.1581		0.67	I	I	0.323
0.100	0.1976		0.11	I	I	0.404
0.120	0.2371			0.67	I	0.484
0.140	0.2766			0.20	I	0.565
0.160	0.3162				0.67	0.646
0.180	0.3557				0.26	0.727
0.200						
0.250						
0.300						

Magl/Mag2 = ratio minor resonance to major resonance
FN = major resonance of transducer and mount combination
I = any minor resonance can be ignored

TABLE E.XII
DETERMINISTIC DATA FILTER CRITERIA

Maximum Error in $|H(j_w)|$ is 5% and Maximum Phase Nonlinearity is 5 Degrees Over Data Range

Filter Type Chebyshev .1dB Number of Poles 8

Data Range (Times FN)	-3dB Filter Frequency (Times FN)	Magl/Mag2 at Various Locations Before its Effects Cannot be Ignored				Normalized Noise Equivalent Bandwidth
		0.2 FN	0.4 FN	0.6 FN	0.8 FN	
0.002	0.0053	I	I	I	I	0.011
0.004	0.0107	I	I	I	I	0.022
0.006	0.0161	I	I	I	I	0.033
0.010	0.0269	I	I	I	I	0.055
0.020	0.0538	I	I	I	I	0.111
0.030	0.0807	I	I	I	I	0.167
0.040	0.1076	0.92	I	I	I	0.222
0.050	0.1345		I	I	I	0.278
0.060	0.1614		I	I	I	0.333
0.080	0.2152		0.92	I	I	0.444
0.100	0.2690			I	I	0.555
0.120	0.3228			0.92	I	0.667
0.140	0.3766			0.21	I	0.778
0.160	0.4304				0.92	0.889
0.180	0.4842				0.30	1.000
0.200						
0.250						
0.300						

Magl/Mag2 = ratio minor resonance to major resonance
FN = major resonance of transducer and mount combination
I = any minor resonance can be ignored

DISTRIBUTION:

1110 J. D. Kennedy
1120 G. E. Hansche
1170 S. A. Moore
1500 W. A. Gardner
1510 A. J. Clark, Jr.
1520 T. L. Pace
1530 W. E. Caldes
1540 R. L. Brin
1550 F. W. Neilson
1580 T. S. Church
1585 P. L. Walter (50)
1710 V. E. Blake, Jr.
2510 D. H. Anderson
2550 E. G. Franzak
4230 M. Cowan
4310 C. C. Burks
4330 E. E. Ives
4340 H. W. Schmitt
4360 J. A. Hood
5520 T. B. Lane
5620 M. M. Newsom
5630 R. C. Maydew
8120 W. E. Alzheimer
8410 R. Baroody
8460 C. M. Tapp
8266 E. A. Aas
3141 T. L. Werner (5)
3151 W. L. Garner (3)
For DOE/TIC (unlimited Release)
DOE/TIC (25)
(R. P. Campbell, 3172-3)